Inhibition of fungal biodeterioration of construction materials using low and high ionizing radiation

THESIS SUBMITTED FOR

THE DEGREE OF DOCTOR OF PHILOSOPHY

(ENGINEERING)

JADAVPUR UNIVERSITY

2023

By

ANIRBAN CHAUDHURI

Index No: D-7/ISLM/100/19

SCHOOL OF ENVIRONMENTAL STUDIES

JADAVPUR UNIVERSITY, KOLKATA-700032,

INDIA

CERTIFICATE FROM THE SUPERVISORS

This is to certify that the thesis entitled **"Inhibition of fungal biodeterioration of construction materials using low and high ionizing radiation"** submitted by **Shri Anirban Chaudhuri** who got his name registered on **November 1, 2019** for the award of **Ph.D. (Engineering)** degree of **Jadavpur University**, is absolutely based upon his own work under the supervisions of Dr. Subarna Bhattacharyya, Dr. Somnath Mukherjee, Dr. Anindita Chakraborty and that neither this thesis nor any part of it has been submitted for either any degree/diploma or any other academic award anywhere before.

Subarna Bhattacharyya 18.12.2023

(Signature of Supervisor with date and official seal)

Subarna Bhattacharyya, PhD
Assistant Professor
School of Environmental Studies
Jadavpur University
Kolkata 700032, INDIA

18.12.2023

(Signature of Supervisor with date and official seal)

R. S. N. MUKHERJEE
Professor
CIVIL ENGINEERING DEPT.
JADAVPUR UNIVERSITY
KOLKATA-700032. (W.B)

Anindita Chakraborty 18.12.2023

(Signature of Supervisor with date and official seal)

डॉ. अनिंदिता चक्रबोर्ती / Dr. Anindita Chakraborty
वैज्ञानिक-एच / Scientist-H
यूजीसी-डीएई कंसोर्टियम फॉर साइंटिफिक रिसर्च, कोलकाता केन्द्र
UGC-DAE Consortium for Scientific Research, Kolkata Centre,
ब्लाक-एल.बी.-८ बिधाननगर / Block-LB-8, Bidhannagar
कोलकाता (प.बं.)-७०० १०६ / Kolkata (W.B.)-700106

THESIS DETAILS

1. Index No. and Date of Registration: D-7/ISLM/100/19 registered on November 1, 2019

2. Title of the Thesis: Inhibition of fungal biodeterioration of construction materials using low and high ionizing radiation

3. Name, Designation & Institution of the Supervisors:

Dr. Subarna Bhattacharyya

Assistant Professor

School of Environmental Studies

Jadavpur University

Kolkata- 700032, India

Dr. Somnath Mukherjee

Professor

Department of Civil Engineering

Jadavpur University

Kolkata- 700032, India

Dr. Anindita Chakraborty

Scientist H

Radiation and Stress Biology

UGC-DAE CSR, Kolkata Centre

4. E-mail ID of the Supervisors: barna_kol@yahoo.com

mukherjeesomnath19@gmail.com

anindita.iuc@gmail.com

5. List of Publications:

(a) Publications Related to Doctoral Work –

(i) Anirban Chaudhuri, Chiradeep Basu, Subarna Bhattacharyya, and Punarbasu Chaudhuri (2019) Development of health risk rating scale for indoor airborne fungal exposure. **Archives of environmental & occupational health (Taylor & Francis)** 75(7): 375-383. DOI: 10.1080/19338244.2019.1676187.

(ii) Anirban Chaudhuri, Subarna Bhattacharyya, Punarbasu Chaudhuri, Mathummal Sudarshan, and Somnath Mukherjee (2020) *In vitro* deterioration study of concrete and marble by *Aspergillus tamarii*. **Journal of Building Engineering (Elsevier)** 32, 101774. DOI: 10.1016/j.jobe.2020.101774.

(iii) Anirban Chaudhuri, Subarna Bhattacharyya, Anindita Chakraborty, Somnath Mukherjee, Mathummal Sudarshan, Chandan Kumar Ghosh, and Punarbasu Chaudhuri (2023) Inhibitory effect of UV and gamma radiation for fungal biodeterioration of concrete: a short-term study for sustainable conservation. **Journal of Cultural Heritage (Elsevier)**. (Revised manuscript submitted).

(b) Other Publications during the Period of Doctoral Research –

(i) Anirban Chaudhuri, Subarna Bhattacharyya (2019) Foldscopic visualization and identification of airborne fungi in museum and library environment. **International Journal of Emerging Technologies and Innovative Research** 6(6): 838-841.

(ii) Anirban Chaudhuri, Subarna Bhattacharyya, and Punarbasu Chaudhuri (2020) *In vitro* susceptibility testing of indoor fungi by Etest. **Asian Journal of Microbiology, Biotechnology & Environmental Sciences** 22(4): 642-647.

(iii) Chiradeep Basu, Subarna Bhattacharyya, **Anirban Chaudhuri,** Shaheen Akhtar, Akash Chatterjee, Biswajit Thakur, Himadri Guha, and Punarbasu Chaudhuri (2021) Assessment of

Potential Damage Factor: A Case Study of St. Paul's Cathedral, Kolkata. **Journal of Heritage Management (SAGE)** 6(1): 53-68. DOI: https://doi.org/10.1177/2455929621108678.

(iv) Subarna Bhattacharyya, Shaheen Akhtar, **Anirban Chaudhuri,** Shouvik Mahanty, Punarbasu Chaudhuri, and Mathummal Sudarshan (2022) Affirmative nanosilica mediated approach against fungal biodeterioration of concrete materials. **Case Studies in Construction Materials (Elsevier)** 17. DOI: https://doi.org/10.1016/j.cscm.2022.e01258.

(v) Eshita Jhahan, Subarna Bhattacharyya, **Anirban Chaudhuri**, Nirmal Sarkar, Shaheen Akhtar, and Punarbasu Chaudhuri (2022) Optimization and application of UVC irradiation for prevention of fungal biodeterioration of vegetable tanned and chrome tanned leather. **Journal of Leather Science and Engineering (Springer)** 4(1): 1-14. DOI: https://doi.org/10.1186/s42825-022-00104-4.

6. List of Patents: Nil

7. List of Presentations in National/International Conferences/Workshops:

(i) Poster presentation on a paper entitled **"Non-destructive restoration technique for conservation of building materials"** authored by **Anirban Chaudhuri,** Subarna Bhattacharyya in 107th Indian Science Congress (3rd January, 2020 to 7th January, 2020) held in University of Agricultural Sciences, Bangalore, India.

(ii) Oral presentation on a paper entitled **"Effect of gamma radiation on inhibition of fungal biodeterioration of concrete"** authored by **Anirban Chaudhuri,** Subarna Bhattacharyya, Anindita Chakraborty, Somnath Mukherjee in an International Conference on "Advances In Smart Materials, Chemical & Biochemical Engineering" (CHEMSMART-22) (16th December, 2022 to 18th December, 2022) held in NIT Rourkela, India.

Dedicated to

My Family

ACKNOWLEDGEMENTS

During my research work in Jadavpur University, I had the opportunity of coming in contact with many persons without whose help and cooperation I could not have completed my work. I would like to convey my sincere gratitude to all who in different ways extended their hands to complete this thesis.

My appreciation would go first and foremost to my PhD supervisors **Dr. Subarna Bhattacharyya**, Assistant Professor, School of Environmental Studies, Jadavpur University, **Dr. Somnath Mukherjee**, Professor, Department of Civil Engineering, Jadavpur University and **Dr. Anindita Chakraborty**, Scientist H, Radiation and Stress Biology, UGC DAE CSR, Kolkata Centre for their respected support and constant guidance during my doctoral research work. In addition to the primary task, they taught me about data management, the value of consistency, thinking styles, and the use of appropriate linguistics while writing research articles. Working under their supervision is a true honour and honour for me.

I want to convey my gratefulness to **Dr. Joydeep Mukherjee**, Professor and Director, School of Environmental Studies, Jadavpur University for giving me such a wonderful opportunity and facility to perform this work.

I would like to mention that this work would not have been possible without the support and encouragement from **Dr. Tarit Roychowdhury**, Associate Professor, School of Environmental Studies, Jadavpur University whose valuable suggestions helped me throughout the work.

I am indebted to **Dr. Reshmi Das**, Assistant Professor, School of Environmental Studies, Jadavpur University for her continuous advice and valuable inputs in my research work.

I would like to express my appreciation to **Dr. Mathummal Sudarshan**, Scientist F, UGC-DAE, CSR, Kolkata centre for helping me analyse my samples using Micro XRF facility at his institute.

I pay my deep sense of gratitude to **Dr. Punarbasu Chaudhuri**, Associate Professor, Department of Environmental Science, Ballygunge Science College, University of Calcutta for helping me analyse my samples using SEM facility at his institute.

I would like to acknowledge **Dr. Anupam Ghosh**, Associate Professor, Department of Geological Sciences, Jadavpur University for helping me analyse my samples using Stereo Microscope facility at his department.

I would like to thank **Dr. Chandan Kumar Ghosh,** Assistant Professor, School of Material Science and Nanotechnology, Jadavpur University, for helping me analyse my samples using FTIR facility at his department.

I would like to convey my gratitude to **Dr. Paramita Bhattacharjee**, Professor, Food technology & Bio-Chemical Engineering, Jadavpur University for helping me irradiated my samples using gamma chamber facility at her department.

I would also like to acknowledge the individual assistance of my lab seniors **Deeblina Di, Sanghamitra Di, Shayontani Di and Tanushree Di** (University of Calcutta). I would also like to thank my laboratory mates **Chiradeep, Riashree, Sangsaptak, Arup, Ankita, Shantanu, Saranya, Tanaya and Hamidul** for their valuable help and co-operation.

I like to pay my sincere thanks to all the **official staff** of School of Environmental Studies, Jadavpur University for their kind help. I would like to express my special gratitude to all the staff of the Jadavpur University research section for their help regarding the disbursement of my fellowship.

I would like to express my special gratitude and thanks to the lab in-charge/technicians **Samrat Sengupta**, **Baisnab Das**, **Prothyush Sengupta, Aparna Dutta and Jaganmoy Biswas** for giving me such attention and time.

I would also like to thank the **School of Environmental Studies, Jadavpur University** as a whole for inviting me into their world and providing me with an excellent work space, instruments and the necessary chemicals for this project.

I am indebted to the **UGC-DAE Consortium for Scientific Research, Kolkata Centre** and **Department of Biotechnology (DBT), Government of India** for endowing me the financial assistance during my research period.

Lastly and most importantly, I would like to pay my special regards to my family for their great support and love. This work would not have been possible without their inputs. I wholeheartedly acknowledge the contributions of **my father, my mother** and **my brother Abhijit** always encourage me to keep going.

STATEMENT OF ORIGINALITY

I, **Anirban Chaudhuri**, registered as a research scholar on **1st November, 2019** with **Registration number: D-7/ISLM/100/19** do hereby declare that this thesis entitled **"Inhibition of fungal biodeterioration of construction materials using low and high ionizing radiation"** contains literature survey and original research work done by the undersigned candidate as part of Doctoral Studies.

All information in this thesis have been obtained and presented in accordance with existing academic rules and ethical conduct. I declare that, as required by these rules and conduct, I have fully cited and referred all materials and results that are not original to this work.

I also declare that I have checked this thesis as per the "Policy on Anti Plagiarism, Jadavpur University, 2019", and the level of similarity as checked by iThenticate software is **12%**.

Signature of Candidate: Anirban Chaudhuri

Date: 18.12.2023

Certified by Supervisors:

(Signature with date and official seal)

18/12/2023

DR. S. N. MUKHERJEE
Professor
CIVIL ENGINEERING DEPT.
JADAVPUR UNIVERSITY
KOLKATA-700032, (W.B.)

Subarna Bhattacharyya 18.12.2023

Subarna Bhattacharyya, PhD
Assistant Professor
School of Environmental Studies
Jadavpur University
Kolkata 700032, INDIA

Anindita Chakraborty 18.12.2023

डॉ. अनिंदिता चक्रबोर्ती / Dr. Anindita Chakraborty
वैज्ञानिक-एच / Scientist-H
यूजीसी-डीएई कंसोर्टियम फॉर साइंटिफिक रिसर्च, कोलकाता केन्द्र
UGC-DAE Consortium for Scientific Research, Kolkata Centre,
ब्लाक-एल.बी.-८ बिधाननगर / Block-LB-8, Bidhannagar
कोलकाता (प.ब.)-७०००३६ / Kolkata (W.B.)-700106

DECLARATION

I hereby declare that this thesis represents my own work and has not been previously included in any thesis or any other institution for a degree, diploma or other academic qualifications. Further, I have acknowledged all sources used and have cited these in the reference section.

I hereby submit the record of my observations for evaluation for the award of the degree of Doctor of Philosophy in Engineering.

Date: 18.12.2023

Anirban Chaudhuri

(Anirban Chaudhuri)

Contents

LIST OF ABBREVIATIONS

%	Percentage
&	And
$	Dollar
^0C	Degree Celsius
ACGIH	American Conference of Governmental Industrial Hygienists
$Ca(OH)_2$	Calcium hydroxide
CFU	Colony Forming Unit
CSH	Calcium Silicate Hydrate
C	Column
cm	Centimeter
DNA	Deoxyribonucleic acid
EDXRF	Energy dispersive x-ray spectroscopy
FTIR	Fourier-transform infrared spectroscopy
ft	Foot
g	Gram
HPLC	High-performance liquid chromatography
H_3PO_4	Phosphoric acid
h	Hour
Kg	Kilogram
KGy	Kilogray
KH_2PO_4	Potassium dihydrogen phosphate
KV	Kilovolt

L	Litre
M	Mix
mA	Milliampere
min	Minute
ml	Millilitre
mm	Millimetre
mM	Millimolar
N	Newton
nm	Nanometre
psi	pounds per square inch
RP	Reverse Phase
Rs	Rupees
SBS	Sick Building Syndrome
s	Second
SEM	Scanning Electron Microscope
UV	Ultraviolet
µg	Microgram
µL	Microlitre
µW	Microwatt
WHO	World Health Organization

ABSTRACT

Fungal growth on concrete is a big challenge for building industries, real estate settlement in the modern world including India. The present study focuses on to prevent the invasive fungal damage in concrete using UVC and gamma radiation. To achieve this aim, fungi was isolated from three distinct locations of the fungal infected surface (4 cm^2 area) of the wall of 200 years old Tagore's house at Jorasanko, north of Kolkata, West Bengal, India by rubbing a sterilized cotton swab at a height of 2.5 m from the ground. Subsequently, the cotton swab was dipped in 1 mL of sterile Czapek Dox broth and then inoculated into the Czapek Dox Agar plates. For seven days, the plates were incubated at 27 °C and slides were prepared for each colony. After microscopic observation, the four fungal strains i.e. *Aspergillus niger, Aspergillus tamarii, Aspergillus flavus* and *Penicillium oxalicum* were identified. Thereafter concrete pieces were inoculated with pure cultures of fungi which were isolated from Tagore's house. The weight loss (%) of concrete piece, pH and color change of the fungal medium, oxalic acid production from HPLC (High Performance Liquid Chromatography) analysis, calcium leaching from micro EDXRF (Energy Dispersive X-ray Fluorescence Spectroscopy) study, SEM (Scanning Electron Microscope) images of fungal colonization on concrete surface after 30 days showed that *A. tamarii* imparted the maximum loss compared to other fungal species. A long term biodeterioration study (Marquez-Penaranda et al., 2016; Wiktor et al., 2009) of M40 and M20 graded concrete cube was subsequently performed with pure culture of *A. tamarii* to observe the changes in the concrete cube. After 180 days, the loss of weight and compressive strength of the infected concrete cubes (M40 and M20) compared to the control were 1.20 ± 0.01%, 2.22 ± 0.04%, 24.34 ± 0.16% and 25.17 ± 0.12% respectively. The fungal development and expansion of fungal hyphae into the interior of concrete cubes, which was deemed to be responsible for crack formation, which clearly visible in the stereo zoom microscope and SEM images. The micro EDXRF analysis further revealed that reduction in calcium mass for M40 and M20 graded concrete were 25.36 ± 0.05% and 15.68 ± 0.09% as well as absence of several spectral bands from FTIR (Fourier Transform Infrared Spectroscopy) study after 180 days which supported the *A. tamarii's* propensity for such deteriorating effect. Dose selection study was then performed for 30 days to find out the changes in properties in the *A. tamarii* infected concrete cube (M20) after exposure of UVC and gamma irradiation in radiation chamber. According to the concrete cube's physical, mechanical, and chemical properties, UVC (5 min) and gamma (0.5 KGy) radiation were required to prevent fungal biodeterioration without any deterioration of concrete cube caused by radiation. Radiosensitivity test (Choi and Lim 2016) was performed to select the most potent dose for complete inhibition of *A.tamarii*. The investigation

reflected that *A. tamarii* was resistant after 5 min UVC and 0.5 KGy gamma exposures in radiation chamber but 20 min UVC and 1 KGy gamma radiation were needed for complete depletion of fungal population. Long term inhibition study was performed with M20 grade concrete for 180 days to observe the efficacy of the selected doses of radiation. Negligible weight losses (0.28 ± 0.09% and 0.72 ± 0.08%) were observed in UVC and gamma exposed infected concrete cubes as well as compressive strength of the cubes were improved compared to only infected samples. Strong stretching bands and greater calcium content (%) were also observed via the FTIR and micro EDXRF study in irradiated as well as infected cubes (66.43 ± 0.06% and 54.11 ± 0.07%) than the only infected ones. The usage of selected ultraviolet and gamma radiation doses demonstrated the effectiveness of minimising these prominent visible and chemical modifications of concrete materials against the growth of *A. tamarii.*

CHAPTER – 1

INTRODUCTION

1.1 Concrete

Concrete is an useful widely accepted composite man-made construction material, mainly constituted with cement, water, sand (fine aggregate) and stone chips (coarse aggregate). By mixing water and cement, chemical reactions known as sol-gel hydration take place. These reactions through different stages bind the different matrices together (Nair et al., 2021). The name "concrete" comes from the Latin term *concretus*, meaning "to grow together" (Surahyo et al., 2019). The concrete freshly mixed before set is known as wet or green concrete whereas after setting and hardening it is known as hardened concrete and to be matured for taking necessary structural strength. Concrete is a cost effective, sustainable choice for different structures because of its strength, durability, versatility, reflectivity and long-lasting. It is easy to create and may be moulded into any shapes and sizes. Concrete is widely used building material in the construction of different structures such as dams, weirs, houses, foundations, fences, roads, bridges, retaining walls, chimneys, marine constructions, sewers, pipes, culverts etc are various examples of civil engineering applications. However deterioration of concrete is an adverse phenomenon of down-gradation of cementitious materials to a lower vulnerable quality that reduce the life of material. It is defined as the loss of structural capacity over time resulting from the action of external agents or the leaching imposes on the material (Sanchez-Silva et al., 2008). When this deterioration is brought about by biological factors, it is termed as biodeterioration, which is an undesired negative change in the properties of a material due to the dominant activities of kind of living organisms (Rose 1981; Hueck 1965; 1968). There is a difference between 'biodegradation' and 'biodeterioration' (Allsopp et al., 2004). When microorganisms modify materials with a positive or useful purpose it is referred to as 'biodegradation' and the negative impacts of a microbial activity is referred to as 'biodeterioration'. Though concrete is not biodegradable but can be deteriorated by the action of biological agents mainly by fungal attack.

1.2 Research focuses on fungal biodeterioration of concrete

In the context of the proposed study it may not be out of the place to mention the fact that fungi are chemoheterotrophic organisms that are common in subaerial and subsurface habitats. Autumn and summer are the prevailing seasons with the highest fungal levels in environment, while winter and spring have the lowest. Geographically, the Southwest, Far West, and Southeast have the highest levels of fungi. *Aspergillus* sp., *Penicillium* sp., *Cladosporium* sp., and nonsporulating fungi which are the most prevalent cultivable airborne

fungi inside throughout all seasons and regions (Di Giulio et al., 2010; Yassin et al., 2010; Reddy et al., 2017). They actively participate in decomposition, as pathogens and mutualistic symbionts of both animals and plants, and as creatures that ruin both natural and manufactured materials (Burford et al., 2003). Most of fungi present in indoors come from outdoor sources in normal houses and buildings (Nevalainen et al., 2015). Generally fungi enter a building through windows and doors, through outside air intakes of the ventilation, heating, and air conditioners, and contaminate building materials and other structural elements. Till date, fungi were thought to exist indoors primarily in the form of spores (in singly or groups). The earlier work carried out by some researchers demonstrated that indoor fungi grown in the culture medium or construction materials, subjected to an air current, able to release fungal fragments, as individual or group wise in form of spores. Moreover, sick building syndrome (SBS) (Sykes 1988) is a global phenomenon and a disease confirmed by the World Health Organization (Thach et al., 2019; Sarkhosh et al., 2021) predominantly by the active fungal ingress. Some of the deterioration effects on building surface are exhibited below (Fig. 1.1).

Fig. 1.1 Surface of concrete walls covered and affected by fungal biofilm **(Kurth et al., 2008)**.

Microorganisms (bacteria, cyanobacteria, fungi, algae, and lichens) play a significant role in the overall deterioration of construction materials, such as concrete, mortar, stone, slurries and paint coatings, glass and metals etc (Pinar and sterflinger 2009; Kurth et al., 2008). Fungi are amongst the most harmful organisms associated with the deterioration of inorganic and organic materials (Urzi et al., 2000). Now a day's mold growth in homes is one of the vital

problems in the house construction industry. In most of the buildings, the main reason of mold growth is seepage. The cement constructed walls of the buildings with internal seepage either due to rains or leakages in washroom or air conditioning system which supports indoor fungal growth. In suitable temperature and humidity for their growth, in form of fungal colony and degrade the properties of concrete, which are dependent on the availability of nutrients and carbon sources. Sometimes in various environments the fungal species are called as bio indicators of indoor air pollution (Cabral 2010). Concrete weathering, abrasion, deterioration, carbonation, corrosion, and chloride ion penetration are caused by physical, mechanical and chemical factors. This phenomenon shortens the concrete's lifespan and hiking the maintenance cost. Fungi release organic acids that react with free lime $Ca(OH)_2$ in the alkaline concrete to form highly soluble calcium salts. The pH in the pores of concrete drops when calcium salts are leached and the cement paste's binding agent's remains to be unstable. As a result, unstable material is easily removed by mechanical impacts and becomes fragile.

It is difficult and expensive to repair or replace deteriorated concrete structures. The annual loss worldwide from fungal attacks on archives, apparel and construction materials are over Rs 2.7 lakh crores (US$40 billion) as stated by Allsopp (2011). In Hamburg, Germany, one percent of the building's cost or Rs 2,28,000 crores ($25–$30 billion), is spent on maintenance annually to combat deteriorating effects to be imposed by biological, physical and chemical invasion (Sand and bock 1991).

In the present investigation, fungi affected historical buildings are taken into consideration and field observations are done. After thoroughly examination, lots of mold in wood, concrete, marble and painting surfaces are physically observed. To collect samples sterile cotton swabs were used to wipe the deteriorated building's walls. The samples were then immediately transferred to Czapek Dox Agar plates. After seven days of incubation the fungal species were identified in compound microscope. This study revealed that fungi present in this heritage building were *Aspergillus niger, Aspergillus tamarii, Aspergillus flavus and Penicillium oxalicum.* This finding motivated the researcher to carry out further research for exploring how the fungal species biologically deteriorates the physical, mechanical, chemical and aesthetic properties of concrete. In this matter, no such integrated study has been carried out in detail in the past to identify the fungi, loss determination and prevention by some important physical radiological phenomenon to eradicate the problem. The present research is addressed for the reduction of such gap.

Most taxa in the kingdom fungi are known for their filamentous growth habit and special ability to develop by extending their hyphal tips. Moreover, filamentous fungi have strong, flexible cell walls that allow them to penetrate into concrete materials to seek and acquire nutrient resources. Indeed, filamentous fungi can colonise and grow in concrete structures under favourable conditions of temperature and moisture, provided they have access to enough nutrients, energy, and organic carbon sources. This can have a detrimental effect on the concrete's physical, mechanical, chemical, and aesthetic properties (Tong 2018). Gene of fungus or phylum of fungi responsible for such corrosion and identification needed for that. Furthermore, necessary methods and assessment for remediation of fungal affected materials is the present scope of study.

To address this critical issue, a variety of techniques have been developed, including the use of fungicide in paints and the use of $Ca(OH)_2$, SiO_2, and ZnO nanoparticles during white wash (Sierra-Fernandez et al., 2017; Aldosari et al., 2019; Heaton et al., 1991). The use of UVC and gamma radiation to prevent microbial contamination of concrete materials has only recently been described in few research studies (Borderie et al., 2012; Kontani et al., 2014; Van Der Molen et al., 1980; Caneva et al., 2008). Radiation-related knowledge on the physical, mechanical, and chemical deterioration of concrete materials was thought to be scarce up till date. With this view point, the present studies has been undertaken to choose an acceptable UVC and gamma radiation exposure dose to prevent fungal biodeterioration of concrete with the least possible loss of the materials in its physical, mechanical, and chemical properties. On fungus inoculated on concrete, a growth environment extremely similar to that actually found on buildings, the effectiveness of the UVC and gamma exposure strategy to restrict the fungal biodeterioration for some time duration was also established.

1.3 Prevention of fungal biodeterioration of concrete

The preservation of a nation’s historic structures is the engineers and architects top priority. Ionizing and non-ionizing radiation have successfully been used in the recent past years to disinfect cultural heritage structures with the assistance of libraries and museum authorities (Fuentes et al., 2022; Bertrand et al., 2023). Additionally, a lot of materials can be irradiated at once. It thus became possible to sterilise, decontaminate, and disinfest foods, cosmetics, pharmaceuticals and medical supplies in addition to doing irradiations for study (Katusin-Razem et al., 2003). This technology does not harm the environment or leave any residue

behind. Therefore, there is no risk to the environment or to conservators/restorers, museum curators and registrars, or operators of irradiation facilities.

According to a recent study, various items may respond differently after exposure to radiation. It is dependent on the radiation dose and the substance (Badarloo et al., 2022; Olarinoye et al. 2023). In addition to eliminating mould, a high radiation exposure also causes the substrate to degrade substantially. With a wavelength of 10 nm to 400 nm, ultraviolet radiation has an electromagnetic spectrum that is shorter than visible light but longer than X-rays. UV radiation is splitted into three groups based on wavelengths: UVA (315–400 nm), UVB (280–315 nm), and UVC (100-280 nm). UVC is the only ray that the ozone layer totally filters off, unlike UVA and UVB. UVC is the portion of the solar spectrum that is particularly destructive to bacteria, fungi, and algae because it contains extremely energy containing photons. In contrast to conventional disinfection methods, gamma rays are electromagnetic waves with tremendous penetrating power that can flow through materials without leaving any toxic trace (Maity et al., 2005; Da Silva et al., 2006). Through ionization, this sterilising procedure directly harms cell DNA, causes mutations, and finally destroys the cell. It also encourages the production of reactive oxygen species (ROS), free radicals, and peroxides through the radiolysis of cellular water, which breaks single and double strands of DNA (McNamara et al., 2003).

The outcome of the present investigation will be helpful for knowledge base research findings of deterioration of concrete materials due to fungal attack in indoor environment and to examine the physical, chemical, mechanical and aesthetic properties. These findings also support for standardization of some non-destructive method such as application of ultraviolet and gamma radiation for reduction of such fungal deterioration. Also, the degradation mechanism of concrete against radiation are investigated and results of gamma ray irradiation tests on cement paste samples also presented to provide a better understanding of the interaction between radiation and concrete.

It is addressed at both the ionizing radiation community (engineers, scientists and technicians working in various field such as environmental technology, radiation technology, radiation chemistry and radiation biology) as well as the conservation community (registrars, curators, conservators, conservation scientists, archaeologists) active in the different fields of cultural heritage (museums, libraries, archive, historical buildings).

1.4 Organization of thesis

This dissertation contains following chapters organized to translate the entire research work under present investigation.

Chapter 1 mainly covers introduction, genesis of the problem statement and brief objective of the work as **introduction**.

Chapter 2 **review of literature** mainly focuses on the brief review of literature of the present research work.

Chapter 3 stated **objective and scope of work**.

Chapter 4 introduces the **methodology** of this dissertation in detail.

Chapter 5 is the **result and discussion** of the present research work.

Chapter 6 stated a **conclusion** of this dissertation as well as recommendation on **scopes of future work**.

Chapter 7 all the research work referred in this dissertation has been listed in the **reference** section.

Chapter 8 contains the **publications and conference proceedings** related to the present research work.

CHAPTER – 2

LITERATURE REVIEW

2.1 Micro-fungi in indoor environment

Majority of time is spending in indoor environments such as houses, schools, colleges, offices for which the quality of indoor air becomes very important. The presence of few numbers of airborne microorganisms in such places a normal, but an increase of their concentration level could be a sign of disease risk factor. When fungi were present in an indoor environment, they were typically very prevalent and difficult to prevent. In an interior environment, microorganisms were usually not spread uniformly. The first stage in identifying the causes and effects of building-related deterioration is the detection and species identification of all fungi present in indoor environments.

A study conducted by Mui et al., (2007) in the air-conditioned offices in Hong Kong, which were comparable to several other Asian cities, *Aspergillus* sp., *Cladosporium* sp. and *Penicillium* sp. were found to be the most prevalent fungal species. This can be explained by the climate of the city, where the daily mean relative humidity ranges from 30 to 97% and the daily maximum and minimum air temperatures are 35 °C and 60 °C, respectively.

A further study conducted by Yassin et al., (2010) revealed that seven genera of fungi, mainly *Aspergillus* species, were isolated from the science laboratory and classrooms of Kuwait University. In the investigation, *Aspergillus niger* and *Penicillium* sp. fungal spores were found.

Similar type of research work was also performed within the passengers (platform, station precinct and passenger carriage) and workers (bedroom, station office and ticket office) activity areas of the Seoul metropolitan subway (Kim et al., 2011). The station precinct and employees' bedroom had some of the highest amounts of airborne fungi among the places that were tested. The genera identified in all activity areas of the subway were *Penicillium* sp., *Cladosporium* sp. and *Aspergillus* sp.

Indoor air of a hospital may affect not only the patient’s health, but it can also have an impact on hospital staff members' interactions with patients. In order to ascertain the abundance and variety of airborne micro-fungi in both indoor and outdoor environments, a further investigation was carried out at the government hospital in Turkey (Okten et al., 2012). According to the findings, there were 2469 bacterial colonies and 1376 micro fungal colonies in the hospital environment. *Cladosporium* sp. had the highest percentage of colonies among

these (33.58%). There were also a few more species discovered, including *Aspergillus* sp., *Penicillium* sp. and *Alternaria* sp.

A study by Naji et al., (2014) showed that *Aspergillus* was the most prevalent genus (48.9%) as discovered in National Museum, Yemen. *A. niger* (25.53%) and *A. flavus* (10.63%) were the two most prevalent species, while *A. fumigatus*, *A. candidus* and *A. ustus* were isolated in low frequency. *Penicillium* and *Cladosporium* were isolated in considerable amounts (14.89 and 12.76%) respectively.

Deterioration factors like viable spore load, species diversity and species dominance in three seasons in the museum in Kolkata, India had been reported by Bhattacharyya et al., (2016). Monsoon season found to be the highest concentration of spores in the museum's living room, while winter season had the lowest concentration in the library. *Paecilomyces* sp. (50.8%) had the highest spore percentage, followed by *Aspergillus* sp. and *Penicillium* sp. However, the eleven dominant fungal species were not evenly dispersed in the indoor environment of the study area throughout the year and significant variations were observed in between different rooms.

A different study was performed in indoor and outdoor air of twelve kindergartens in Rasht, Iran (Chegini et al., 2020). The predominant genera of the airborne fungi in kindergartens were *Aspergillus flavus*, *Aspergillus terreus*, *Penicillium* sp., *Cladosporium* sp., *Alternaria* sp., *Ulocladium* sp. and *Rhodotorula* sp. Staszowska (2023) investigated the prevalence of airborne fungi in the library of the Lublin University of Technology, Poland. The study revealed the presence of most common airborne fungi such as *Aspergillus* sp., *Penicillium* sp. and *Cladosporium* sp.

2.2 Biodeterioration of concrete structures

In this section, comprehensive reviews of literatures highlighting the fungal influences on concrete structures were presented. After construction, concrete is typically resistant to biological attack because of its high alkalinity (Sand 1987). Biodeterioration can be broadly classified into three main categories: (a) biophysical (b) biochemical and (c) aesthetic, depending on the biodeteriogens, the type of the material, and environmental conditions (Gaylarde et al., 2003). In many regions of the world, the environmental deterioration of concrete infrastructure is a major, widespread, and expensive issue. Following are some of

the research studies which have been carried out to evaluate the deterioration of concrete by microorganisms.

Perfettini et al., (1991) discovered that the overall porosity of cement samples (discs with thickness 4 mm and diameter 70 mm) increased to 31% after 11 months of exposure to *A. niger* in comparison to the uninoculated control, which had a porosity similar to about 20%. *A. niger's* production of oxalic acid and the creation of insoluble calcium oxalate perhaps be responsible for the similar amount of Ca that leached under both the circumstances.

Melanin and other extracellular polymerization products from fungi are the main causes for the pigmentation (Krumbein et al., 1992). Wollenzien et al., (1995) isolated the filamentous and micro colonial fungi which majorly came from the stone monuments in the Mediterranean region. Melanin production is a characteristic of the majority of strains. In dry, humid and warmth environments, melanin synthesis was thought to be essential for the survival of micro colonial fungi on rock. Roughness on the concrete surface is typically caused by the erosive action of water or the friction of structural parts with other materials (Ribas-Silva 1995).

Research work was performed to evaluate the biodeterioration of concrete by fungus, and to measure calcium release and weight loss of the concrete specimens (Gu et al., 1998). Studies showed that the presence of *Fusarium* sp. promotes concrete deterioration. This study tracked the weight variations of concrete samples that were exposed to fungus for up to 120 days. Once the precipitates were gently brushed off by a brush, a concrete sample exposed to *Fusarium* sp. showed up to 6% weight loss. However, during the incubation phase, inoculation with *Fusarium* sp. considerably improved the process of calcium release from concrete. On the outside of the test samples, released calcium may have formed soluble precipitates with organic acids generated by fungus. Moreover, SEM micrographs (Fig. 2.1) revealed that fungus were capable of etching concrete and extending the fungal hyphae into the concrete's core, expanding the damaged area and increasing porosity (Gu et al., 1998; Gaylarde et al., 2003).

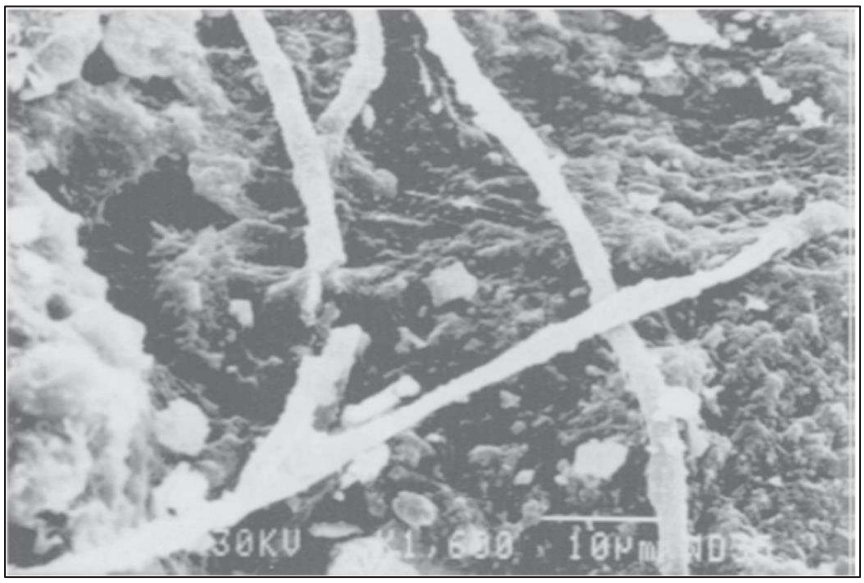

Fig. 2.1 Fungus hyphae observed on the deteriorated surface of a concrete bridge pier submerged in a contaminated river **(Gaylarde et al., 2003)**.

Mehta (1999) explored whether the calcium salts that are produced when calcium hydroxide reacts with oxalic, tartaric, tannic, humic, hydrofluoric or phosphoric acid fall under the category of insoluble, non-expansive calcium salts. In the alkaline concrete (pH around 13), lactic and acetic acid react with free lime $Ca(OH)_2$ to form highly soluble calcium ions. If the salts are leached, the pH in the pores of the concrete drops, which makes the cement paste's binding agents unstable and then easily eliminated by mechanical impacts from washing or animals. In another study, Sanchez-Silva et al., (2008) found that microorganisms affect the concrete mainly by eroding the exposed concrete surface, decreasing the protective cover depth and increasing porosity that accelerate cracking and other problems.

A three-month investigation on the bio-deteriorative effects of several fungal strains on a cementitious matrix was developed by Wiktor et al., (2009). The main impact of the results was aesthetical biodeterioration. Findings indicated that fungal growth had been taking place under these experimental circumstances since the first week of incubation. In particular, hyphae were seen inside the matrix of samples injected with *Alternaria alternata* and *Coniosporium uncinatum*, penetrating via the cracks caused by the accelerated weathering of the matrix. These measurements allowed us to estimate the depth of microbial colonisation at 130 μm. While periodic acid schiff (PAS) staining revealed that the true extent of microbial growth on and within the matrix, as the later confirmed by SEM observations of cross section

showing the penetration of hyphae inside the matrix, stereomicroscopy observations revealed that microbial growth was only noticed on the surface of specimens.

The effect of the activity of sulfur oxidizing bacteria (SOB) on concrete structures has been linked mainly to weight loss and compressive strength (Marquez-Penaranda et al., 2016). Here, samples of cement mortar exposed to an environment high in H_2S were inoculated with pure cultures of *Acidithiobacillus thiooxidans* and *Halothiobacillus neapolitanus*. Over the course of 300 days, physical property changes were measured. After 300 days, weight loss in the samples inoculated with *Acidithiobacillus thiooxidans* and *Halothiobacillus neapolitanus* was 4.6 and 2.4%, respectively. Samples inoculated with the consortium lost more than half (52%) of their initial strength, whereas control samples did not exhibit any significant strength differences. Algae present in mixing water or on the surface of the aggregate either reduces bond by combining with the cement or decreases the strength of the concrete by entraining a lot of air (Duggal 2017).

Yakovleva et al., (2018) inoculated concrete beams (160 × 40 × 40 mm) with *Penicillium brevicompactum*, submerged the lower half in a culture medium, and exposed the upper surfaces to a humid environment. After a short incubation period of 28 days, surfaces that were both immersed and exposed exhibited signs of fungal degradation. Yet, in this instance, compared to the uninoculated control, Ca leaching of immersed and exposed concrete inoculated with fungus increased by roughly 41 and 32%, respectively. No significant changes in the percentage of other trace elements were detected (Fig. 2.2). The flexural and compressive strengths of infected concrete were also decreased, compared to the control samples. It was interesting to note that concrete samples with greater initial strengths were less likely to experience strength loss as a result of fungus infection. As a result, *A. niger* lowered the flexural and compressive strengths of concrete with an initial compressive strength of 400 kg/cm^2 by 0.46 and 1.5% respectively and for concrete of higher initial compressive strength equivalent to 1000 kg/cm^2 they were reduced to a smaller extent by 0.21 and 0.41% respectively.

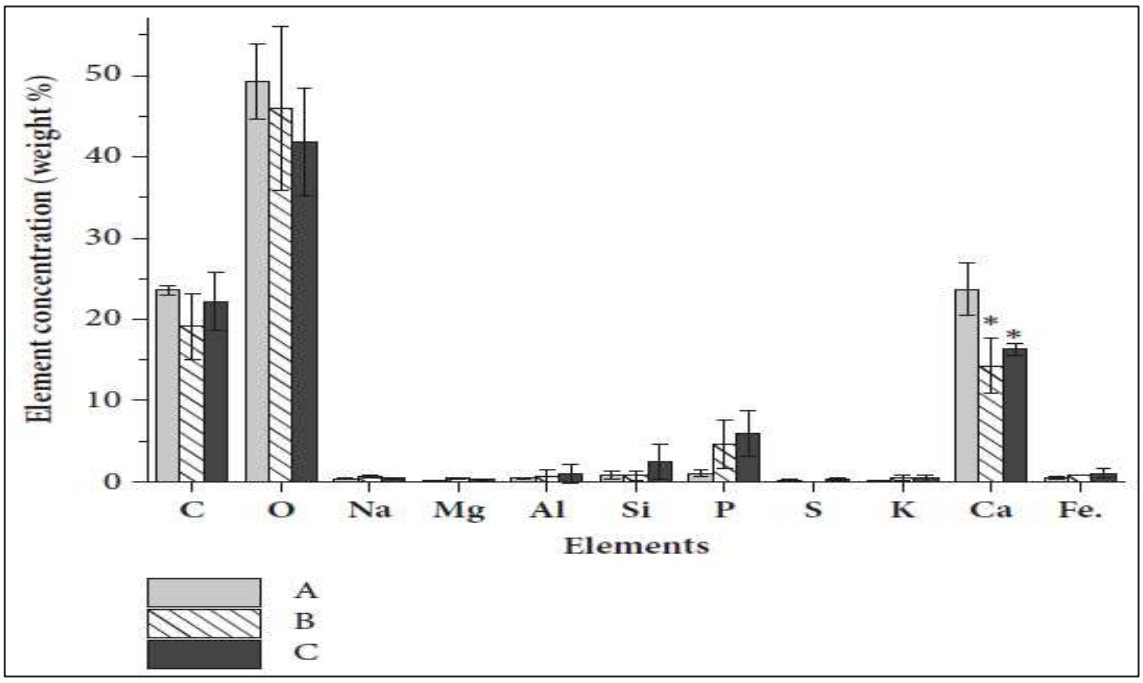

Fig. 2.2 Composition of components in concrete surface layer A) without treatment; B) surface totally submerged in *P. brevicompactum* culture medium for 28 days; C) concrete surface in contact with air in container for 28 days **(Yakovleva et al., 2018)**.

Organic acids were metabolic waste products released by fungi to change (acidify) and improve the growing circumstances of their immediate external environment. These acids react with calcium and play a significant role in the chemical biodeterioration of concrete. The main filamentous fungus and often released organic acids implicated with concrete fungal influenced degradation (FID) are listed in Table 1. Environmental factors had an impact on the types and amounts of organic acids released, which had significant repercussions for the development of FID (Magnuson and Lasure 2004). The reaction between organic acids released by fungi and the Ca^{2+} ions in concrete that resulted in the formation of soluble Ca salts that cause Ca leaching and insoluble Ca salts that cause expansion attack is what drives the degradation mechanism (De Windt and Devillers 2010). Citric acid was shown to be the most aggressive acid and oxalic acid to be the least aggressive acid for cementitious materials, according to Bertron (2014).

Table 1 Organic acids released by *Aspergillus* sp. that are involved in FID.

Fungal taxa	Organic acids	Reference
***Aspergillus* sp.**	Oxalic	Dutton and Evans (1996)
	Oxalic, acetic, formic, fumaric, gluconic, glyoxylic and itaconic	Sterflinger (2000)
	Succinic	Vazquez et al., (2000)
	Oxalic, citric, acetic, fumaric, pyruvic, gluconic, lactic, formic, propionic and butyric	Jestin et al., (2004)
	Oxalic, citric, succinic, gluconic	Rashid et al., (2004)
	Oxalic, citric, succinic, gluconic	Fomina et al., (2007)
	Oxalic, gluconic	Chuang et al., (2007)
	Oxalic, acetic, lactic, citric, malic, ascorbic, butyric, fumaric, formic, gluconic, itaconic, isobutyric, propionic, succinic and tartaric	Liaud et al., (2014)
	Oxalic, acetic, lactic, citric, malic, tartaric	Yakovleva et al., (2018)
	Oxalic, acetic, lactic, citric, malic, fumaric, succinic	Nonthijun et al., (2023)

Hydrolytic enzymes, such as proteases and lipases, were discovered to be secreted by *Aspergillus* strains isolated from old concrete buildings as reported by Ilinskaya et al., (2018). A secreted enzyme known as keratinase as characterized with filamentous fungi including *Aspergillus*, *Fusarium* and *Trichoderma*, reacts with amino acids to form thin ettringite needles that cause cracks in concrete (Cody et al., 2001; Kumar and Kushwaha 2014). Ettringite formation in fresh concrete plays a very promising role by decreasing the setting time and enhancing the early strength of the concrete matrix due to hydrous in nature. Nevertheless, ettringite creation in hardened concrete as shown in Fig. 2.3 might result in the development of cracks, indicating that this formation was one of the mechanisms causing fungal influenced degradation (FID) of concrete (Hanehara and Oyamada 2010). These mechanisms would permit the infiltration of water, nutrients, and organic matter as well as additional infiltration of acids and enzymes, that establish a favourable environment within the concrete matrix for promoting fungal colonisation and growth. Internal pressure might potentially cause fragmentation and disintegration as fungal hyphae penetrate in deeper region into the concrete matrix. This could result in wider crack formation, increased surface exposure and ultimately more fragile degradation (Ilinskaya et al., 2018; Sterflinger 2000). The impact of microorganisms on concrete structures can be categorised according to how they affect concrete surfaces, concrete matrices, cracking and crack progression as seen by Scanning Electron microscope (Amann et al., 1990).

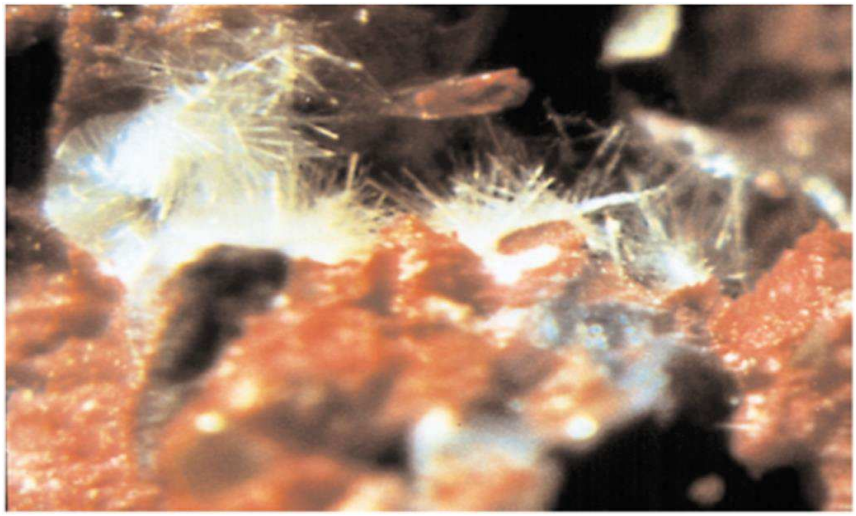

Fig. 2.3 Formation of ettringite in hardened concrete structures **(Portland cement association, 2001)**.

A possible framework (Fig. 2.4) of the chemical and physical mechanisms involved in the fungal influenced degradation of concrete as descried by Ilinskaya et al., (2018). At first fungi formed a biofilm on concrete which was followed by the excretion of organic acids by the fungi. The organic acids reacted with calcium within concrete and formed soluble calcium salts resulting in leaching of calcium as well as insoluble calcium salts causing expansion attack. Fungi could secrete enzymes in addition to organic acids, combined with amino acids also secreted by fungus to form thin ettringite needles. Therefore calcium leaching, expansion attack and volume increased porosity and cracks were formed. Salts and water percolated through these cracks which initiated corrosion. As a result, the number of spore increased and surface growing hyphae penetrated into the concrete materials and caused further degradation.

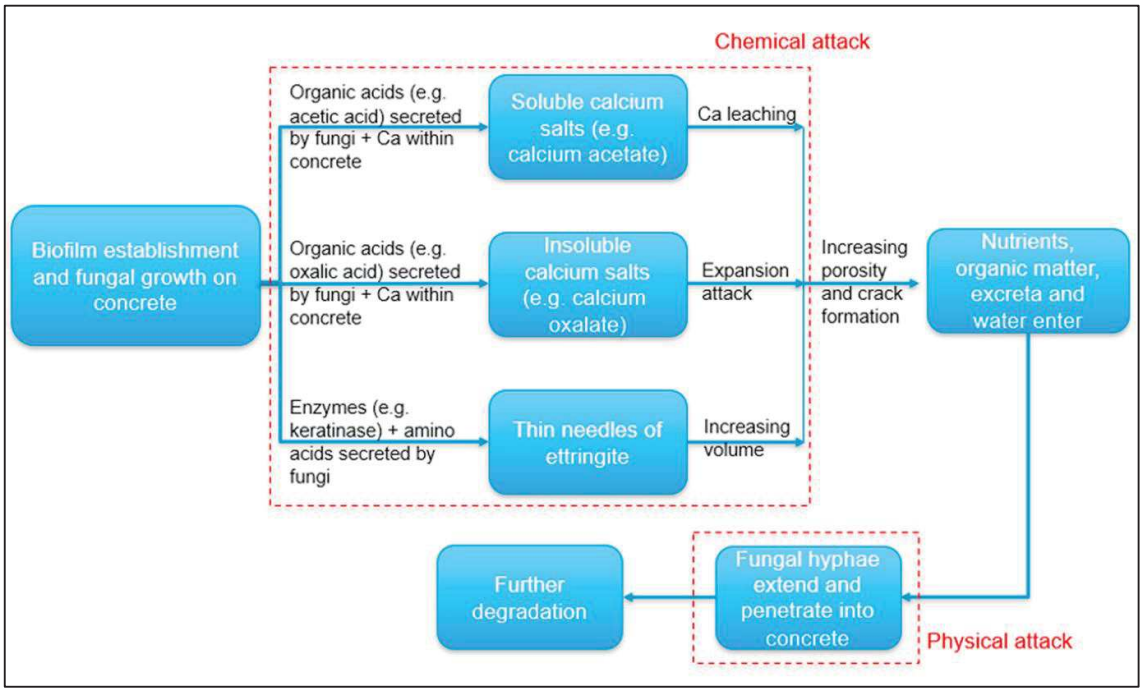

Fig. 2.4 Hypothetical framework of the chemical and physical mechanisms involved in FID of concrete **(Ilinskaya et al., 2018)**.

2.3 Overview of methods to control the biodeterioration of concrete

2.3.1 Biological Methods

2.3.1.1 Biocidal treatments with compounds of natural origin

Both organic and inorganic materials may be treated with natural biocides, which were seen as being safer for people and more environmentally friendly. Several of these products were

extracted from plants and can be used as essential oils, crude extracts, or in their pure form. According to Tayel et al., (2016), plant burning fumes can be used as a powerful substitute to chemical fungicides because they totally sterilise the fumigated archive while leaving no changes to the colour or surface structure of the specimens. Also, since fumes were removed after treatment, residues did not remain in the treated materials and fumes did not promote the growth of additional microorganisms.

Volatile extracts obtained from *Illicium verum*, the flower buds of *Coptis chinensis*, *Quercus infectoria*, *Phellodendron amurense* and *Syzygium armoaticum* were successfully tested with isolated fungal biofilm on the stone monuments in South Korea (Jeong et al., 2018). Eugenol, which was separated from clove extract, demonstrated the strongest antifungal properties. The stable emulsifiers Tween and Span were combined with the volatile organic molecule. In order to prevent the formation of bacterial biofilm, Bogdan et al., (2018) studied in vitro the antibacterial activity of weed extracts and their integration into waterborne paints. The extracts were collected from *Dipsacus fullonum, Rapistrum rugosum*, *Raphanus sativus*, *Nicotiana longiflora,* and *Sinapis arvensis* weeds, being vegetables extensively used in traditional medicine as antibacterial substances. Results of this investigation have showed that the *Nicotiana longiflora* based paint was effective in preventing the growth of biofilms caused by *Staphylococcus aureus* and *Escherichia coli*.

To remove biofilm from a travertine wall at the Sapienza University in Rome, essential oils obtained from *Origanum vulgare*, *Thymus vulgaris*, and *Calamintha nepeta* and their primary components (carvacol, thymol, and pulegone) were prepared within a hydrogel matrix composed of Calcium chloride, Gelrite, polyvinyl acetate, and Acemoll CC (Genova et al., 2020). Strong antimicrobial activity was showed by *Thymus vulgaris* and *Origanum vulgare* essential oils in in vitro assays, and this activity was subsequently confirmed in situ applications on biofilm recovered from beneath the floor mosaic tesserae in the Greco-Roman archaeological site of Solunto, Sicily (Italy) (Casiglia et al., 2020). According to a separate study, biofilm growth was significantly impacted by the antibacterial activity of a 15% solution of *T. vulgaris* essential oil. The two main chemotypes found were carvacrol and thymol. Recently, the volatile components of the same essential oils, *T. vulgari and O. vulgare*, were utilised to stop the fungus *Aspergillus flavus* from causing biodeterioration processes (Palla et al., 2020).

2.3.2 Chemical Methods

2.3.2.1 Traditional chemical biocides

Biocides were used to curb the outbreak, but they largely failed over time (Gu 2003). However partly found effective, but the use of biocide had some unfavourable consequences, particularly in terms of ecotoxicology. Martin-Sanchez et al., (2012) carried out a separate research to addressing the community of fungi, distinguished by black stains, in the Lascaux Cave, France where a *Fusarium solani* outbreak took place. Two samples of the black stains were taken before and after the biocidal treatment, respectively, to test the antifungal efficacy of the substance. The "Devor Mousse" biocide that was employed was mostly made of compounds such quaternary ammonium, 2-octyl-2H-isothiazol-3-one, benzalkonium chloride, and Parmetol. A new breakout of black spots appeared after applying biocide for an exposure time of four months, and they gradually started to fill the cave. According to Nugari and Salvadori (2017), ethylene oxide, which has been banned in many nations due to its carcinogenic and mutagenic properties, was the only gas for fumigation (the use of poisonous gases in airtight boxes) that was effective against insects and fungus.

It is frequently necessary to conduct in situ pilot tests to calibrate biocidal treatments on the specific study scenario (species, site) if a biocide strategy is intended to reduce microbial development on a heritage surface. Favero-Longo et al., (2017) investigated of five biocides (BiotinT, BiotinR, DesNovo, Preventol RI80 and Lichenicida 464) against lichens which revealed that various biocidal agents and application techniques showed wide variation on efficacies against every species examined. Also, the effectiveness of a biocidal treatment against a particular species of lichens varies amongst different heritage sites. Des 50 and BiotinT, two other commercial biocides that were more efficient against gram positive bacteria than gram negative, were applied to non-pathogenic bacteria (Dresler et al., 2017).

Recent studies have looked upon the effectiveness, durability, and environmental advantages of organic biocide agents. Two commercial biocides, Preventol RI80 (didecyldimethylammonium chloride, 2-octyl-2H-isothiazole), and Biotine T (2-octyl-2H-isothiazole and Quaternary Ammonium Salts) were used against lichen thalli to test the physiological recovery of the thalli. After the application of biocides, a significant physiological change was noted. It was discovered that Preventol R180 was more efficient and altered quickly the physiological processes (Vannini et al., 2018). An investigation through laboratory research and field testing, Jeong et al., (2018) found that the antifungal

capability of the compound Eugenol derived from natural medicinal clove was stronger. It was found to be significantly reduced the microbial activity and shown excellent anti-fungal efficacy. Fungicides made from vegetable essential oils show promising and are safe for the environment.

Dimethyl sulfoxide (DMSO) in a solvent gel has been utilised as the active ingredient to remove microbial colonisation on stone as an alternative to conventional biocides and contrasted to biocides currently used in heritage conservation (Toreno et al., 2018). DMSO solvent gel was shown to be effective at cleaning stone and was seen as a feasible alternative to commercial biocides because it was affordable, easy to use, and did not interfere with pigments. The Auschwitz-Birkenau State Museum in Oswiecim, Poland, disinfects new and historical objects with vaporised hydrogen peroxide, which has comparable effects to ethylene oxide, according to more recent study (Anna et al., 2020).

2.3.2.2 Nanoparticles

Gutarowska et al., (2012) investigated a case study in Poland for exploring efficacies of nanoparticles on eradication of fungal ingress on masonry concrete structures. They found *Aspergillus* sp., *Aureobasidium* sp., *Alternaria* sp., *Penicillium* sp., *Cladosporium* sp., *Chrysonila* sp., *Paeciliomyces* sp., *Trichoderma* sp., *Rhizopus* sp., *Mucor* sp., and *Botrytis* sp. were the most prevalent fungi discovered in six museums in this country and archives in Poland. They showed that the microorganisms on the surface of the documentary heritage works could be effectively removed by a concentration of 10-100 nm nanosilver particles at 90 ppm.

The introduction of metal oxide nanoparticles as additives quickens chemical processes during initial hydration, strengthening cement composites. The amount of calcium silicate hydrate (C-S-H) in the concrete increases as a result of the reaction between the metal oxide nanoparticles such as TiO_2, Al_2O_3, Fe_2O_3, SiO_2 and the $Ca(OH)_2$ contained in the concrete. This phenomenon imparted more compaction, lowering the permeability, and improves the mechanical properties of the material (Hanus and Harris 2013).

In vitro tests conducted by Van der Werf et al., (2015) revealed that the bioactive characteristics of Estel1100/ZnO nanocomposite material against the mould *Aspergillus niger* be favourable. The findings of this investigation showed that zinc oxide nanoparticles (ZnO NPs) can be used in matrices at a tenfold higher concentration than silver nanoparticles (Ag

NPs) without changing the substrate colour and exerting long-lasting bactericidal activity on the substrates. CuO/SiO_2 nanocomposites were developed by Zarzuela et al., (2017) using the sol-gel method used as multifunctional protective coatings for historical structures. They investigated a reference laboratory yeast and bacterium on slabs under laboratory condition and they established that the most plausible mechanism for the biocidal impact is the release of Cu^{2+} ions.

Nanoparticle has been found to be an extremely powerful additive for modifying the cementing products, even at very low concentrations (Reches 2018). The main modifications was accomplished with an exposure a 1-2-hour reduction in setting time, a 4 to 75% increase in diffusivity, a 5 to 25% increase in strength, and a 0–30% increase in residual strength for thermal durability. Due to their small size and huge surface area, nanoparticles have a special reactivity. As biocides for masonry materials, two nanocomposites based on titanium dioxide and silver nanoparticles had been employed successfully (Becerra et al., 2019).

A separate study as carried out by Bhattacharyya et al., (2022) showed that fungal species such as *Aspergillus tamarii* weakens the physical, chemical and mechanical properties of concrete hence deteriorate, but the use of silicon oxide nanocoatings can successfully stop the fungus growth as well as prevent deterioration. The apparent aesthetic modifications apparently take place due to the contamination by fungus through the colour change of cube surface although the nanocoated concrete cubes showed a slighter alteration compared to the biodeteriorated cubes. The stereo graphs showed that the fungus-infected concrete surface was more exposed than the nanocoated ones. Due to rapid carbonation and calcium ion leaking into the media, biodegraded cubes of higher alkalinity than nanocoated ones and capable of changing the chemical composition were seen by SEM images (calcite crystal formation). Furthermore, the FTIR and EDXRF analyses validated the chemical alterations for which in the larger context influence the concrete's weight and compressive strength.

2.3.3 Physical Methods

2.3.3.1 UVC irradiation

Van Der Molen et al., (1980) did a pioneer work on the use of UV irradiation to prevent biofouling of heritage structural materials. To treat some of the portions of the walls invaded by microorganisms at St. Stephanus Church, Pilsum, Germany the authors created a Mobile Ultra Violet Unit (MUVU). They indicated that UV treatments were effective in eliminating microorganisms, but any details regarding the type, power, or time of UV exposure has been

not mentioned. A separate study as carried out by Ishida et al., (1991), showed that UVC light (254 μW/cm²) killed most *Candida* organisms within 5 min. Certain fungi can grow after phototrophic cells die on the excreted organic matter because they are resistant to UVC because of pigments like melanin. This was found to be disadvantage that needs to be considered while using this practise.

When exposed to UV light, species that can thrive in both aquatic and terrestrial settings, like cyanobacteria, have developed survival mechanisms. The aquatic *Tolypothrix* UU 2434 was destroyed after exposure to UVC for half an hour, in contrast to the terrestrial *Tolypothrix*, *T. byssoitka*, which was isolated from the stone surface of the Sun Temple in Konark, India (Adhikary and Sahu 1998). It was found that exposure to UVC light for 45 min was enough for inactivation of fungi (Ozcelik 2007).

According to Caneva et al., (2008), UVC irradiation could be utilised to eliminate microorganisms contaminating heritage materials. They also reported that only UVC irradiation is not the unique method for preventing the spreading of microorganisms on structural materials such as paper, wood, concrete, etc. in addition to harmful effect on the material properties.

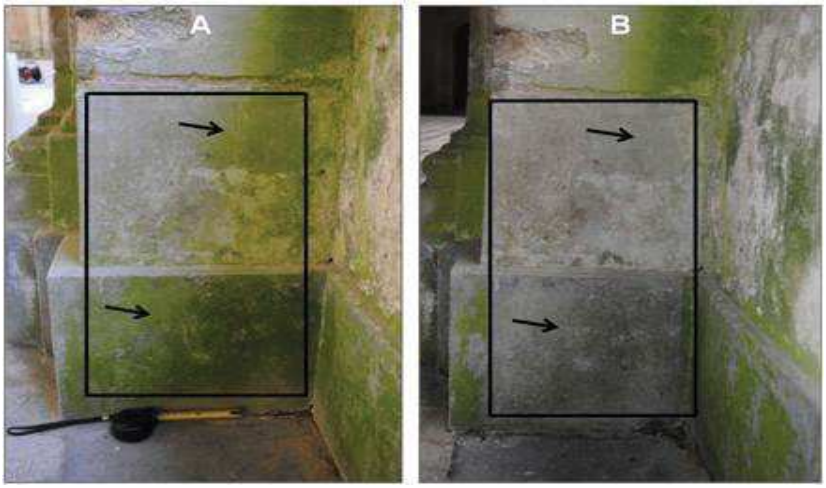

Fig. 2.5 UVC treatment on a green algae contaminated wall **(Borderie et al., 2012)**.

Research laboratory for historical monuments tested the effects of UVC treatment on a green algae-infested wall (Borderie et al., 2012). The study was conducted in the Department of Aisne, France. A 16 hour UVC exposure treatment with 30W was applied during the night. Fig. 2.5 shows observations from this initial test. Before the treatment, the algal biofilm

covered a significant portion of the wall in the first image [2.5(A)]. The algal biofilm was greatly affected by the 16 hour UVC treatment [2.5(B)], confirming by shown a total discoloration and entirely disappearing.

Cyanobacteria, which kill through photosynthesis and eukaryotic algae, were both harmful by prolonged exposure to UVC radiation (PS II is extremely susceptible due to their protein absorption) (Borderie et al., 2015). In addition, Pfendler et al., (2018) asserted in situ UVC treatment was more effective, quicker, less expensive, and ecologically friendly than chemical treatment. However, several radiation treatments were necessary to treat biofilms due to the layers of cells arranged upon each other and the low penetration of UV light.

2.3.3.2 Gamma irradiation

According to Hassanein (1987), *Aspergillus flavus* grew more rapidly at lower gamma radiation doses, and was completely inhibited at 3000 Gy. Irradiation at 0.5 KGy gamma dose completely eliminated degradation by *Alternaria alternata* (Barkai-Golan et al., 1993). Also 750 Gy was the critical dose for inhibiting the degraded fungi. However, radiation resistance in filamentous fungi varies greatly, ranging from being highly radiation resistant to being extremely radiation susceptible (Mironenko et al., 2000). A further study were carried out by da Silva et al., (2006) to determine the gamma radiation dose at which fungi may be rendered inactive. Representatives of *Acremonium*, *Aspergillus*, *Cladosporium*, *Fusarium*, *Penicillium* and *Trichosporon* were among the fungi that were isolated, identified, and treated in a Co^{60} irradiation unit with doses ranging from 14.5 to 25 KGy. The fungi needed to be killed by a minimum dose of 16 KGy.

Unlike UV radiation, gamma radiation can profoundly penetrate objects; as a result, the applied inhibitory dose will be felt throughout the entire object (Ponta 2008). According to Geba et al., (2014), raising the irradiation dose above 10 KGy had a significant impact on the tested specimens' mechanical resistance and loss of elasticity.

From an archaeological painted coffin, Geweely et al., (2014) isolated *Alternaria alternata*, *Aspergillus niger*, *Aspergillus ochraceous*, *Cladosporium herbarum*, *Curvularia eragrostidis*, *Fusarium moniliforme* and *Penicillium expansum*. Experiments were then carried out to determine the effectiveness of gamma sterilisation on the fungal degradation of the painted coffin. XRD, EDX with SEM, and FTIR were applied for analysis and the inquiry. The

growth parameter rapidly dropped to approach the lethal dose at 2000 Gy when the gamma radiation exposure grew over 250 Gy.

A wooden cashbox that was a Korean cultural artifact and was kept at a local museum was subjected to gamma radiation for decontamination (Choi and Lim 2014). The isolated strains were *Aspergillus niger*, *Penicillium verruculosum* and *Trichoderma viride*. Each strain's susceptibility to gamma radiation was evaluated, and radiation at a dose of 5 KGy rendered it inactive. The cash box was thus gamma radiated with the above dose and consequently disinfected. When the wooden currency box was retested to look for biological contamination two months following its radiation, no fungi was traceable.

According to Craeye et al., (2015), compressive strength found to be reduced as total radiation exposure is progressively increased. Also, they discovered that samples that had been exposed to radiation for a longer period of time at higher dose rates (1.36 KGy/h), had a greater loss in compressive strength. Low radiation rates (2–8 Gy/h) did not show this impact. Furthermore, weight loss in cement products was seen under irradiation; likely to be related to the loss of unbound, physically bound, and chemically bound water. Yet, in conditions of high radiation exposure, the atomic structure of some aggregates used in concrete may change from crystalline to deformed amorphous (Field et al., 2015).

2.3.4 Advantage and drawbacks of the control methods

On the basis of all these methods as described above can be summarized below in tabular form.

	Control Strategy	**Advantages**	**Drawbacks**
Biological Methods	Biocidal treatments with compounds of natural origin.	Safer for people and more environmentally friendly than conventional biocides. Easy to apply. Effective against a large range of microorganisms.	Not selective against particular biodeteriogens. The harvesting season, geographic region, and other agronomic factors all affect the extract composition. Only few products available on the market.

Chemical Methods	Traditional chemical biocides	Effective against a large range of microorganisms. Affordable and simple to apply.	It creates environmental toxicity. Possible changes of biofilm structures favouring the development of more dangerous biodeteriogens. Effectiveness over long run is very low.
	Nanoparticles	Effective at very low concentrations. Easy to apply.	Not selective against particular biodeteriogens. Produce strain. Surface morphology was modified. Product prices are high.
Physical Methods	UVC irradiation	Do not expose people, the environment, or cultural heritage to any harmful chemicals. Do not release any toxic residual element into the environment.	Organic historical materials like wood, stone, and concrete can become damaged by frequent use. Low penetration in substrates and in biofilms that is quite thick. Not selective against specific biodeteriogens.
	Gamma Radiation	Do not expose people, the environment, or cultural heritage to any harmful chemicals. High penetration in substrates and in biofilms that is quite thick.	Organic historical materials like wood, stone, and concrete can become damaged by frequent use. Limited use in remote locations. Require specialized staff. Costly.

2.4 Critical review of earlier literature

- The research work done on this topic till now focusses on isolation and identification of airborne fungi in different indoor environment.
- Subsequently variation in weight, strength and elemental composition of concrete due to the infection of few microorganisms has been reported by some research groups.
- Also, the inhibition of biodeterioration of concrete materials using nanoparticles during white wash, application of fungicide in paints has been performed by different researchers.
- A specific study on the fungal biodeterioration of concrete with potent airborne fungus for some time duration has not been explored yet and hence a long term laboratory scale study to focus on this aspect is proposed.
- Another potential area to investigate is the inhibition of fungal biodeterioration of concrete materials using different doses of ultraviolet and gamma radiation which is also required further in this work.

CHAPTER – 3

OBJECTIVES AND

SCOPE OF WORK

3.1 Objectives of work

The objective of the present work is to explore and evaluate biodeterioration potential for concrete specimen due to invasion of some potent airborne fungi along with assessment of physico-chemical change of the infected concrete materials with radiation effect for resisting fungal effect.

Following specific objectives are also considered for the present study:

- To isolate and identify some potent airborne micro-fungi from ambient air as well as fungal infected concrete wall of the building.
- To evaluate the biodeterioration of concrete materials using fungus (*Aspergillus tamarii*) as biodegrading agent.
- To standardize some non-destructive method i.e. application of ultraviolet and gamma radiation for inhibition of such microbial degradation.
- To interpret the fungal deterioration and inhibition effect on concrete materials by various standard tests and material testing analyses.

3.2 Scope of work

Following scope of work are undertaken to achieve the objective of the study:

- Identification of sampling location followed by sampling of airborne micro-fungi in different indoor environment.
- Isolation and identification of fungi from deteriorated walls of the 200 years old heritage building.
- Preparation of medium for fungal propagation including its sterilization and standardisation.
- Preliminary study of biodeterioration of concrete pieces by immersing into fungal spore containing Czapek Dox medium.
- Preparation of concrete cubes for biodeterioration and inhibition study for some time exposure.
- Standardize some non-destructive method (application of UV and gamma radiation) for prevention of such microbial degradation.
- Interpretation of results of fungal deterioration and prevention of fungal attack on concrete specimens by conducting some instrumental test such as SEM, HPLC, EDXRF, FTIR and stereo microscope observations.

CHAPTER – 4

MATERIALS AND METHODS

Chapter 4 deals and describes the methodology adopted for targeting the objective.

4.1 Isolation of fungal species from ambient air

4.1.1 Fungal sampling locations

The location of sampling sites were chosen at different places such as library, computer room, creche, cafeteria, beauty parlour salon and separately one outdoor (control) area located in Kolkata, India. All indoor sampling sites were closed and air-conditioned at the time of sampling. The average humidity was kept as 66% and the temperature fluctuates between 22 and 27 °C. Temperature and humidity was measured using infrared MESTEK thermometer (Model IR01C). Different locations of grabbing samples are shown in Fig. 4.1.

Fig. 4.1 Sampling locations: (a) library; (b) computer room; (c) creche; (d) cafeteria; (e) salon; (f) outdoor (control).

4.1.2 Preparation of agar plates

For the necessary culture of yeasts and moulds, both Rose Bengal Agar (RBA) medium (Ottow and Glathe 1968) and Potato Dextrose Agar (PDA) medium (Westphal et al., 2021) were used. PDA medium was prepared with potato infusion (200 g/l), dextrose (20 g/l), agar (15 g/l) at a pH of 5.6 (CyberScan pH 510). The composition of RBA was papaic digest of soybean meal (5 g/l), dextrose (10 g/l), mono-potassium phosphate (1 g/l), magnesium sulfate (0.5 g/l) and Rose Bengal (0.050 g/l) at a pH of 7.2 ± 0.3 (CyberScan pH 510). After carefully maintaining the pH for both medium, the ingredients were properly mixed in distilled water before being autoclaved at 15 pounds per square inch (psi) pressure for 15 min. 20 mL of medium was then added to each sterile petri plate, and left until it hardened. Before sampling, the plates were kept at a temperature 4 °C in a deep freezer.

4.1.3 Sampling procedure

The fungal spores were collected with Two-Stage Viable Andersen Cascade Impactor. On agar plates, it can pick up 95–100% of the viable particles larger than 0.8 microns. The plates were labelled and acclimated at room temperature before being used for air sampling. They were carried out taped to one another in an icebox. After reaching the chosen location, the impactor was placed at a relatively undisturbed location inside the room. Then, in a sequential manner, each set of medium plates was take out and put to the second stage, with its corresponding matching pair in the first stage. For both of these medium, Andersen sampler was run for 15 min at each sampling sites. Each stage was carefully opened once it was finished off, then the plates were removed, and the lid was put on top before the air could enter to contaminate it. The plates' lids were closed by tapping with hands to prevent them from reopening during transported, and they were then brought to the lab where they were kept in an incubator for 7 days at 27 °C. Colony growth was visible on the plates after 7 days in the incubator. After staining with lacto phenol cotton blue, each colony was examined with a compound microscope (LEICA ICC50 HD) at 100× magnifications.

4.1.4 Fungal load determination

The term "colony-forming unit" (or "CFU") refers to a measurement of the quantity of viable fungi in a sample. The following equation was used to determine the amount of fungi per cubic metre of air:

$$\textbf{Colony} - \textbf{forming unit} = \frac{\mathbf{1000P}}{\mathbf{RT}}\,\mathbf{CFU/m^3}$$

Where P = number of counted colonies on the sample plate after correction using positive hole conversion table (Andersen 1958), T = time (15 min), R = rate of air sampling (14 L/minute).

4.2 Isolation of fungal species from damp walls

4.2.1 Location of fungal sampling

The subject area for our current study was the Tagore residence in Jorasanko, Kolkata, India. Our study site, which was 200 years old and 6 m above sea level, was close to the Hooghly River (Fig. 4.2). It was built in the 18th century. Throughout the entire year, the weather was warm and humid. The temperature varies between 24 and 38 ^{0}C in the summer and between 12-27 ^{0}C in the winter. Around 1582 mm of rain falls annually on average between June and September. These data have been collected from India Meteorological Department, Ministry of Earth Sciences, Government of India.

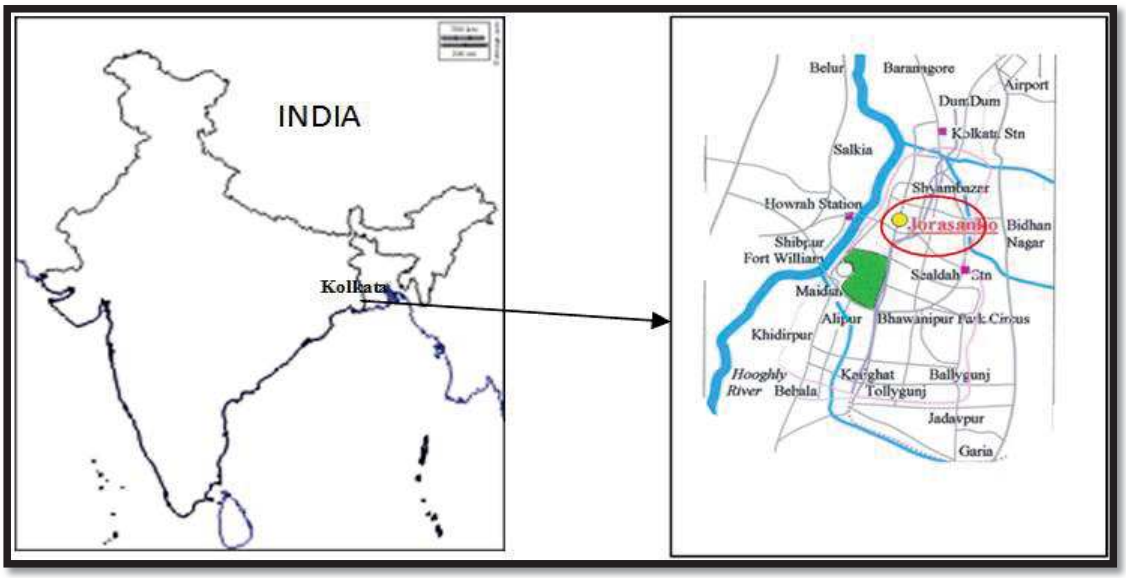

Fig. 4.2 Location map of our sampling site **(Mukherjee et al., 2016)**.

This old edifice serves as an example of the nation's cultural history, which was highly valued in society. Additionally, this museum preserves information about the history of the Tagore family and the Bengal region, including furniture, antique manuscripts, books, photos, oil paintings, and newspapers.

4.2.2 Fungal growth in cardinal directions

Cardinal direction (north, south, east and west) of exposure influences the fungal colonisation in the concrete wall. The least growth was observed in the south and east walls, which might have been caused by their longer exposure to sunlight leading to changes in surface moisture. The largest fungal growth was observed on the north and west walls which were exposed to wind-driven rain. The main source of moisture is the wind-driven rain that affects the hygrothermal performance of building enclosure, which supports noticeable mould formation.

4.2.3 Procedure of sampling

Temperature and humidity at Tagore's home at the time of isolation were 27 ^{0}C and 50% respectively. Fungi was isolated from three distinct locations of the fungal infected surface (4 cm^2 area) of the wall of Tagore's house by rubbing a sterilized cotton swab at a height of 2.5 m from the ground. Subsequently, the cotton swab was dipped in 1 mL of sterile Czapek Dox broth and then inoculated into the Czapek Dox Agar plates. For consequently seven days, the plates were incubated at 27 °C. Different fungal species produce different types of colony patterns, with some colonies having different colours or by shapes (irregular to circular). After 7 days of incubation, slides were prepared for each colony using lacto phenol cotton blue as a stain in a laminar air flow chamber and observed under compound microscope (LEICA ICC50HD). The fungi were then identified based on their microscopic structure and colonial morphology. Also, the identification of these strains had been done by Agharkar Research Institute (ARI), Pune, Maharashtra, India.

4.3 Selection of predominant fungus for adverse effect

This study was performed to select most potent fungal strain involved in biodeterioration of concrete. Concrete pieces (250 mm^2 surface area) were used for this study. The detailed methods were explained in subsequent section.

4.3.1 Preparation of fungal spore suspension

In a conical flask, semi-synthetic fungal (Czapek Dox) medium (Szatmari et al., 2015) was prepared with sodium nitrate (2 g/l), dipotassium hydrogen phosphate (1 g/l), potassium chloride (0.5 g/l), magnesium sulphate (0.5 g/l), ferrous sulphate (0.01 g/l), sucrose (30 g/l), and agar (20 g/l) at a pH of 7.3 ± 0.2 (CyberScan pH 510). The medium was then sterilised for 20 min at 121 ^{0}C and 1.0546 kg/cm^2 pressure. After that, the sterile medium in the conical

flask was tilted at an angle of 45^0 and left to solidify. With the aid of a sterilised inoculating loop, a loop of fungal culture was collected and streaked over the agar surface in a conical flask.

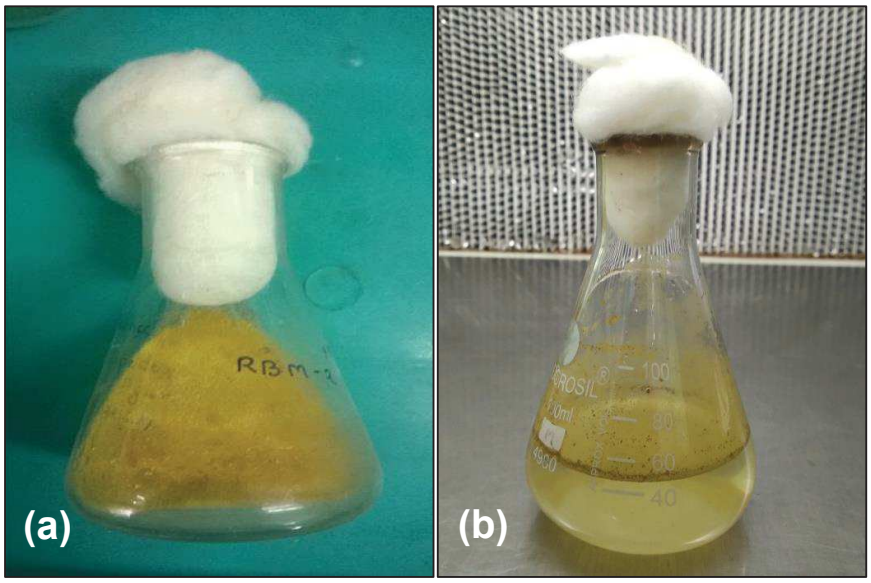

Fig. 4.3 Preparation of: (a) agar slant; (b) spore suspension of fungus.

The agar slants were then kept in an incubator at 27 ^{0}C, the temperature necessary for growth of fungi [Fig. 4.3(a)]. The fungal spores (1.8 x 10^5 spores/ml) in the slants were combined with the autoclaved distilled water after the 7-day incubation period [Fig. 4.3(b)]. Finally, fungal spore suspensions for each fungus species was filled into a sterilized conical flask and kept them ready for use.

4.3.2 Experimental set up

70 mL test tubes were used for this study. Each test tube was filled with 20 mL of Czapek Dox medium. The Czapek Dox medium which composed of 2 g sodium nitrate, 1 g dipotassium hydrogen phosphate, and 30 g sucrose in 1000 mL of distilled water. The pH of the medium was maintained at 7.3 ± 0.2 (CyberScan pH 510). Next the sample concrete pieces chosen were dipped into the medium. Magnesium sulphate, potassium chloride and ferrous sulphate were absent in the medium because these salts were already present in concrete samples. After that all the above test tubes were put in an autoclave for sterilization. After sterilization, the medium was cooled at ambient temperature (27 ± 5 ^{o}C). At last 2 mL of each fungal spore suspensions was added in that particular test tube with the help of 5 mL

pipette in laminar airflow chamber. The entire set up (Fig. 4.4) was kept in an incubator for 30 days at a temperature of 27 ºC and a relative humidity of 75%.

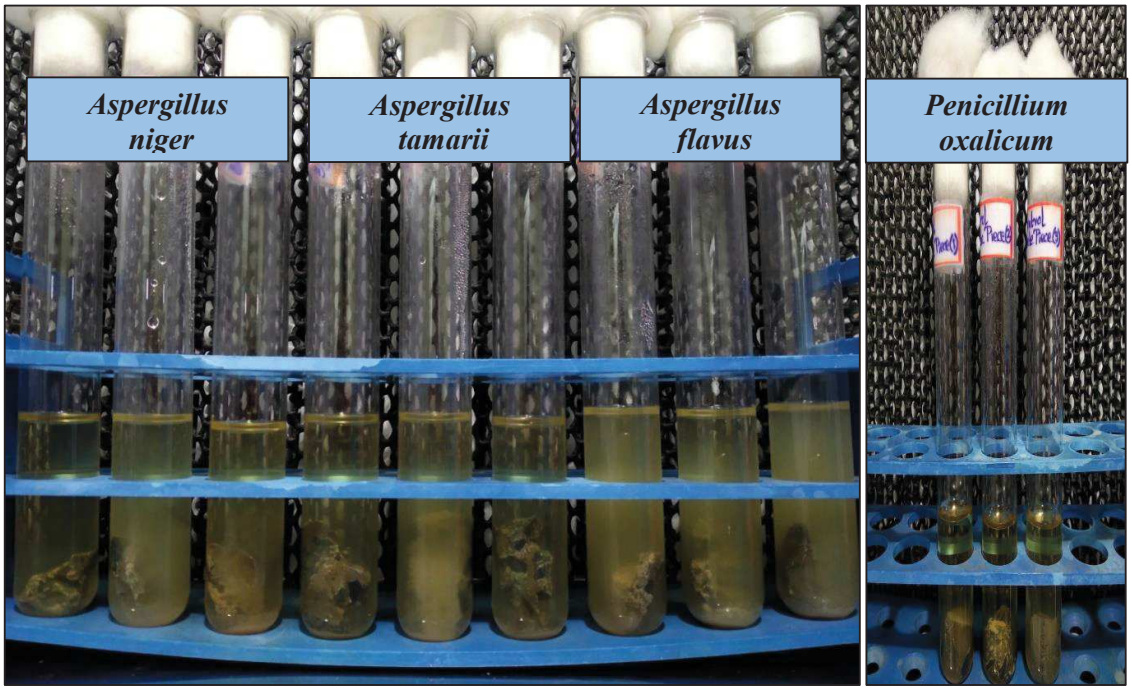

Fig. 4.4 Set-up of test tubes for selection of most potent fungus.

4.4 Biodeterioration study

4.4.1 Preparation of concrete cubes

Portland cement (53 Grade), fine aggregate and coarse aggregate were uniformly hand mixed manually. Then water was added to this ingredients mixture and hand mixing until the concrete was homogeneous and was the necessary consistency achieved. Cube of cast iron moulds [(10 cm × 10 cm × 10 cm) and (5 cm × 5 cm × 5 cm)] were cleaned and smeared with lightly oil as necessary. After that, the freshly mixed concrete (M40 and M20) was appropriately poured into the mould and tamped with a compacting rod to remove any air pockets that might exist in the concrete. The iron mould was slightly lifted and dropped after tamping every layer, to close the top surface of each layer. The last layer of concrete mix should slightly overflow the mould. Finally the concrete was levelled off with a trowel to give a flat smooth surface with the top of the iron mould kept at ambient temperature for 1 day. After removal of concrete cubes at the end of 24 h, it was submerged into clean water for 28 days for curing. The cube specimen was removed from the water after specified curing

time and dried for 3 days at room temperature. Fig. 4.5 depicts the process of preparing concrete cubes.

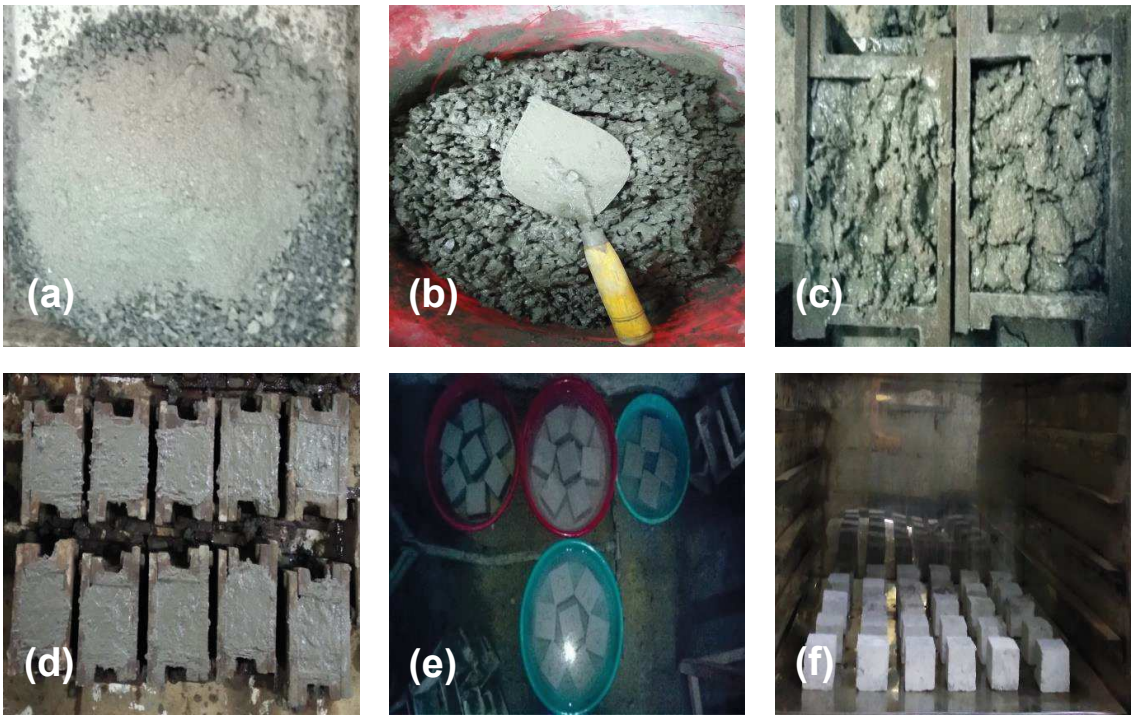

Fig. 4.5 Cube preparation: (a) Cement, fine aggregate and coarse aggregate (1:1.5:3); (b) Concrete mix; (c) Concrete is poured in the mould; (d) Level the top surface and smoothen it with a trowel; (e) Test specimens are put in water for 28 days curing; (f) Dried in hot air oven.

4.4.2 Experimental set up of concrete cubes

Airtight plastic containers [(38 cm × 26 cm × 18 cm) and (30 cm × 20 cm × 15 cm)] were used for biodeterioration test. Utilizing surface sterilization, the containers were cleaned. M40 and M20 graded concrete cubes were kept in the containers containing sterilized (121 °C temperature at 15 psi pressure for 15 min) Czapek Dox medium (pH 7.3 ± 0.2) and injected with the spore suspension of most potent fungus (*A. tamarii*) (Fig. 4.6). In intervals of 60 days, it was observed for 180 days. Additionally, a control was run for 180 days in sterile Czapek Dox medium. At a temperature of 27 ºC and a relative humidity of 75%, the full set was incubated.

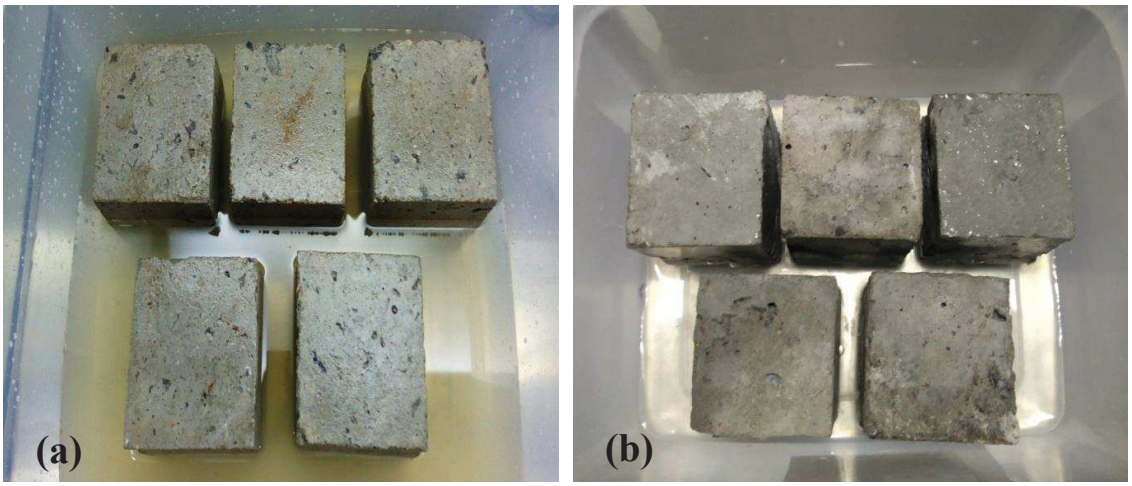

Fig. 4.6 Experimental set up for deterioration test of: a) M40 grade concrete (10 cm x 10 cm x 10 cm); b) M20 grade concrete (5 cm x 5 cm x 5 cm) cubes.

4.5 Selection of radiation dose

4.5.1 Radiosensitivity test of *A. tamarii*

The fungus that was isolated from deteriorated walls of the Tagore's residence at North Kolkata, was used to calculate the necessary dose needed to inactivate fungus on axenic cultures. The most dominant fungus (*A. tamarii*) from the preliminary study was inoculated on Petri dishes with Czapek Dox Agar and incubated at 27 ^{0}C for 2 days. Following incubation period the cultures were exposed to a ^{60}Co gamma source for irradiation at 20 ^{0}C with exposure doses of 0.5, 0.75, 1.0 KGy (1.27 KGy/h) and UVC exposure of 5, 10, 15, 20 min respectively. The UVC light (Philips TUV 11W) of intensity 625 µw/cm² and 254 nm peak was used in the current investigation. The distance between light and applied surface of plate was 15 cm. After irradiation the plates were incubated at 27 ^{0}C for 7 days. The controls were grown on Czapek Dox Agar and kept under the same conditions as the treated fungus. On the first, fourth and seventh days after irradiation, the colony diameter was measured to check for fungal development in comparison to the colony diameter measured just before irradiation and to the controls. All these biological assays were done in triplicate. The protocol used in this followed by Choi and Lim (2016) and da Silva et al., (2006).

4.5.2 Radiation on concrete cubes

4.5.2.1 Arrangement of concrete cubes

Airtight sterilized plastic boxes (24 cm × 19 cm × 9 cm) and 5 cm × 5 cm × 5 cm concrete cube (M20) were both used for current study. In separate plastic containers, the formed concrete cubes were placed in various arrangements that were observed after 30 days. The arrangements included a biodeterioration set (cubes were infected with *A. tamarii*), inhibition sets (cubes were inoculated with same fungus and exposed to multiple doses of ultraviolet and gamma radiation), a control set (non-infected and non-irradiated), and multiple control sets (cubes were irradiated with multiple doses of both radiation).

4.5.2.2 Experimental set up for radiation application

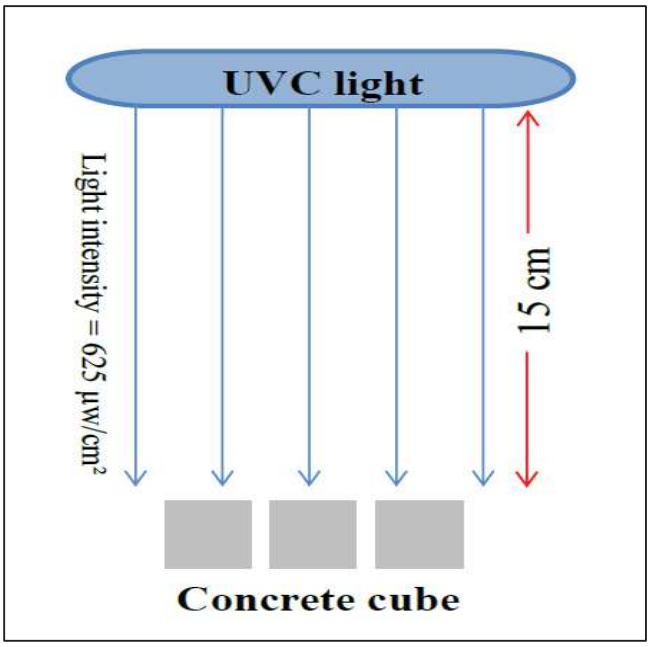

Fig. 4.7 An illustration of the concrete cubes exposed to UVC light.

Using a paint brush, spore suspension of *A. tamarii* was applied on the concrete cubes (biodeterioration and inhibition) within polyethylene boxes before adding autoclaved Czapek Dox medium ($1/10^{th}$ height of cube) in laminar air flow cabinet. The control sample i.e. non-infected and non-irradiated sample was run in sterile Czapek Dox medium. Then an incubator was used to keep the boxes for control (non-infected and non-irradiated) and biodeterioration (infected) at a constant temperature of about 27 ± 2 ^{0}C and a relative humidity of 50 ± 2% for 7 days.

The inhibition sets before irradiation was also maintained at the same temperature and humidity level in order to see the fungal growth on the concrete cube's surface visually. At the 8th day, the inhibition (infected and irradiated) cube samples were exposed to UVC light for 5, 10, 15 and 20 mins on the irradiation chamber. In the present investigation, UVC light (Philips TUV 11W), with a peak of 254 nm and a 625 µw/cm² intensity was used. The distance between light and surface of concrete cube was 15 cm (Fig. 4.7).

Fig. 4.8 Concrete cubes were irradiated with selected dose in gamma radiation chamber.

For gamma radiation, inhibition concrete cubes were subjected to a ^{60}Co gamma source for irradiation (Fig. 4.8) at 20 ^{0}C with exposure doses of 0.5, 0.75 and 1.0 KGy (1.27 KGy/h) at UGC DAE, Consortium for Scientific Research, Kolkata Centre. A Fricke Dosimeter was used to measure the rate of radiation dose (ASTM 2007). The same dosages of UV and gamma radiation were also applied to the control cubes (irradiated). Finally, the control (irradiated) and inhibition (infected and irradiated) concrete cubes were put into the cleaned plastic boxes which contained the same medium (sterile). Both setups were incubated at the same humidity and temperature for thirty days of retention time.

4.6 Inhibition study with selected radiation dose

4.6.1 Arrangements of concrete cubes

This study was conducted in airtight plastic boxes (24 cm × 19 cm × 9 cm). Surface sterilizing was used to clean the box. Both infected sets (cubes were infected with *A. tamarii* and exposed to a selected dose of ultraviolet and gamma radiation from previous study) and multiple control sets (cubes were exposed to a preselected dose of ultraviolet and gamma radiation) were included in the arrangements.

4.6.2 Experimental set up

The M20 graded concrete cubes (5 cm × 5 cm × 5 cm) for infected sets were initially coated with a spore suspension of same fungus using a paintbrush inside a plastic container. After that, sterile Czapek Dox medium (1/10th height of cube) was added into the plastic box. The box was then placed into the incubator at 27 ^{0}C for 7 days. After 7 days of incubation period, concrete cubes (infected) were exposed with the selected dose (from dose selection study) of ultraviolet and gamma radiation. The control cubes were also irradiated with the same dose of radiations. After cleaning the boxes and addition of fresh sterile (121 ^{0}C temperature at 15 psi pressure for 15 min) Czapek Dox medium (pH 7.3 ± 0.2), the exposed concrete cubes (control and infected) were finally placed inside for 180 days at 27 ^{0}C temperature and 75% relative humidity.

4.7 Characterization of concrete cube

4.7.1 Weight variation

Losing weight was considered to be a significant biodeterioration study indicator (Grbia and Vukojevia 2009; Bielefeldt et al., 2010). After drying the pieces, the pieces were weighed before and after the experiment since, if any water had been soaked during the inoculation process, it would have been eliminated during oven-drying. Each sample's weight was averaged over three measurements. Equation was used to compute the weight loss variation.

$$\Delta \mathbf{W} = \frac{\mathbf{W_1} - \mathbf{W_2}}{\mathbf{W_1}} \times \mathbf{100}$$

Where, ΔW is the weight loss variation (%), W_1 = Initial dry weight of each cube before test, W_2 = Final dry weight of each cube after test.

4.7.2 Compressive strength variation

Concrete's compressive strength as quantifiable parameters is its most valuable structural property. The cube samples were positioned between the Aimil Prime Automatic Compression Testing Machine (AIM317E-MU-1) platens with care to ensure that the cube's axis was aligned with the platen's centre of thrust (Fig. 4.9). Load was steadily added until the cube failed. The compressive strength of a concrete cube was calculated by dividing the load at failure by the area of the specimen. Following expression was used to estimate the compressive strength of the concrete.

Fig. 4.9 Aimil Prime Automatic Compression Testing Machine (AIM317E-MU-1).

$$\textbf{Compressive Strength} = \frac{\textbf{Maximum load (N)}}{\textbf{Cross sectional area (mm}^2\textbf{)}}$$

Three cube specimens were removed from the boxes after 60 days of incubation and broken in a universal testing machine. The compressive strength of concrete cubes was determined to be the average of the three results.

4.7.3 HPLC analysis for determination of organic acids

High-performance liquid chromatography (HPLC) is the most trustworthy method due to its great sensitivity, straightforward operation, outstanding reproducibility, and capacity to concurrently detect several organic acids. However, there is a limited study reported in the literature of finding organic acids in the fungal culture medium so far. In present study, high performance liquid chromatography was used for the detection of organic acids present in the fungal medium which may be a probable reason to deteriorate concrete cubes.

Fig. 4.10 High Performance Liquid Chromatography (LC-20AT Shimadzu Liquid Chromatograph).

The HPLC system (LC-20AT Shimadzu Liquid Chromatograph, Kyoto, Japan) (Fig. 4.10) was equipped with a manual injection mechanism and 20 µL sample loop, a valve unit and a system controller. The UV detector was set at 210 nm and operated using Shimadzu LCsolution software. The RP C18 column 4.6 x 150 mm was used for the separation. At room temperature, an isocratic flow was used. Mobile phase was 20 mM KH_2PO_4 adjusted to pH 2.5 with H_3PO_4 and a flow rate of 1 ml/min. The injection volume for the reference sample solutions was 20 µL. The samples, buffers, and stock solutions of each standard compound were all made with HPLC grade water (Merck).

4.7.4 EDXRF analysis for determination of elemental composition

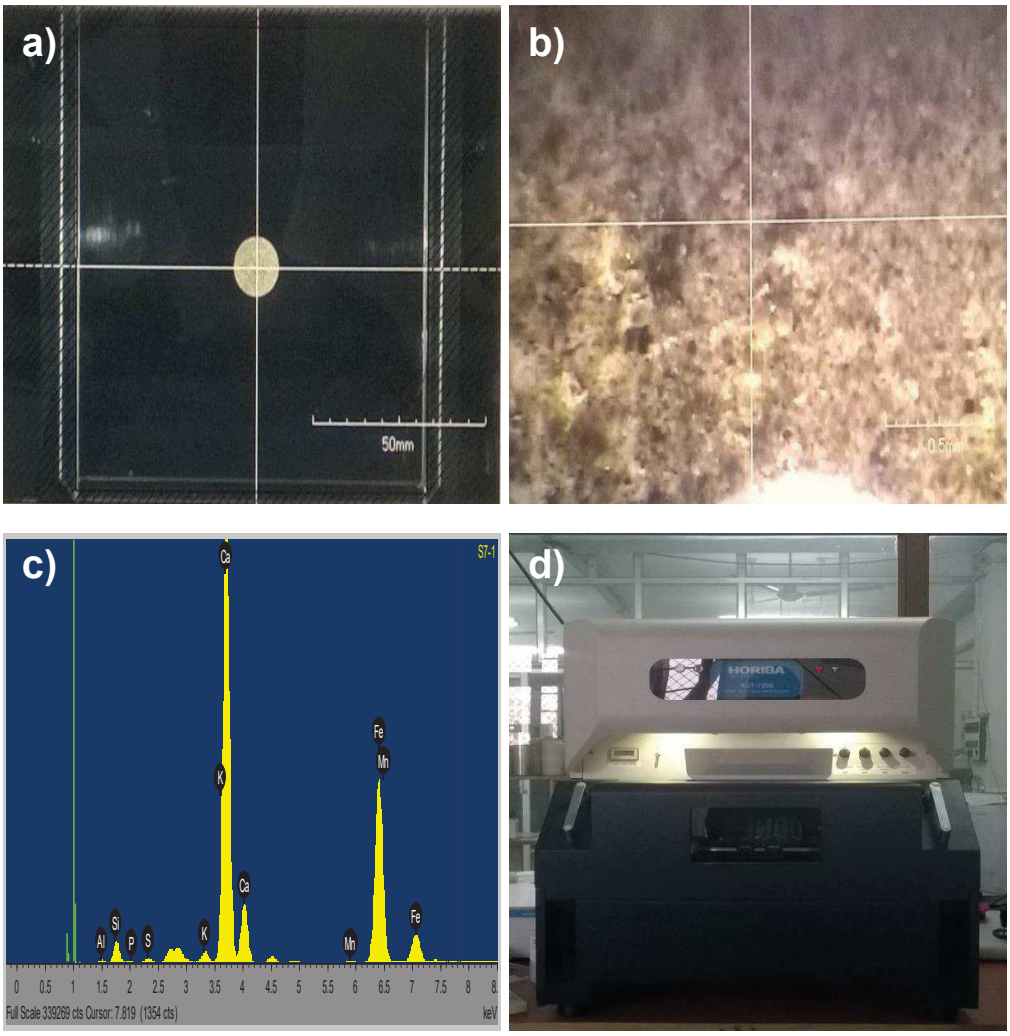

Fig. 4.11 EDXRF images: a) the pellet as viewed on-screen b) surface of the pellet c) chromatogram representing peaks of different elements d) micro EDXRF machine (Horiba Scientific, XGT-7200).

The Energy Dispersive X-ray fluorescence (EDXRF) spectrometry has been effectively used all over the world to analyse sediment and plant materials since it is multi-elementary, quick, non-destructive, and sensitive (ppm level). The concrete cubes were broken down into powder, and 2 g of each powder sample were used to make pellets (1 mm thick and 13 mm in diameter) by a tabletop pelletizer (pressure 110-130 kg/cm^2 for 2 min.). The pellets were measured in triplicates for quantitative elemental analysis in micro EDXRF (Horiba Scientific, XGT-7200) (Fig. 4.11), which was composed of an oil-cooled Rh anode X-ray tube (maximum voltage 50 kV, current 1 mA). Filters were used to take measurements for

400s in vacuum condition for the best element detection, and nExt software was used for quantitative analysis. A 12.5 mm^2 Si (Li) semiconductor detector with liquid nitrogen cooling was used to find the X-rays (resolution 150 eV at 5.9 keV).

4.7.5 FTIR analysis for determination of functional groups

A useful technique for identifying unidentified spectra found in construction materials is Fourier-transform infrared spectroscopy (FTIR). The effects of temperature, relative humidity, and pollution on concrete were investigated using reflection IR measurements. In the present work, fungal contribution to degradation was discovered using IR spectroscopy (PerkinElmer Spectrum 100) (Fig. 4.12). The literature has been written extensively about FTIR analysis of building materials (Ramachandran and Beaudoin 2000). Since it would reveal the essential structural details and organic functional groups contained in the concrete powder samples, all FTIR spectra were taken in the mid IR range between 4000 and 400 cm^{-1}. Each data point's transmittance % for these spectra was recorded. The measurements were made three times for each sample.

Fig. 4.12 Fourier-transform infrared spectroscopy (Perkin Elmer Spectrum 100).

4.7.6 SEM analysis for observation of fungal growth

SEM (ZEISS EVO-MA 10) (Fig. 4.13) is an electron microscope that uses a focused electron beam to scan a sample's surface in order to produce images of the sample. The signals produced by the electrons interactions with the sample's atoms reveal details about the surface topography and composition. Its purpose is to investigate the surfaces of solid specimens. Additionally, it may look at any pollution on the surface and locate crystalline structures. It produces high resolution, three dimensional photographs.

Fig. 4.13 Scanning Electron Microscope (ZEISS EVO-MA 10).

SEM examination was carried out by mounting broken small pieces of concrete (10 mm thickness) on brass stubs using carbon tape and taking micrographs at a magnification of about ×2000.

4.7.7 Stereo zoom microscope for surface observation

A stereo zoom microscope (Discovery, V8) (Fig. 4.14) is an optical device that uses light that is reflected from an object's surface rather than being transmitted through it to observe a sample at low magnification. The microscope uses two distinct optical pathways, two objectives, and two eyepieces to provide the left and right eyes slightly different viewing angles. This arrangement produces a three-dimensional visualization of the testing sample. In stereo microscopes, there are primarily two categories of magnification systems. One kind is fixed magnification, in which a paired set of objective lenses with a predetermined degree of magnification is used to accomplish primary magnification. The alternative is zoom or pancratic magnification, both of which have a fixed range of continually variable magnification.

Fig. 4.14 Stereo zoom microscope (Discovery, V8).

4.8 Statistical analysis

For each of the specimen sample, experiments were performed in triplicate and standard deviation has been shown as error bars and values in results and discussion chapter 5. In order to compare the differences between the mean values of control (non-infected and non-irradiated) and biodeteriorated (infected) concrete specimens as well as control (irradiated) and inhibition (infected and irradiated) specimens, the Student's *t*-test was also carried out for all experiments.

CHAPTER – 5

RESULTS AND DISCUSSION

5.1 Selection of most dominant fungus for adverse effect

5.1.1 Identification of micro-fungi isolated from ambient air

The majority of the colonies were found circular and greenish in colour in RBA plate, followed by round shape big black colonies and a few that were cottony white in colour. Most of the colonies were detected on PDA in the form of tiny green and cottony black forms. In this investigation, several distinct fungal genera were isolated and identified from the sampling sites (Fig. 5.1).

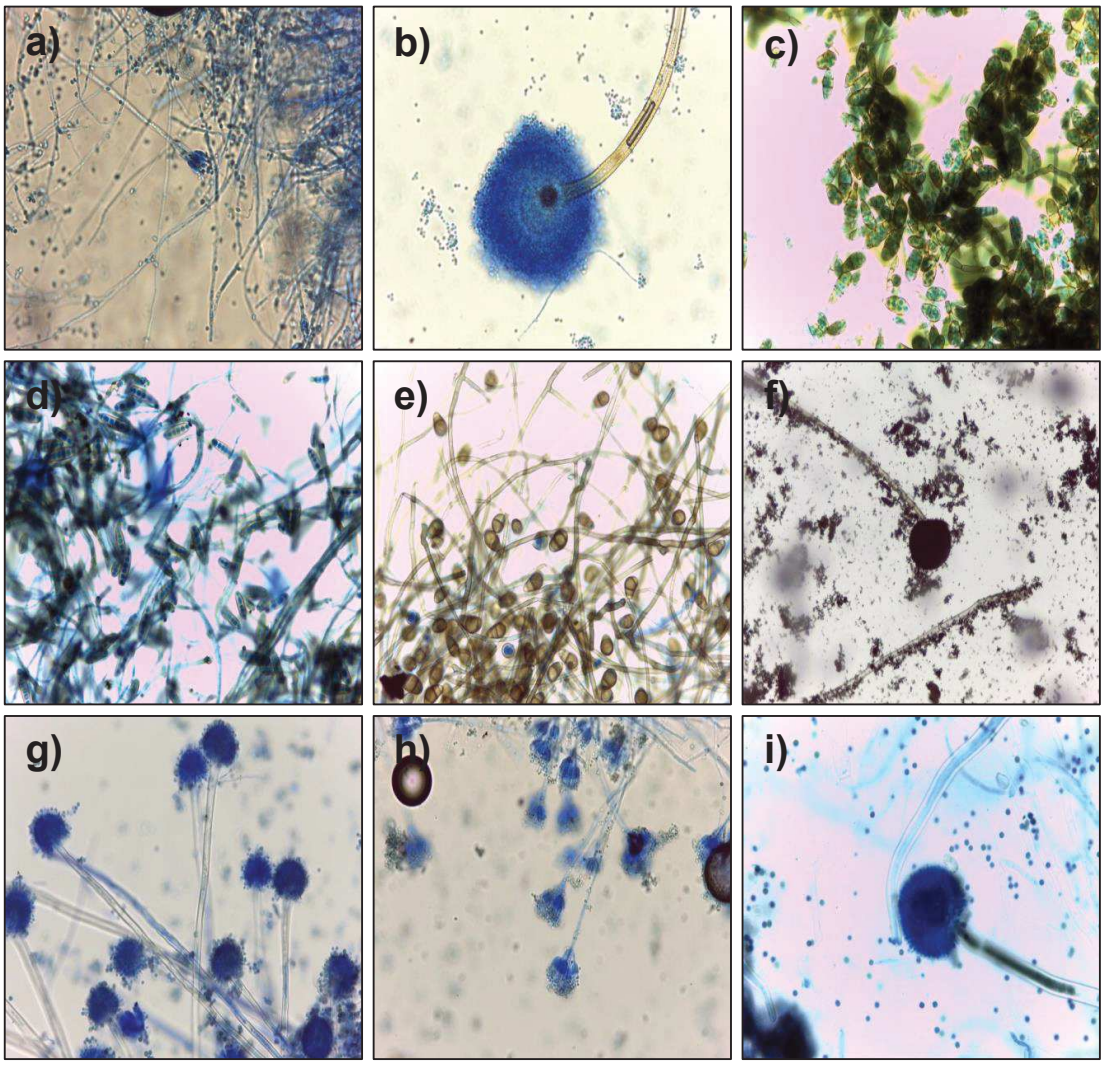

Fig. 5.1 Compound microscope images (100× magnification) of: a) *Penicillium* sp. from library; b) *Aspergillus* sp. from library; c) *Diasporium* sp. from computer room; d) *Alternaria* sp. from computer room; e) *Alternaria* sp. from creche; f) *Aspergillus* sp. from creche; g) *Aspergillus* sp. from cafeteria; h) *Penicillium* sp. from cafeteria; i) *Aspergillus* sp. from salon.

Aspergillus sp., *Penicillium* sp., *Paecilomyces* sp. and *Rhizopus* sp. were the dominating genera in library [Fig. 5.2(a)]. *Aspergillus* sp., *Penicillium* sp., *Paecilomyces* sp., *Cladosporium* sp., *Curvularia* sp., *Alternaria* sp. and *Diasporium* sp. were found in computer room [Fig. 5.2(b)]. This finding can be attributable to the regular exchange of air through windows and the transport of spores by student's feet. Two common fungal species i.e. *Aspergillus* sp. and *Penicillium* sp. were also identified from the indoor air of creche, cafeteria and salon [Fig. 5.2(c), Fig. 5.2(d) and Fig. 5.2(e)]. Aquino et al., (2013) discovered fungal contamination in the dust taken from the cafeteria, which is in contrary to the present observations. Moreover, *Alternaria* sp. and *Curvularia* sp. were also found in the air sampled from creche and salon. Similar to the present study, Martins et al., (2010) observed filamentous fungal growth in creche. While other slow-growing fungal species including *Alternaria* sp., *Cladosporium* sp., *Curvularia* sp. and *Paecilomyces* sp. were detected in RBA medium, *Aspergillus* sp. and *Penicillium* sp. were mostly found in PDA medium.

5.1.1.1 Diversity and density of airborne micro-fungi

In the air sampled from library, *Penicillium* sp. was the most abundant species (461.89 CFU/m^3, or 60.62%), followed by *Aspergillus* sp. (209.52 CFU/m^3, or 27.50%) and *Rhizopus* sp. (52.37 CFU/m^3, or 6.87%) [Fig. 5.2(a)]. The similar pattern was seen in the air taken from a salon (Fig. 5.2(e)), where *Aspergillus* sp. (71.42 CFU/m^3 or 44.12%) and *Penicillium* sp. (38.09 CFU/m^3 or 23.52%) were the two most dominating genera. An earlier study of this kind was conducted in 257 saloons in the four selected areas of Ibadan, the capital of Oyo state, Nigeria which revealed that the most prevalent genera was *Aspergillus* sp. and *Penicillium* sp. followed by *Fusarium* sp. and *Mucor* sp. (Sarah and Ee 2017). The highest percentage of culturable airborne fungi in outdoor environment [Fig. 5.2(f)] during monsoon season was found for *Aspergillus* sp. (395.23 CFU/m^3, or 70.37%) followed by *Penicillium* sp. (114.27 CFU/m^3, or 25.92%).

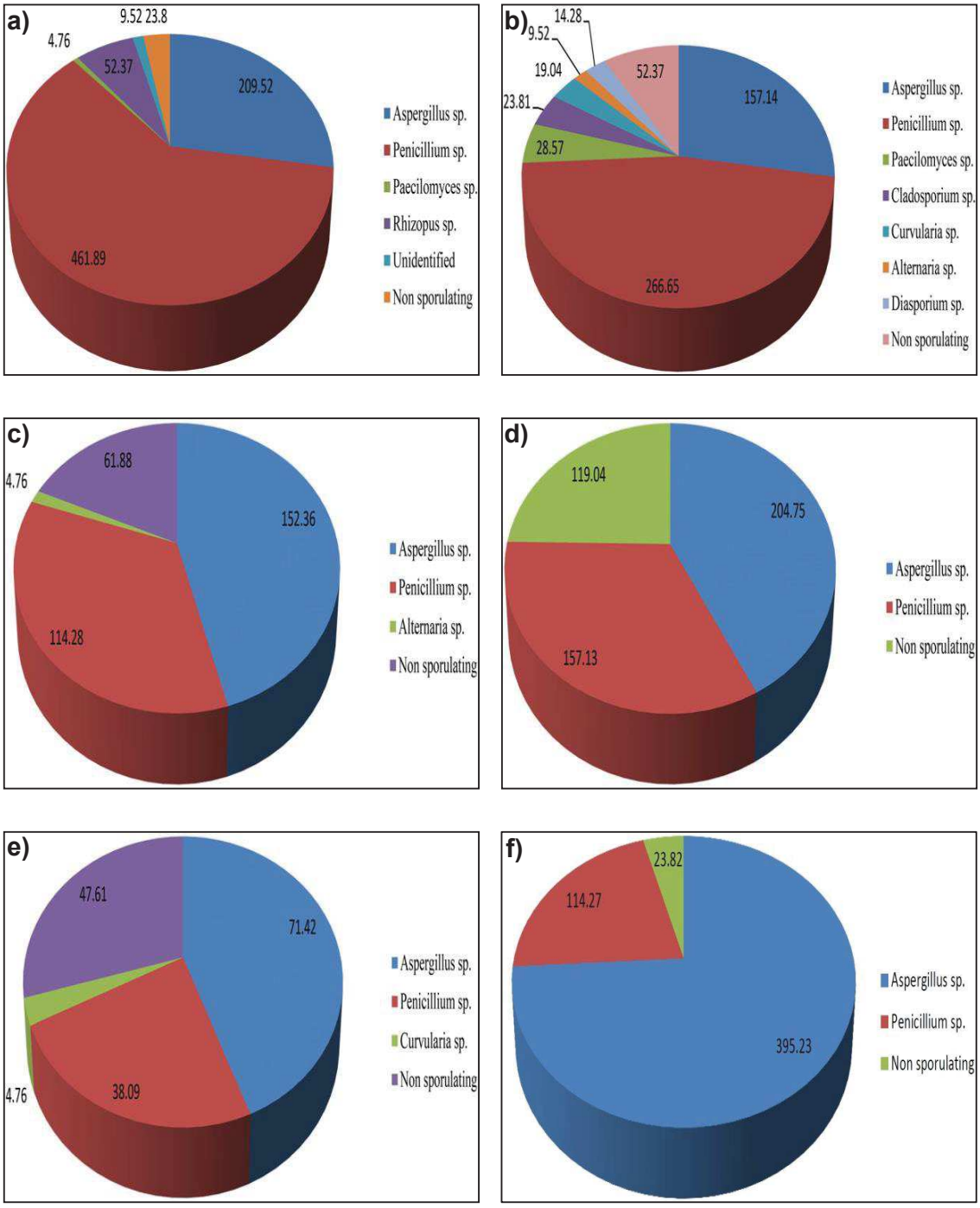

Fig. 5.2 Density (CFU/m^3) of microflora in: a) library; b) computer room; c) creche; d) cafeteria; e) salon; f) outdoor.

The recommended standards of the American Conference of Governmental Industrial Hygienists (ACGIH), which were 100 CFU/m^3, were exceeded in all five sites, including the library (761 CFU/m^3), computer room (571 CFU/m^3), creche (328 CFU/m^3), restaurant (480

CFU/m^3), and beauty salon (161 CFU/m^3) (Fig. 5.3). Due to many factors, including the presence of FGPS and frequent air exchange with the outside, only the computer room and library exceeded the World Health Organization (WHO) recommended limits (500 CFU/m^3), but the beauty salon had some of the cleanest air. The beauty salon had the lowest fungal load (161 CFU/m^3), possibly as a result of the authorities' greater attention to maintaining its cleanliness; otherwise, waste products like used nails, hair, oil, foam and tissues from the salon could be viewed as a source of fungal growth in the salon's indoor environment (Murthy et al., 2000).

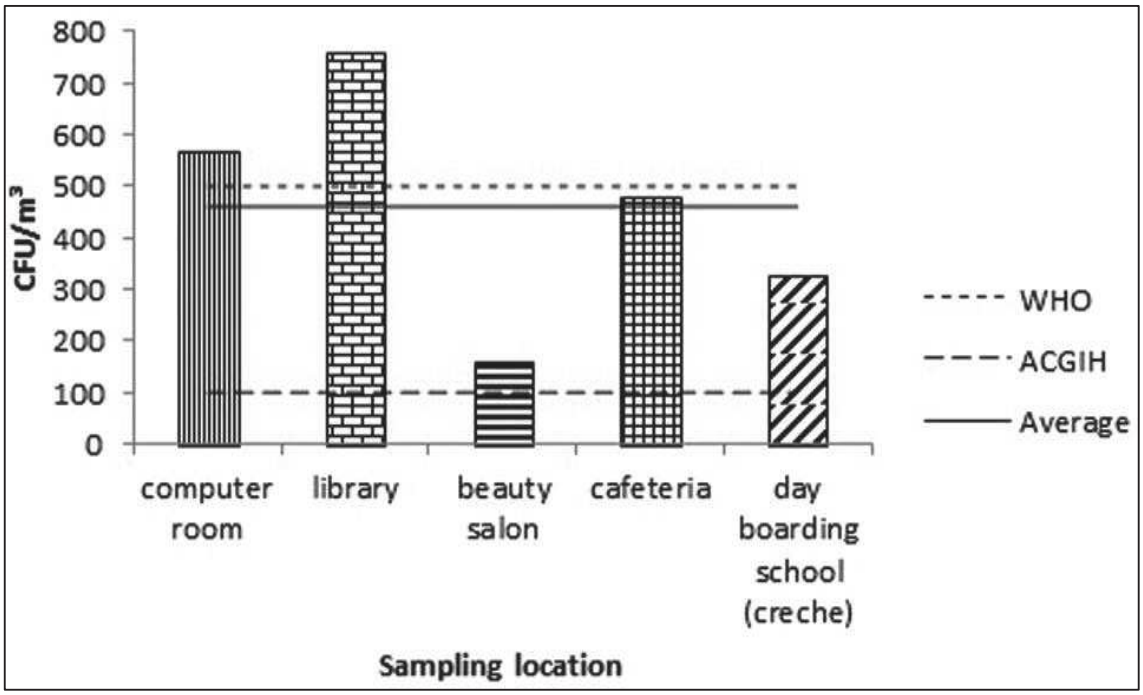

Fig. 5.3 Fungal density (CFU/m^3) in various indoor locations with ACGIH and WHO guidelines.

5.1.2 Identification of micro-fungi isolated from damp walls

After microscopic observation, the highest number of colony in this heritage building was found for *Aspergillus* sp. followed by *Penicillium* sp. Also, these strains had been identified from Agharkar Research Institute, Pune, India. The four fungal strains i.e. *Aspergillus niger, Aspergillus tamarii, Aspergillus flavus* and *Penicillium oxalicum* (Fig. 5.4) were identified from Tagore's house. *Aspergillus* sp. followed by *Penicillium* sp., *Alternaria* sp. was the most encountered in the different studies (Basu et al., 2021; Skora et al., 2015; Sterflinger 2010).

Another study by Chaudhuri and Bhattacharyya (2019) showed that 6 genera of fungi, mainly members of the genus *Aspergillus*, were isolated from museum and library environments.

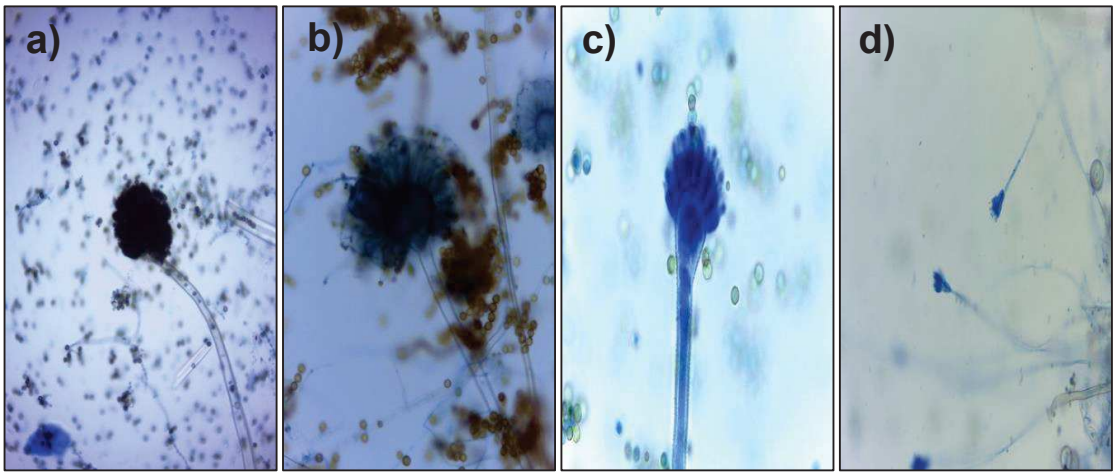

Fig. 5.4 Compound microscope images (100× magnification) of: a) *Aspergillus niger*; b) *Aspergillus tamarii*; c) *Aspergillus flavus*; d) *Penicillium oxalicum.*

5.1.3 Selection of most adverse fungi for present study

5.1.3.1 Colour change of fungal medium

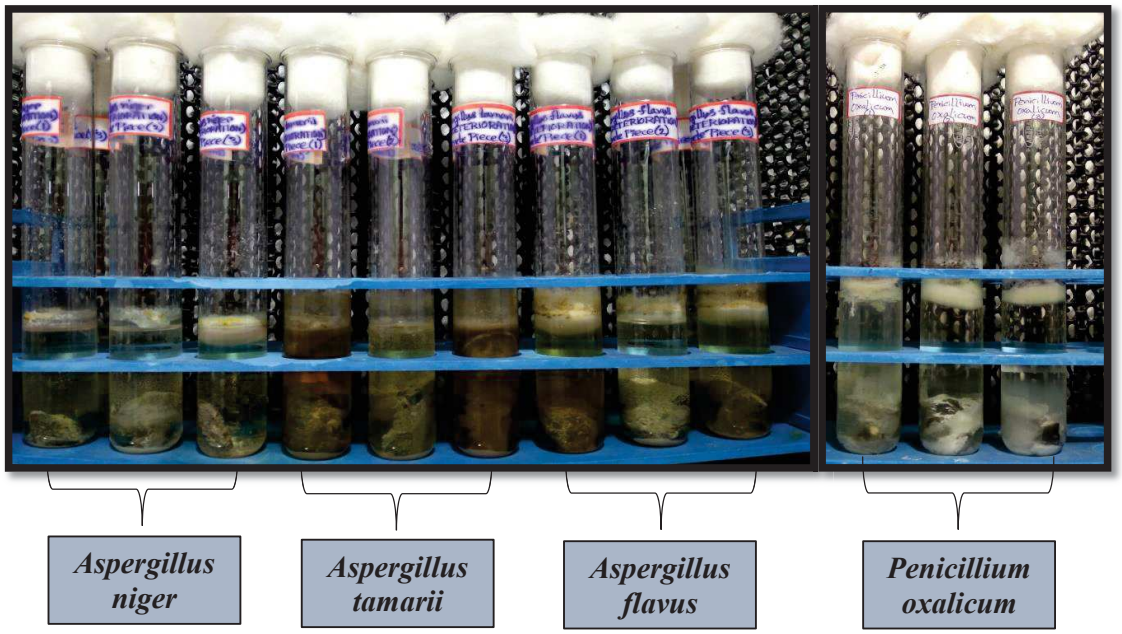

Fig. 5.5 Experimental set up of test tube (n = 3) study after 30 days incubation period for preliminary biodeterioration test.

After 30 days of incubation, heavy fungal growth was observed on all the above test tubes. *Aspergillus tamarii* particularly produce yellowish brown pigments. That's why the color of the Czapek Dox medium within the test tubes for *Aspergillus tamarii* changed from yellowish to yellowish brown compared to other species (Fig. 5.5). The pigmentation is mostly brought on by melanin and other extracellular polymerization products produced by fungus (Krumbein et al., 1992).

5.1.3.2 Change in pH

Fig. 5.6 demonstrated the pH variation in correspond to growth of fungi after deterioration effect. The initial pH of Czapek Dox medium was maintained at 7.3 ± 0.20. In the present investigation change in pH of the medium for *Aspergillus flavus* was noted as 9.48 ± 0.03 followed by *Penicillium oxalicum* (9.42 ± 0.01), *Aspergillus tamarii* (9.30 ± 0.03) and *Aspergillus niger* (9.25 ± 0.02) respectively (Fig. 5.6). Throughout the incubation period, calcium was released from the concrete samples that had been inoculated with fungi. As a result, pH of the fungal growth medium was increased i.e. alkaline. A study by Gu et al., (1998) found that the leaching of calcium ions from the concrete causes pH levels to rise in batch cultures that have been inoculated with *Fusarium* sp.

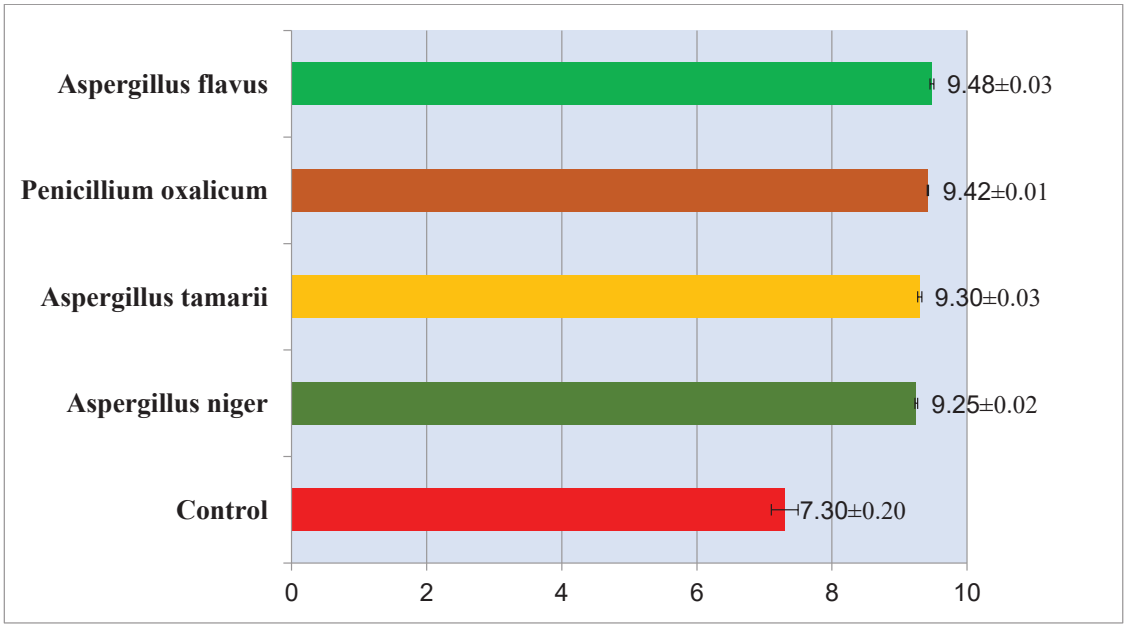

Fig. 5.6 pH variation of fungal growth medium (n = 3) after 30 days biodeterioration study.

5.1.3.3 Loss of weight

Loss of weight in percentages for the concrete pieces after 30 days of incubation is presented in Table 5.1. Concrete pieces infected with *Aspergillus niger*, *Aspergillus tamarii*, *Aspergillus flavus* and *Penicillium oxalicum* showed weight losses of 1.89 ± 0.08%, 2.84 ± 0.06%, 2.57 ± 0.08% and 2.45 ± 0.02% respectively and statistically significant ($p < 0.05$) compared to the control after 30 days of incubation period (Table 5.1). The secretion of organic acid by fungi deteriorates concrete materials through the formation of soluble and insoluble calcium complexes. These complexes were precipitated from the concrete materials, resulted in increased weight loss, calcium leaching, porosity and permeability (George et al., 2013; Giannantonio et al., 2009). According to the percentage weight loss it was observed that *Aspergillus tamarii* attributed maximum deterioration for concrete. Similar observation of reduction in weight of concrete after fungal infection has been cited in earlier studies (Bhattacharyya et al., 2022; Marquez-Penaranda et al., 2016; Gu et al., 1998).

Table 5.1 Weight loss percentage of concrete pieces (n = 3) after 30 days of incubation.

	Initial weight (gm)	Final weight (gm)	Difference (gm)	Loss (%)	Average loss (%)	Standard deviation (%)
Control	5.71 5.82 5.59	5.71 5.82 5.59	0 0 0	0 0 0	0	0
Aspergillus niger	6.64 6.77 5.56	6.51 6.64 5.46	0.13 0.13 0.10	1.95 1.92 1.80	1.89	0.08
Aspergillus tamarii	6.46 5.51 5.93	6.28 5.35 5.76	0.18 0.16 0.17	2.78 2.90 2.86	2.84	0.06
Aspergillus flavus	6.16 6.45 5.66	6.00 6.28 5.52	0.16 0.17 0.14	2.60 2.63 2.47	2.57	0.08
Penicillium oxalicum	6.51 6.14 5.37	6.35 5.99 5.24	0.16 0.15 0.13	2.46 2.45 2.42	2.45	0.02

5.1.3.4 Organic acid analysis

In the current investigation, organic acids that were present in the fungal medium and can damage concrete pieces were also found using high performance liquid chromatography (HPLC). The concentrations of standard oxalic, malic and fumaric acids as found is illustrated in Fig. 5.7, Fig. 5.8 and Fig. 5.9 were 120, 200 and 0.2 µg/ml respectively. At least three concentrations of standard compounds were diluted and analysed.

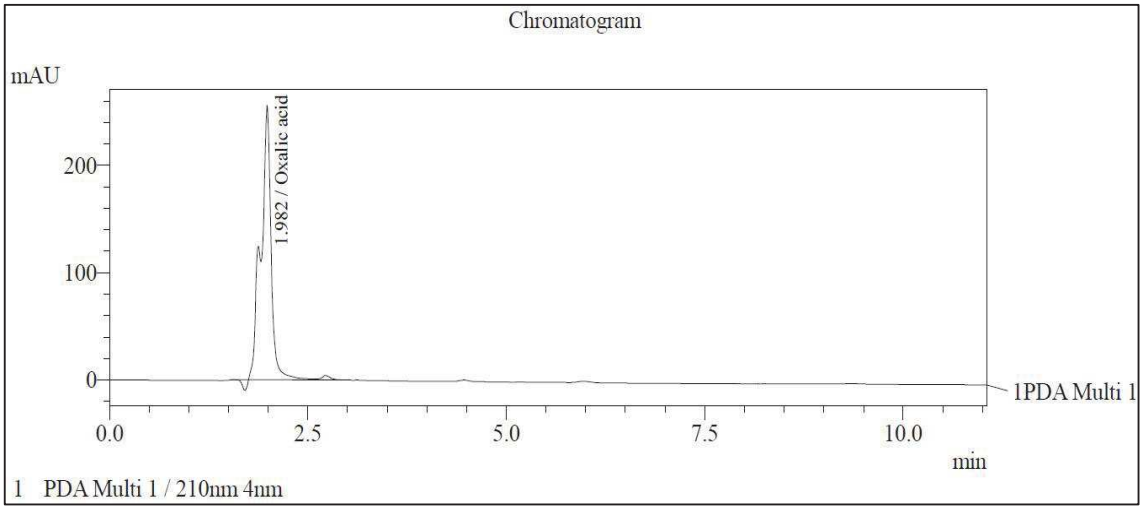

Fig. 5.7 HPLC chromatograph of standard oxalic acid solution (120 µg/ml).

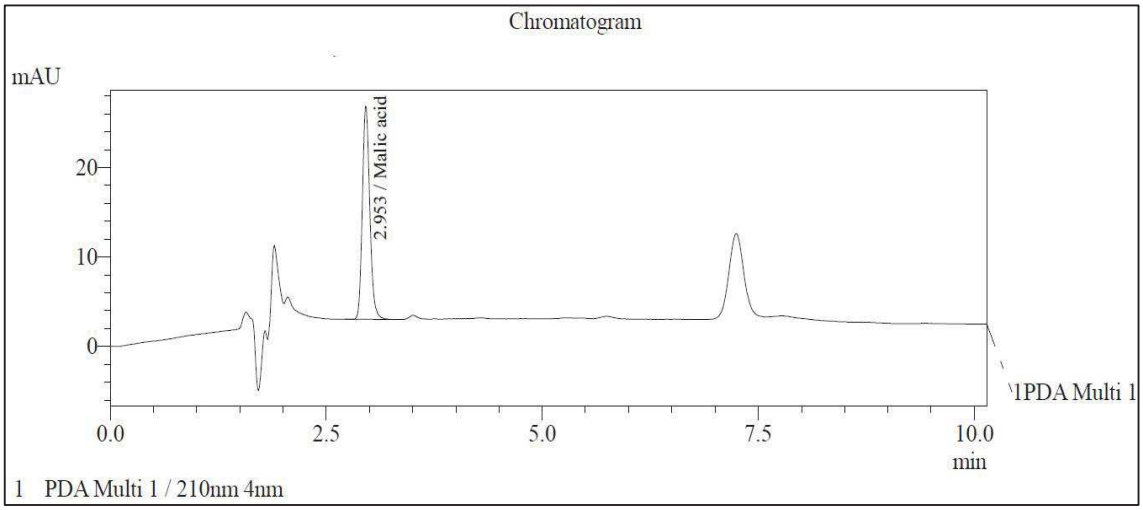

Fig. 5.8 HPLC chromatograph of standard malic acid solution (200 µg/ml).

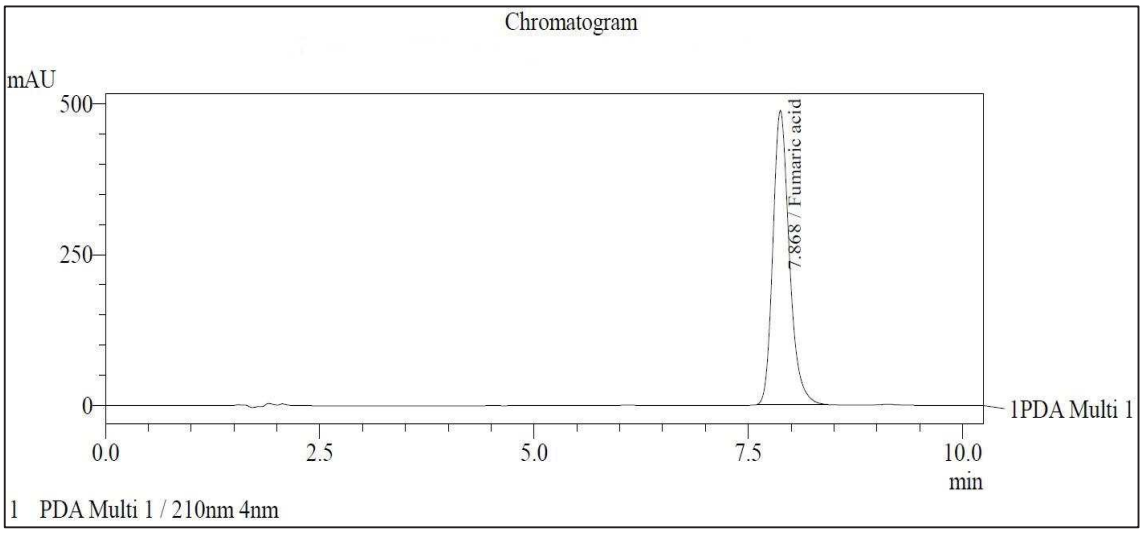

Fig. 5.9 HPLC chromatograph of standard fumaric acid solution (0.2 µg/ml).

The composition of organic acids in the liquid medium of *A. niger*, *A. tamarii, A. flavus and P. oxalicum* were also analysed. The results demonstrated that after 30 days of incubation the fungal medium contained oxalic acid, malic acid and fumaric acid respectively (Fig. 5.10, Fig. 5.11, Fig. 5.12 and Fig. 5.13). The contents of oxalic acid and malic acid with large differences between the solutions of *A. niger*, *A. tamarii and A. flavus* were detected. Moreover, *Aspergillus* sp. has greater ability to secrete organic acids and greater adaptation to acidic conditions compared to *P. oxalicum* (Li et al., 2016). These acid reacts with $Ca(OH)_2$ in concrete and forms insoluble salts (Eq. 1 and Eq. 2) such as calcium oxalate (CaC_2O_4) and calcium malate ($C_4H_4CaO_5$) and soluble salts (Eq. 3) calcium fumarate ($C_4H_2CaO_4$) responsible for expansion attack and leaching of calcium. Moreover, the majority of fungi like *Aspergillus*, *Penicillium* and *Fusarium* excreted acetic, citric, oxalic, malic, lactic, fumaric, gluconic, propionic, itaconic and succinic acids which resulted in corrosion of the concrete structures (Liaud et al., 2014).

$$Ca(OH)_2 + C_2H_2O_4 \rightarrow CaC_2O_4 + 2H_2O \text{.....} (1)$$

$$Ca(OH)_2 + C_4H_6O_4 \rightarrow C_4H_4CaO_5 + 2H_2O \text{.....} (2)$$

$$Ca(OH)_2 + C_4H_4O_4 \rightarrow C_4H_2CaO_4 + 2H_2O \text{.....} (3)$$

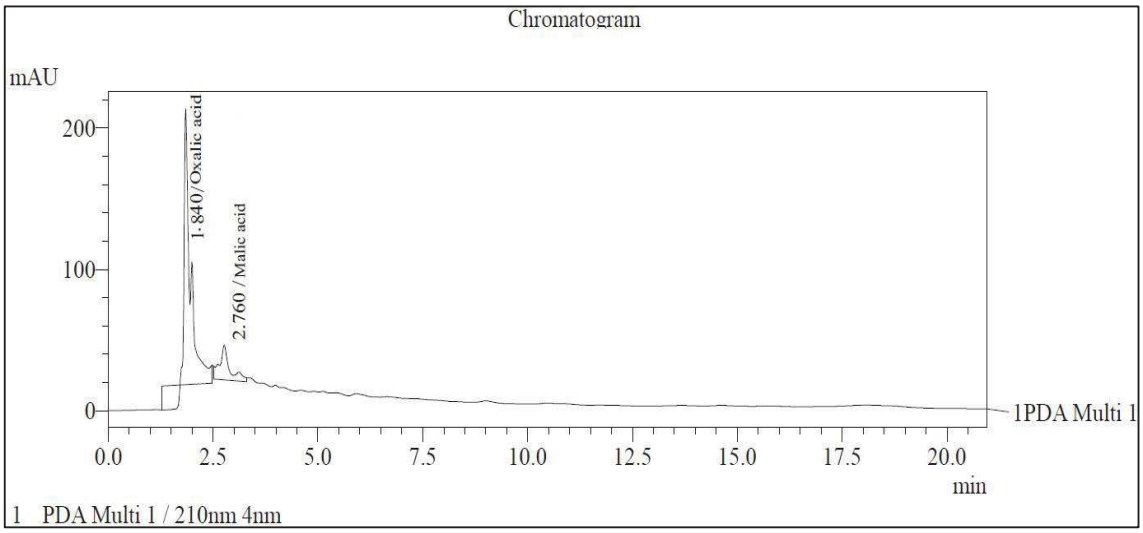

Fig. 5.10 HPLC chromatograph of *Aspergillus niger* infected medium.

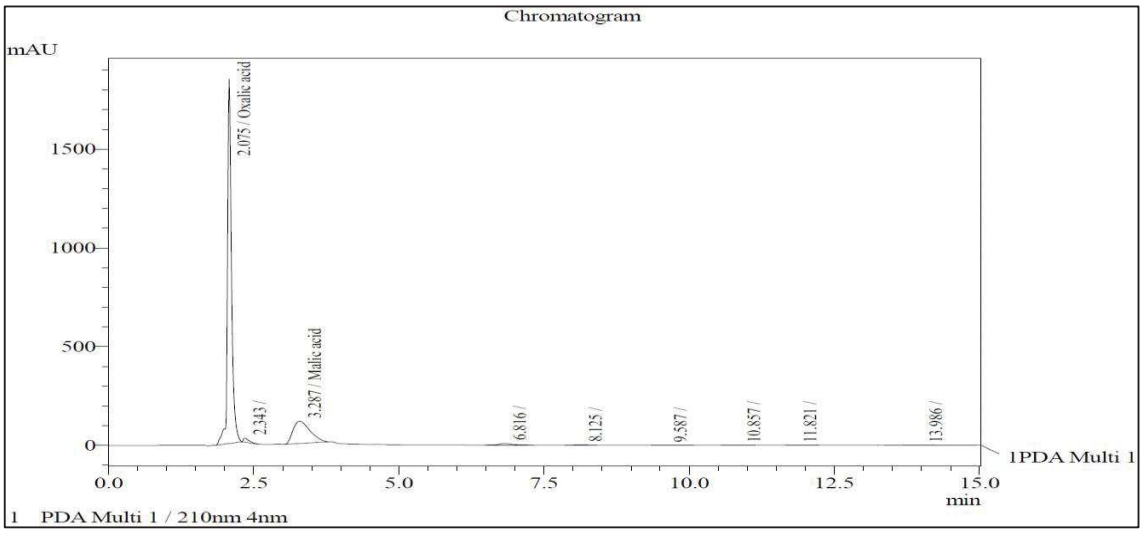

Fig. 5.11 HPLC chromatograph of *Aspergillus tamarii* infected medium.

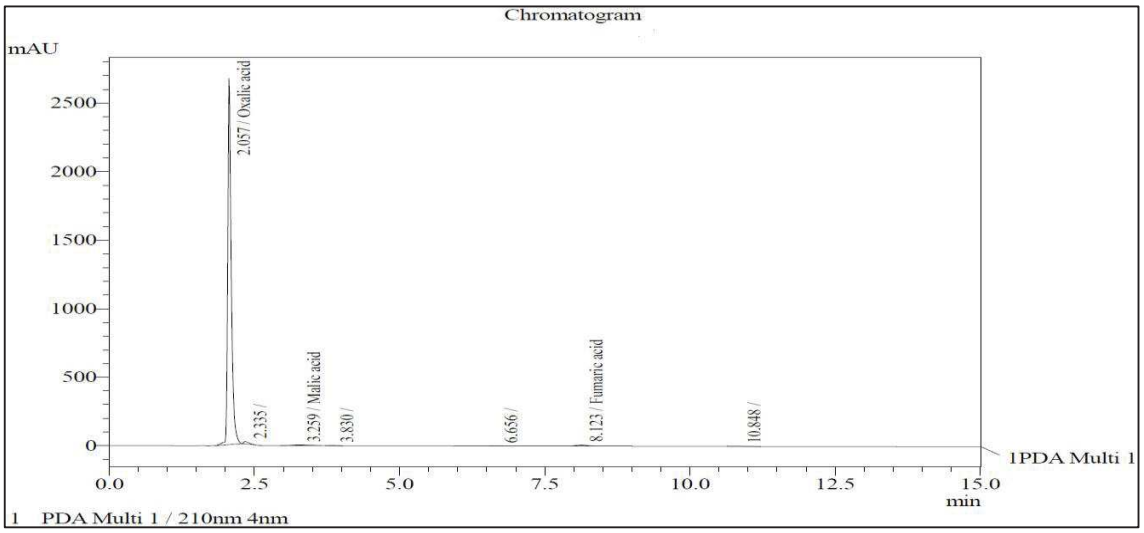

Fig. 5.12 HPLC chromatograph of *Aspergillus flavus* infected medium.

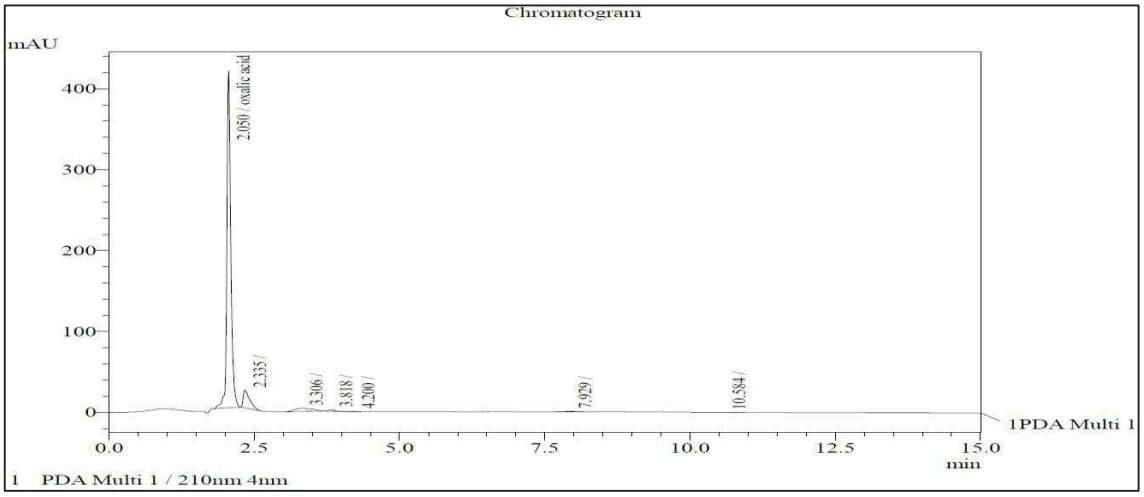

Fig. 5.13 HPLC chromatograph of *Penicillium oxalicum* infected medium.

5.1.3.5 SEM observation

5.1.3.5.1 Fungal growth

The control specimens showed no signs of fungi growing on them. After being exposed to *A. niger*, *A. tamarii*, *A. flavus*, and *P. oxalicum*, concrete samples were analysed under a scanning electron microscope to measure the degree of microbial colonisation. In the SEM pictures (Fig. 5.14), it was observed that spores grow quickly on concrete surfaces. Wiktor et al., (2009) demonstrated that fungal growth starts to develop after the first week of incubation on cement specimens confirmed by SEM observations.

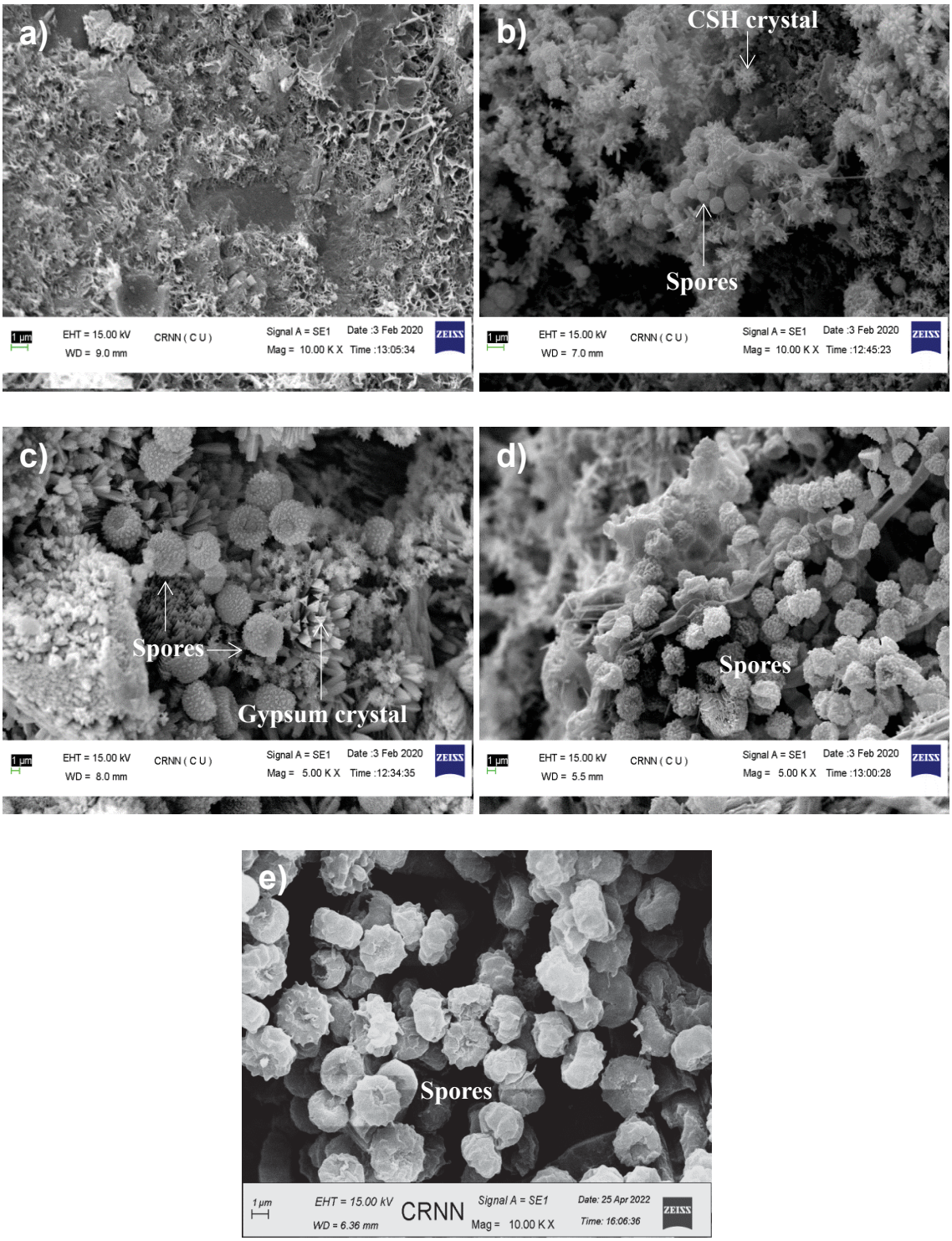

Fig. 5.14 SEM images of: a) Control; b) *Aspergillus niger*; c) *Aspergillus tamarii*; d) *Aspergillus flavus*; e) *Penicillium oxalicum* exposed concrete samples after 30 days of incubation.

5.1.3.5.2 Crack formation

A few interesting results were obtained with the specimens inoculated with *A. niger* and *A. tamarii*. SEM images (Fig. 5.15) clearly evidenced that fractured crack surfaces of *A. niger* and *A. tamarii* infected concrete samples were also observed by scanning electron microscope. Amann et al., (1990) studied earlier and found that the impact of microorganisms on concrete structures can be categorised based on how they affect the surfaces of the concrete and the matrices that produce cracking and encourage crack growth. Cracks in concrete are logical because it is permeable in nature and one of the natural vulnerabilities of concrete. Water and other salts percolating through these cracks initiate corrosion, and reduce the concrete's lifespan. In contrast to our present observations, Gaylarde et al., (2003) exhibited deteriorated surface of a concrete bridge pier due to fungal effect.

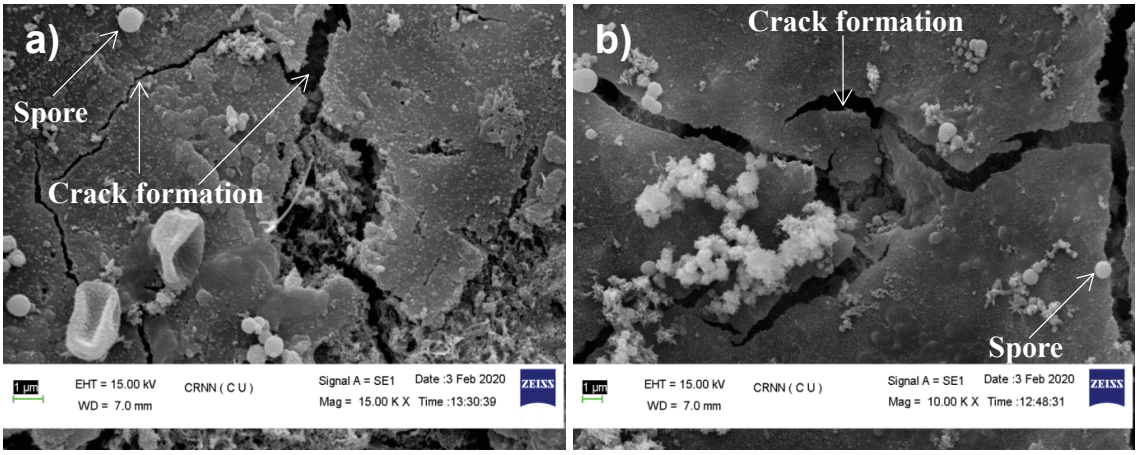

Fig. 5.15 SEM images of crack formation on: a) *A. tamarii*; b) *A. niger* exposed concrete samples.

5.1.3.5.3 Ettringite formation

SEM images of *A. tamarii* infected concrete samples depicted the formation of ettringite needles (Fig. 5.16). Fungi can secrete enzymes which interact with amino acids, that released by fungi, to generate thin needles of ettringite. Ettringite formation in hardened concrete has been reported that a potential property to lead for crack development and perhaps the reason for one of the mechanisms causing fungal influenced deterioration of concrete (Hanehara and Oyamada 2010).

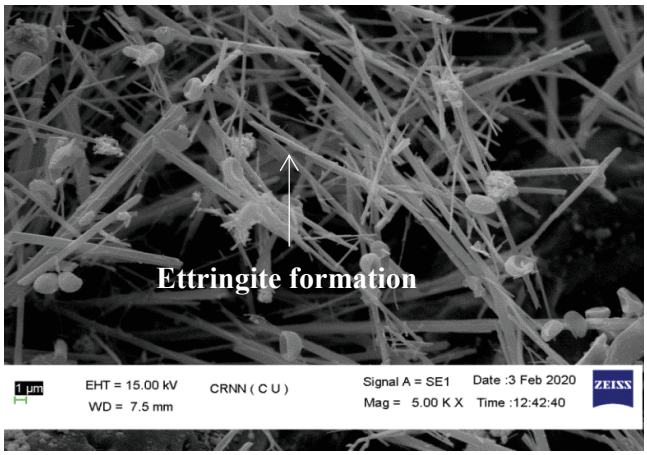

Fig. 5.16 Ettringite formation in *A. tamarii* infected concrete samples.

5.1.3.6 Variation in elemental composition

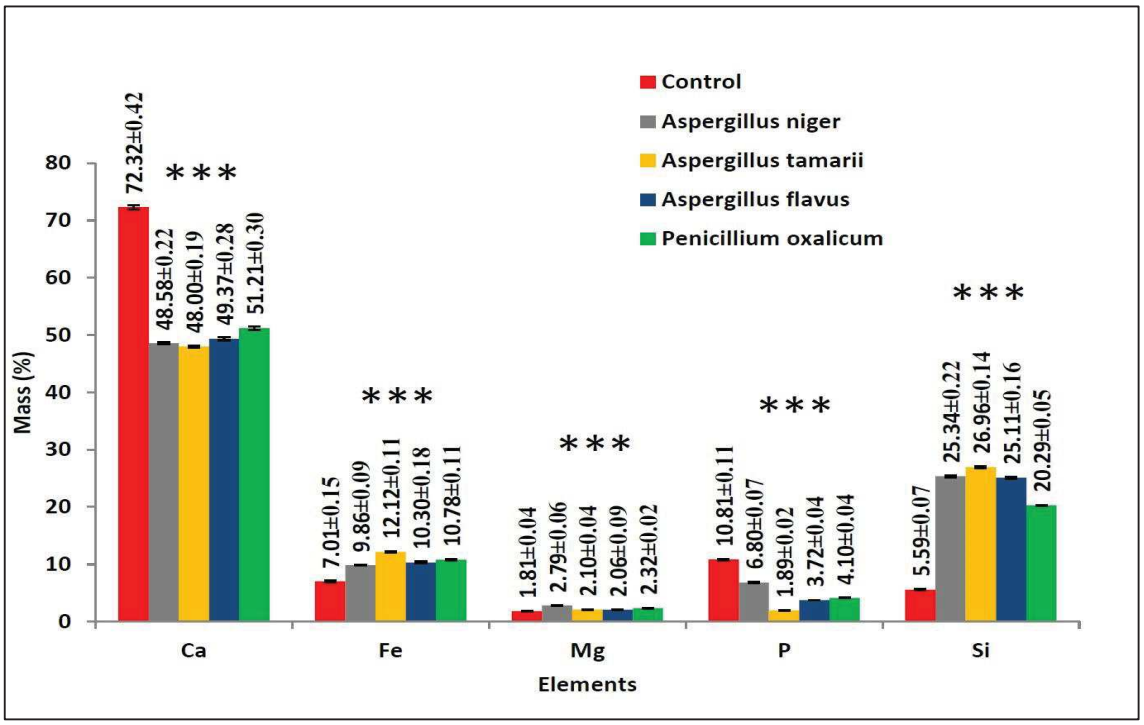

Fig. 5.17 Mass fraction of different elements of concrete pieces (n = 3) after 30 days of incubation. The asterisks above columns indicate the *p*-value (*t*-test between the control and fungal infected sample): ***, $p < 0.001$.

The percentage of calcium was decreased with time for fungal infected samples. The calcium percentage of *A. niger*, *A. tamarii*, *A. flavus* and *P. oxalicum* inoculated concrete were decreased ($p < 0.001$) to 48.58 ± 0.22%, 48.00 ± 0.19%, 49.37 ± 0.28% and 51.21 ± 0.30%

respectively as compared to the control specimens (72.32 ± 0.42%). Also, it was shown earlier in the literature that fungi contributed for the leaching of calcium from the concrete cube (Sanchez-Silva et al., 2008). The primary elements in concrete found were silicon, and calcium, with phosphorous, magnesium and iron present in small quantity (Fig. 5.17). In addition, the level of other elements like magnesium and iron were slightly increased ($p < 0.001$) after 30 days of deterioration study. The calcium leaching rate increased over time, which resulted in a rise in silicon concentration (Fig. 5.17). The increase of SiO_2 indicated the formation of very porous SiO_2 gels in the outermost degraded zones. Besides these, trace levels of manganese, zinc, chromium, titanium and nickel were noted initially but these eventually faded over time or consumed by the fungus as their microbial nutrients for metabolic activity for their growth.

With the view point of weight loss, fungal growth observation, crack and ettringite formation, color changes and pH of fungal medium, excretion of organic acids, change in elemental composition, it may be confirmed that *Aspergillus tamarii* enhanced maximum deterioration effect on concrete in different ways. Hence, all subsequent investigations in the present research were carried out with *Aspergillus tamarii* only as candidate microorganism.

5.2 Biodeterioration study

5.2.1 Weight loss

Experimental control concrete cubes exhibited weight losses of 0.59 ± 0.01%, 0.63 ± 0.01% and 0.85 ± 0.02% for M20 grade and 0.26 ± 0.11%, 0.39 ± 0.01% and 0.53 ± 0.12% for M40 grade concrete respectively (Table 5.2 and Table 5.4) after 6 months of incubation because Czapek Dox medium contains various compounds (chlorides or possibly nitrates) which accelerate calcium leaching (Wiktor et al., 2009). The weight loss in the M20 and M40 graded concrete cubes were studied after exposed with *Aspergillus tamarii* in the laboratory condition. After incubation of 2, 4 and 6 months, 1.61 ± 0.06%, 1.78 ± 0.14% and 2.22 ± 0.04% weight losses have been observed for M20 graded concrete cubes whereas for M40 graded cubes 0.53 ± 0.11%, 0.78 ± 0.01% and 1.20 ± 0.01% weight losses respectively as shown in Table 5.3 and Table 5.5.

Table 5.2 Percentage weight loss for M20 grade control concrete cubes (n = 3).

Time period	Weight (Kg)		Weight loss (Kg)	% loss	Average loss (%)	Standard deviation (%)
	Initial	Final				
After 2 month	0.336 0.331 0.340	0.328 0.329 0.338	0.002 0.002 0.002	0.59 0.60 0.58	0.59	0.01
After 4 month	0.315 0.325 0.310	0.313 0.323 0.308	0.002 0.002 0.002	0.63 0.62 0.65	0.63	0.01
After 6 month	0.352 0.340 0.360	0.349 0.338 0.357	0.003 0.003 0.003	0.85 0.88 0.83	0.85	0.02

Table 5.3 Percentage weight loss for M20 grade *A. tamarii* infected concrete cubes (n = 3).

Time period	Weight (Kg)		Weight loss (Kg)	% loss	Average loss (%)	Standard deviation (%)
	Initial	Final				
After 2 month	0.320 0.315 0.356	0.315 0.310 0.350	0.005 0.005 0.006	1.56 1.59 1.68	1.61	0.06
After 4 month	0.300 0.346 0.310	0.295 0.340 0.304	0.005 0.006 0.006	1.67 1.73 1.94	1.78	0.14
After 6 month	0.320 0.308 0.316	0.313 0.301 0.309	0.007 0.007 0.007	2.18 2.27 2.21	2.22	0.04

Table 5.4 Percentage weight loss for M40 grade control concrete cubes (n = 3).

Time period	Weight (Kg)		Weight loss (Kg)	% loss	Average loss (%)	Standard deviation (%)
	Initial	Final				
After 2 month	2.495 2.480 2.480	2.485 2.475 2.475	0.010 0.005 0.005	0.40 0.20 0.20	0.26	0.11
After 4 month	2.515 2.520 2.535	2.505 2.510 2.525	0.010 0.010 0.010	0.40 0.40 0.39	0.39	0.01

After 6 month	2.490 2.485 2.520	2.475 2.470 2.510	0.015 0.015 0.010	0.60 0.60 0.39	0.53	0.12

Table 5.5 Percentage weight loss for M40 grade *A. tamarii* infected concrete cubes (n = 3).

Time period	Weight (kg)		Weight loss (kg)	% loss	Average loss (%)	Standard deviation (%)
	Initial	Final				
After 2 month	2.485 2.495 2.535	2.470 2.485 2.520	0.015 0.010 0.015	0.60 0.40 0.59	0.53	0.11
After 4 month	2.525 2.545 2.530	2.505 2.525 2.510	0.020 0.020 0.020	0.79 0.78 0.79	0.78	0.01
After 6 month	2.505 2.510 2.500	2.475 2.480 2.470	0.030 0.030 0.030	1.19 1.19 1.20	1.20	0.01

All these results tabulated in Table 5.2 through Table 5.5 are plotted in bar diagram which is shown in Fig. 5.18.

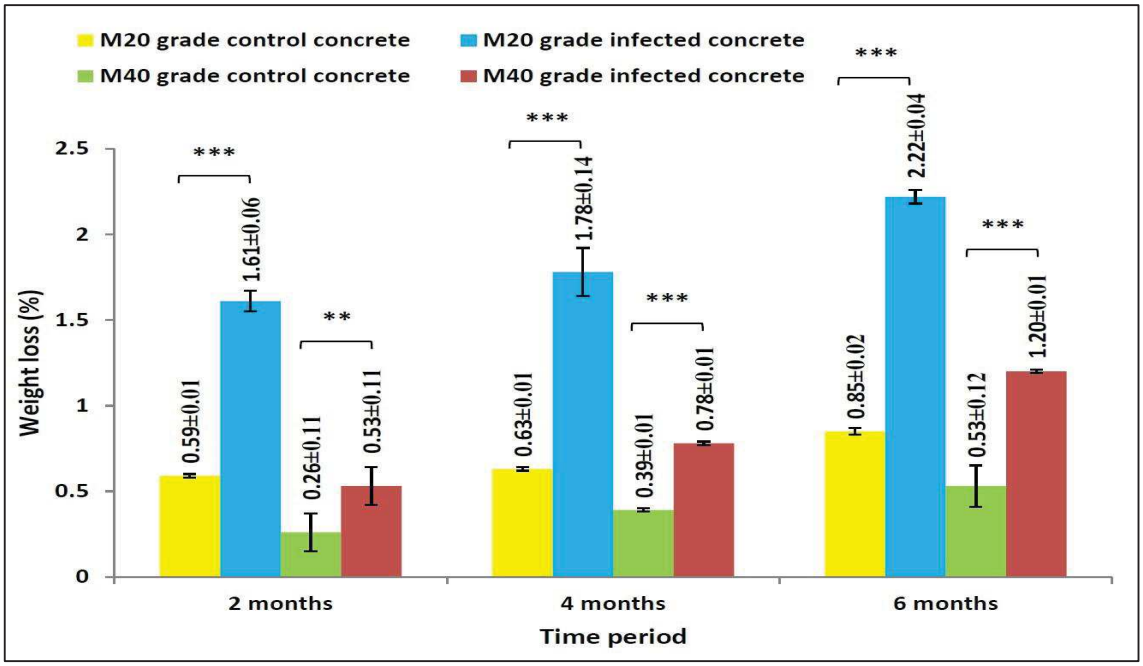

Fig. 5.18 Weight loss of M20 and M40 grade control and infected concrete cubes (n = 3). The asterisks above columns indicate the *p*-value (*t*-test between the control and infected sample): ** $p < 0.01$, *** , $p < 0.001$.

It was observed that the weight loss were increased in every time interval for M20 and M40 grade concrete cubes after infected with *A. tamarii* (Fig. 5.18). Interestingly the weight loss in M20 grade concrete cubes was more compared to the M40 grade cube in every interval because M40 grade concrete is less permeable than M20 grade concrete. The decrease in permeability helps in improving sulfate and chemical attack resistance, resistance to corrosion and chloride penetration. A similar observation were noticed earlier by Gu et al., (1998) using *Fusarium* sp. in concrete sample, where after 2 and 4 months, 1.5 and 6% weight losses were previewed. However no results are cited so far with *A. tamarii* and composite effects. In another study by Marquez-Penaranda et al., (2016) an attempt to use *Acidithiobacillus thiooxidans* and *Halothiobacillus neapolitanus* in concrete (M30) samples showed that 0.5%, 1.8%, 1.8% and 0.1%, 0.3%, 1.3% of weight losses after an incubation period of 2, 4 and 6 months respectively. The weight loss of concrete cube indicates towards the deterioration of concrete.

5.2.2 Compressive strength loss

The average peak load at which the concrete cube was broken down, decreases in every time period for fungal specimens as well as control specimens (Table 5.6 and Table 5.7). This maximum breaking load divided by the cross-sectional area gives the compressive strength for concrete cubes. The average of the three values for every two month interval was taken as the compressive strength of concrete. So, the compressive strength of the low and high graded control concrete cubes after 2, 4 and 6 months of studied period were 19.20 ± 0.14, 18.78 ± 0.09, 18.50 ± 0.08, 43.90 ± 0.08, 43.66 ± 0.05 and 43.28 ± 0.05 N/mm^2 respectively (Table 5.6 and Table 5.7). Also the average strength of *A. tamarii* infected M20 grade concrete cubes after 6 months was found to be decreased less (19.74 ± 0.11 N/mm^2 to 14.77 ± 0.06 N/mm^2) compared to M40 grade concrete cubes (44.00 ± 0.30 N/mm^2 to 33.29 ± 0.09 N/mm^2).

Table 5.6 Compressive strength (N/mm^2) loss for M20 grade control and infected concrete cubes (n = 3).

	Control concrete cube				Infected concrete cube			
Time period	Load (KN)	Compressive strength (N/mm^2)	Average strength (N/mm^2)	Standard deviation (N/mm^2)	Load (KN)	Compressive strength (N/mm^2)	Average strength (N/mm^2)	Standard deviation (N/mm^2)
Initial (after 28 days curing)	49.5 49.0 49.5	19.80 19.60 19.80	19.74	0.11	49.5 49.0 49.5	19.80 19.60 19.80	19.74	0.11
After two month	48.1 48.3 47.6	19.24 19.32 19.04	19.20	0.14	44.3 44.0 43.2	17.72 17.60 17.28	17.53	0.22
After four month	47.1 46.7 47.1	18.84 18.68 18.84	18.78	0.09	37.9 38.6 38.0	15.16 15.44 15.20	15.26	0.15
After six month	46.3 46.0 46.4	18.52 18.40 18.56	18.50	0.08	37.1 36.8 36.8	14.84 14.74 14.72	14.77	0.06

Table 5.7 Compressive strength (N/mm^2) loss for M40 grade control and infected concrete cubes (n = 3).

	Control concrete cube				Infected concrete cube			
Time period	Load (KN)	Compressive strength (N/mm^2)	Average strength (N/mm^2)	Standard Deviation (N/mm^2)	Load (KN)	Compressive strength (N/mm^2)	Average strength (N/mm^2)	Standard deviation (N/mm^2)
Initial (after 28 days curing)	453.9 458.5 407.8	45.39 45.85 40.78	44.00	0.30	438.9 443.5 437.8	43.89 44.35 43.78	44.00	0.30
After two month	438.0 439.4 439.5	43.80 43.94 43.95	43.90	0.08	410.1 413.5 412.8	41.01 41.35 41.28	41.21	0.18
After four month	437.1 436.0 436.7	43.71 43.60 43.67	43.66	0.05	351.3 346.5 349.6	35.13 34.65 34.96	34.91	0.24
After six month	433.4 432.4 432.5	43.34 43.24 43.25	43.28	0.05	333.0 333.8 331.9	33.30 33.38 33.19	33.29	0.09

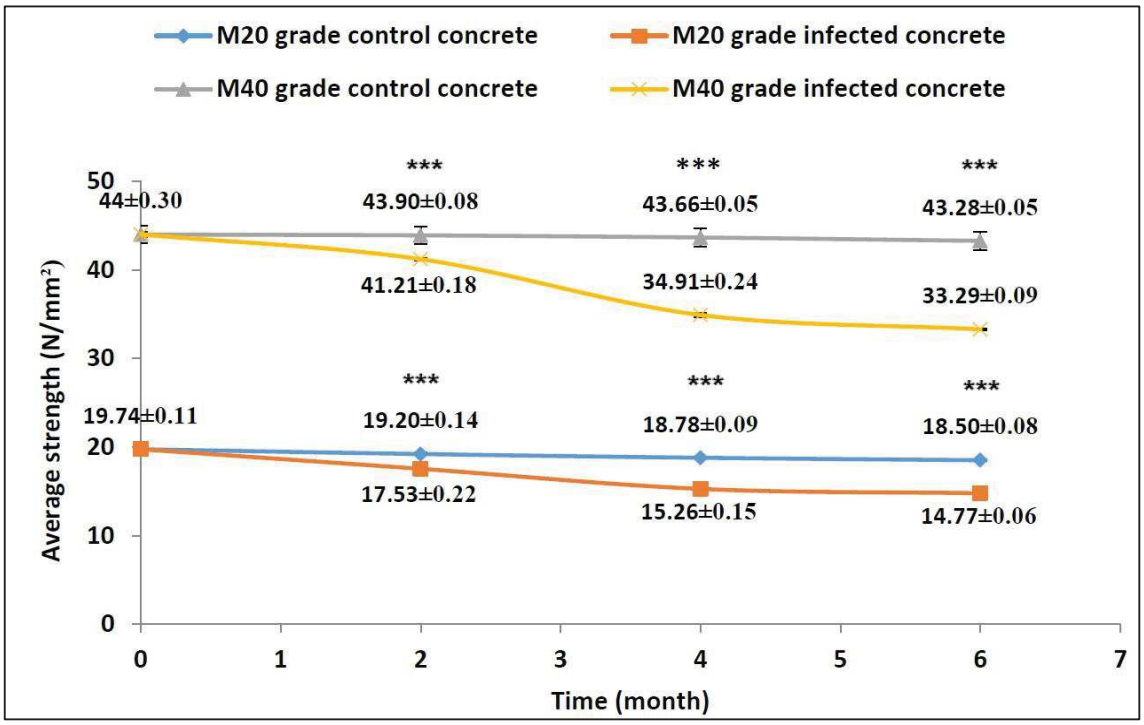

Fig. 5.19 Compressive strength (N/mm^2) loss of M20 and M40 grade concrete cubes (n = 3) after exposure to *A. tamarii.* The asterisks above lines indicate the *p*-value (*t*-test between the control and infected concrete sample): ***, $p < 0.001$.

Experimental data showed that the inoculation with *A. tamarii* accelerates the degradation process which reduced the cubes compressive strength (Fig. 5.19). Similar comparative findings in respect of compressive strength analysis are found in a different study of sewer samples, where microbial production of acids reduced compressive strength (Davis et al., 1998). The present study demonstrates that *A. tamarii* grew on the cube surface and penetrates with their hyphae as shown in SEM images (Fig. 5.27). This is likely one of the main causes of the compressive strength decreasing as incubation time increases (Aldosari et al., 2019).

Furthermore the percentage strength loss of 2, 4 and 6 months infected concrete samples are 6.34 ± 0.12%, 20.66 ± 0.26%, 24.34 ± 0.16% for M40 grade and 11.20 ± 0.04%, 22.70 ± 0.10%, 25.17 ± 0.12% for M20 grade respectively (Table 5.8). Interestingly, as may be expected, concrete samples with higher strengths were less susceptible to strength loss as well as less permeable compared to the lower grade. Marquez-Penaranda et al., (2016) attempted to use *A. thiooxidans* and *H. neapolitanus* in concrete (M30) samples showed that 3%, 12%, 18% and 4%, 11%, 12% of compressive strength was observed after incubation of 2, 4, 6

months respectively with respect to control. Hence it is established that fungal infected concrete are liable for losing the compressive strength in sizeable quantity.

Table 5.8 Percentage strength loss of M20 and M40 graded infected concrete cubes (n =3).

Time period (months)	Compressive strength loss (%)	
	M20 grade	M40 grade
2 months	11.20	6.34
4 months	22.70	20.66
6 months	25.17	24.34

5.2.3 Organic acid analysis

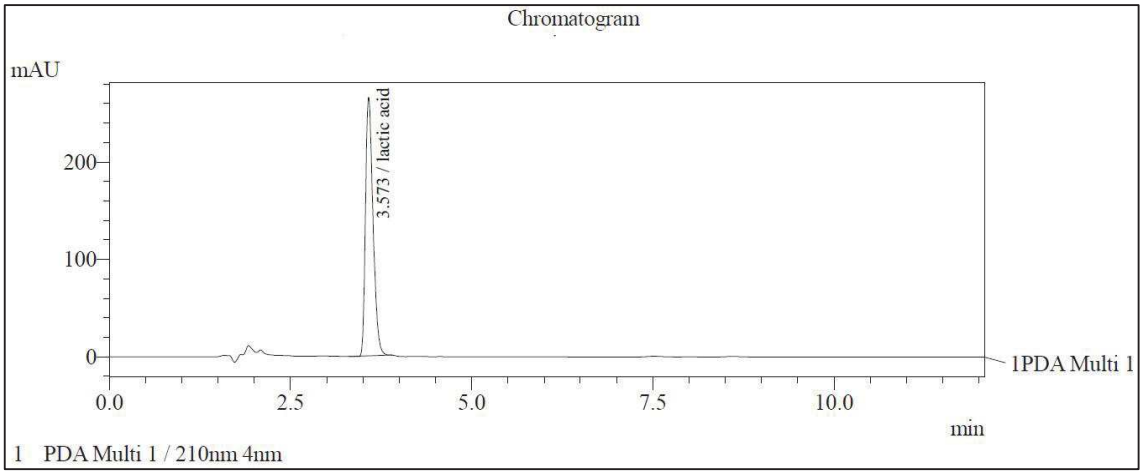

Fig. 5.20 HPLC chromatograph of standard lactic acid solution (1000 µg/ml).

The organic acids which present and shown in Fig. 5.22 in the *A. tamarii* infected medium that probably damage the concrete cubes were found using high performance liquid chromatography. The HPLC chromatograph of standard lactic (1000 µg/ml) and acetic (625 µg/ml) acids were shown in Fig. 5.20 and Fig. 5.21 respectively whereas chromatograph of standard oxalic (120 µg/ml) and malic (200 µg/ml) acids illustrated in Fig. 5.7 and Fig. 5.8. At least three concentrations of standard compounds were diluted and analysed.

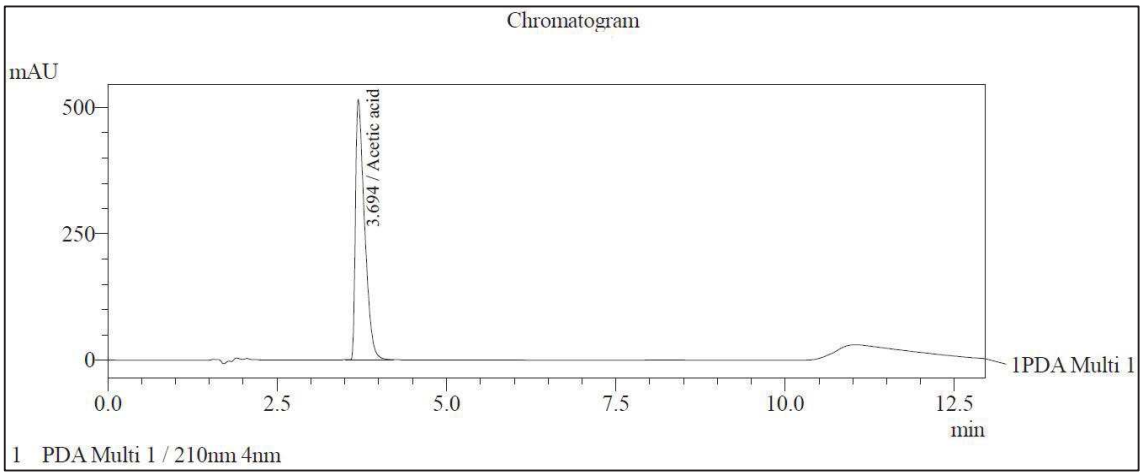

Fig. 5.21 HPLC chromatograph of standard acetic acid solution (625 µg/ml).

HPLC analysis for organic acid production after 6 months indicated four significant peaks identified as oxalic acid, malic acid, lactic acid and acetic acid (Fig. 5.22). Peak identification was established when sample peak retention times matched those of pure organic acid standards. Only two organic acid were found in the earlier (after 1 month), while four acid were found (Fig. 5.22) after 6 months. During the growth process *A. tamarii* continuously secretes organic acids to regulate pH of its surroundings, which might contribute in the promotion of its own growth.

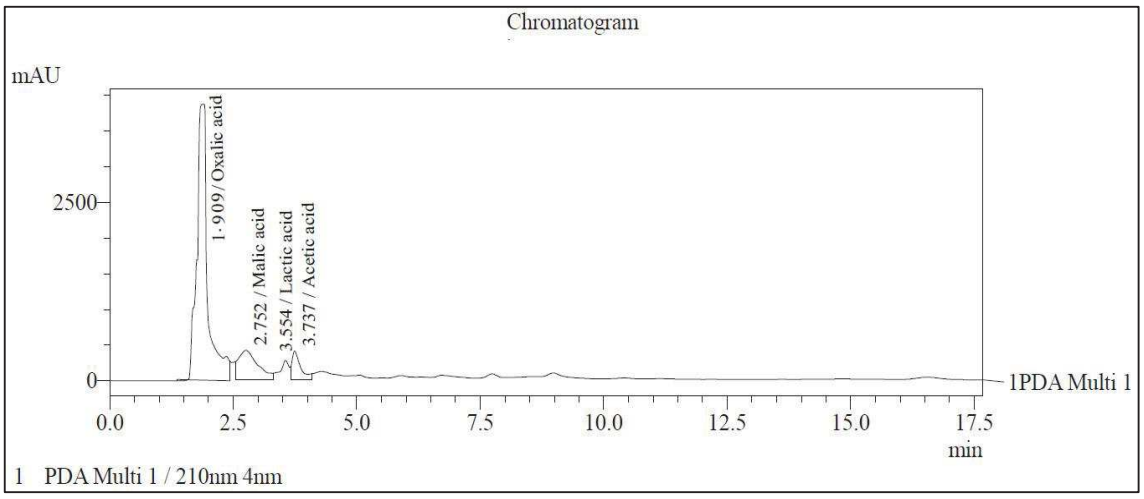

Fig. 5.22 HPLC chromatograph of 6 months liquid medium of *A. tamarii* infected concrete cubes.

It was also observed that oxalic acid dominates the acidity (from the fungus) due to its high concentration. Similar type of findings was also noticed in liquid culture medium of edible

fungi and showed that oxalic acid was present in greater quantity followed by malic acid and citric acid (Yu et al., 2020). Also the contents of oxalic acid and malic acid were also increased after 6 months of incubation compared to 1 month study. These acids could react with calcium hydroxide [$Ca(OH)_2$] in concrete and forms soluble salts (Eq. 3 and Eq. 4) such as calcium lactate [$Ca_3(C_6H_5O_7)_2$] and calcium acetate [$(CH_3COO)_2Ca$], which results in calcium leaching and insoluble salts (Eq. 1 and Eq. 2) i.e. calcium oxalate (CaC_2O_4) and calcium malate ($C_4H_4CaO_5$) causing the entire concrete structure to expand under pressure. SEM images of the biodeteriorated concrete samples revealed precipitation of calcium oxalate crystal, which was associated with and encrusting fungal hyphae [Fig. 5.27(d)]. Mycogenic mineral crystallisation on such a large scale might be considered an expansion attack on concrete, leading to increased cracking [Fig. 5.27(e)] and a sharp decline in the concrete mechanical resistance (Fig. 5.19).

$$Ca(OH)_2 + C_2H_2O_4 \rightarrow CaC_2O_4 + 2H_2O \quad \text{(1)}$$

$$Ca(OH)_2 + C_4H_6O_4 \rightarrow C_4H_4CaO_5 + 2H_2O \quad \text{(2)}$$

$$3Ca(OH)_2 + 2C_6H_8O_7 \rightarrow Ca_3(C_6H_5O_7)_2 + 6H_2O \quad \text{(3)}$$

$$Ca(OH)_2 + 2CH_3COOH \rightarrow (CH_3COO)_2Ca + 2H_2O \quad \text{(4)}$$

5.2.4 Variation in elemental composition

EDXRF analysis was conducted to determine the elements that were present in the concrete cube. Silicon and calcium were the main constituents in concrete, with magnesium, aluminium, and iron being present to a lesser level (Fig. 5.23 and Fig. 5.24). During the progress of time, the calcium content found to be decreased ($p < 0.001$). The percentage of calcium of M40 grade control concrete was 34.24 ± 0.06% and after 6 month fungal infection it reached 25.36 ± 0.05% (Fig. 5.24). Similarly, calcium concentration in M20 grade control concrete was 69.63 ± 0.12% and after 2, 4 and 6 month fungal exposure interval it reached 43.63 ± 0.18%, 31.46 ± 0.22% and 15.68 ± 0.09% respectively (Fig. 5.23). Moreover, it has been also noted that fungal activity helps in the calcium leaching process from concrete cubes (Sanchez-Silva and Rosowsky 2008). Obviously, the rate of calcium leaching was less in M40 grade cube that can explain on the basis of compressive strength of the concrete cube and also porosity of the M20 grade concrete cubes for hyphae penetration to the substrate was more compared to the M40 graded cubes.

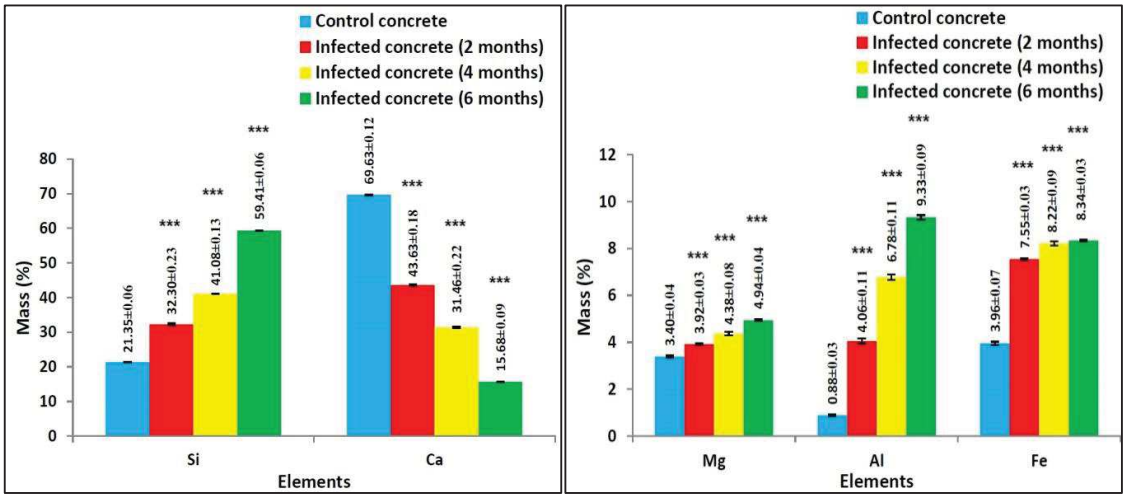

Fig. 5.23 Mass fraction of different elements for control and *A. tamarii* infected M20 grade concrete samples (n = 3). The asterisks above columns indicate the *p*-value (*t*-test between the control and infected concrete sample): ***, $p < 0.001$.

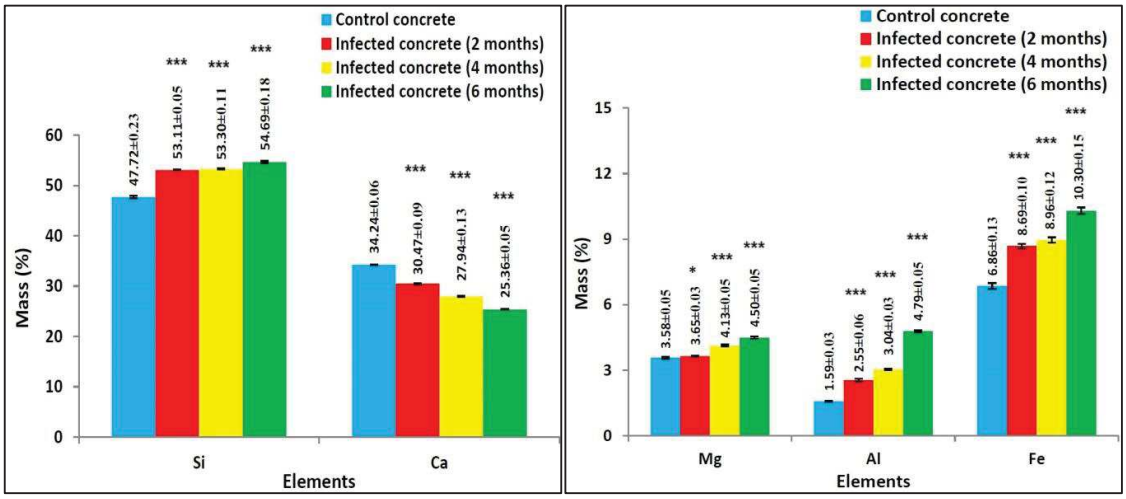

Fig. 5.24 Mass fraction of different elements for control and *A. tamarii* infected M40 grade concrete samples (n = 3). The asterisks above lines indicate the *p*-value (*t*-test between the control and infected concrete sample): *, $p < 0.05$, ***, $p < 0.001$.

Also, during a six-month study on deterioration, the concentration of other elements like aluminium, magnesium, silicon, and iron was increased (Fig. 5.23 and Fig. 5.24). As the calcium leaching rate accelerated over time, silicon content also increased ($p < 0.001$) to this effect. It has been presumed that the increased ($p < 0.001$) concentration of iron and magnesium in the solution perhaps came from the Czapek Dox medium used which was for the experiment. The increase of SiO_2 and Al_2O_3 indicated the production of very porous SiO_2

and Al gels in the outermost damaged zones. In addition to these, trace amounts of chromium, manganese, nickel, titanium and zinc were noted initially but due to leaching these also faded over time. Similar type of research work were also done by Yakovleva et al., (2018) and compared to present study as noted after 28 days of fungal inoculation. The percentage of calcium decreased followed by increment of silicon, iron, aluminium and magnesium after the above period.

5.2.5 Variation in functional groups

The FTIR characterisation of *A. tamarii* that infected M20 and M40 grade concrete after 3 and 6 months was compared with the findings of the control sample in the present study. Fig. 5.25 and Fig. 5.26 shows FTIR analysis plot for *A. tamarii* infected M20 and M40 grade concrete in the range 4000-400 cm^{-1}. The IR spectrum for control concrete showed the presence of portlandite [$Ca(OH)_2$] at 3640 cm^{-1} (O-H stretching vibrations) which was vanished in *A. tamarii* infected samples. The transformations of portlandite occur during the leaching and carbonation of concrete. During the ageing of concrete, carbonation is a natural process of Portland cement (Wiktor et al., 2009). Calcium carbonate was formed at the time of carbonation process. A strong symmetric stretching absorption band (C-O) of calcite at wavenumber 1400, 874 and 611 cm^{-1} became medium in *A. tamarii* infected M40 grade concrete samples (Fig. 5.26). Also this band was absent in M20 grade concrete after 3 and 6 months fungal inoculation (Fig. 5.25).

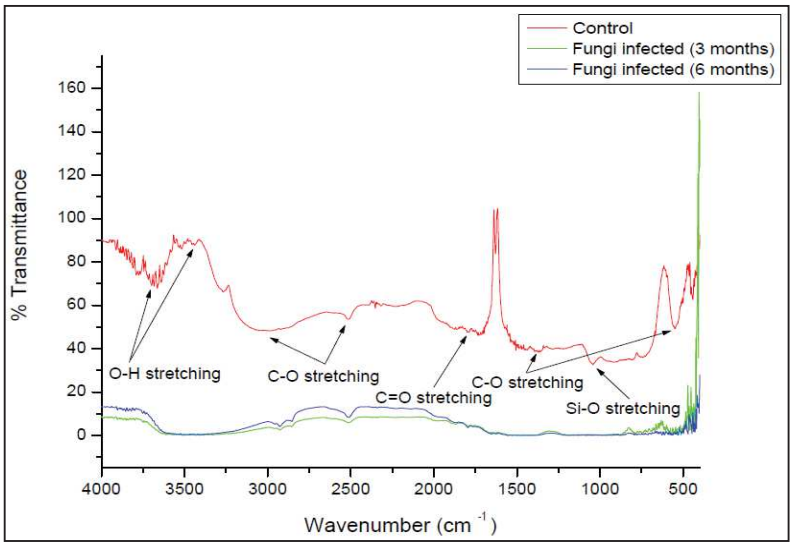

Fig. 5.25 Mid-infrared spectra of control and *A. tamarii* infected M20 grade concrete in the range 4000-400 cm^{-1}.

The control sample showed an envelope-shaped medium with symmetric band of 3450 cm^{-1} attributable to O-H, which after 3 and 6 months of incubation became weak and very weak for M40 grade concrete and ultimately totally absent in M20 grade concrete. This O-H band can be misleading because the sample has absorbed water. Hydrogen bonding might alter the band shape and position. A weak asymmetric stretching band (Si-O) from C-S-H of the quartz (crystalline silica) was evident from 980 cm^{-1} to 1000 cm^{-1}, that result extremely weak in high graded concrete and totally disappearing in low graded concrete after 3 and 6 months biodeterioration study (Fig. 5.25 and Fig. 5.26). The shift in the Si-O band seen in the current study is comparable with the research work of Ghosh et al., (1980) and Wiktor et al., (2011) in which Si-O polymerized to orthosilicate units (SiO_4^{4-}) at the time of weathering process.

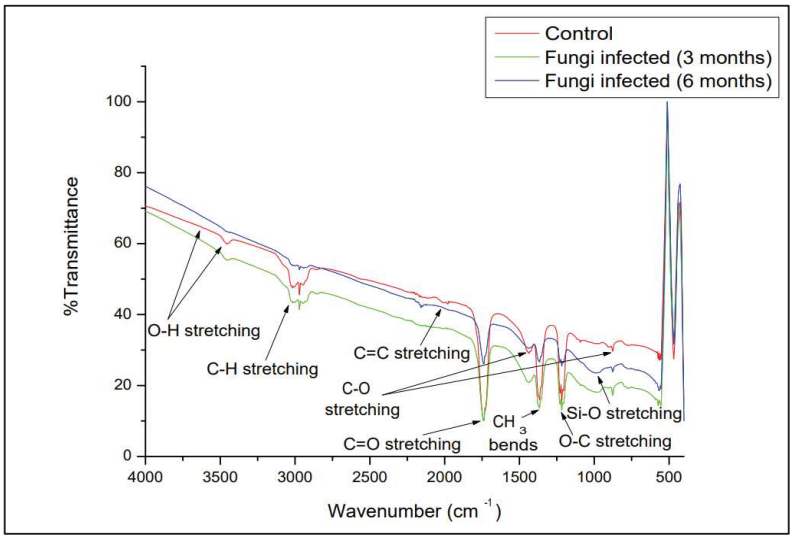

Fig. 5.26 Mid-infrared spectra of control and *A. tamarii* infected M40 grade concrete in the region 4000-400 cm^{-1}.

Water, carbonate, and silicate were the three main bands found from FTIR analysis of concrete deterioration (Fig. 5.25 and Fig. 5.26). The control sample also had certain other bands, such as O-C (1200 cm^{-1}), CH_3 (1350 cm^{-1}), C=O (1730 cm^{-1}), and C-H (3000 cm^{-1}) which became moderate in 6 months *A. tamarii* infected M40 grade and absent in the M20 grade concrete sample because these bands were gradually weakened and then broken by the action of fungus over time. It relies on the concrete's pH, texture, mineral content, and relative percentage of mineral contents. This was directly related to the variation in concrete cube weight loss and compressive strength loss. As the bands found to be weakened or disappeared, the hydration products changed, weakening the matrix and crack formation occurs [Fig. 5.27(e)]. Salts and water entering by these concrete cracks lead to corrosion

(Ilinskaya et al., 2018). The weight and compressive strength were thereby reduced consecutively.

5.2.6 Microscopic observation

5.2.6.1 Scanning electron microscopy

Experimental results on the basis of SEM analysis has been shown in Fig. 5.27.

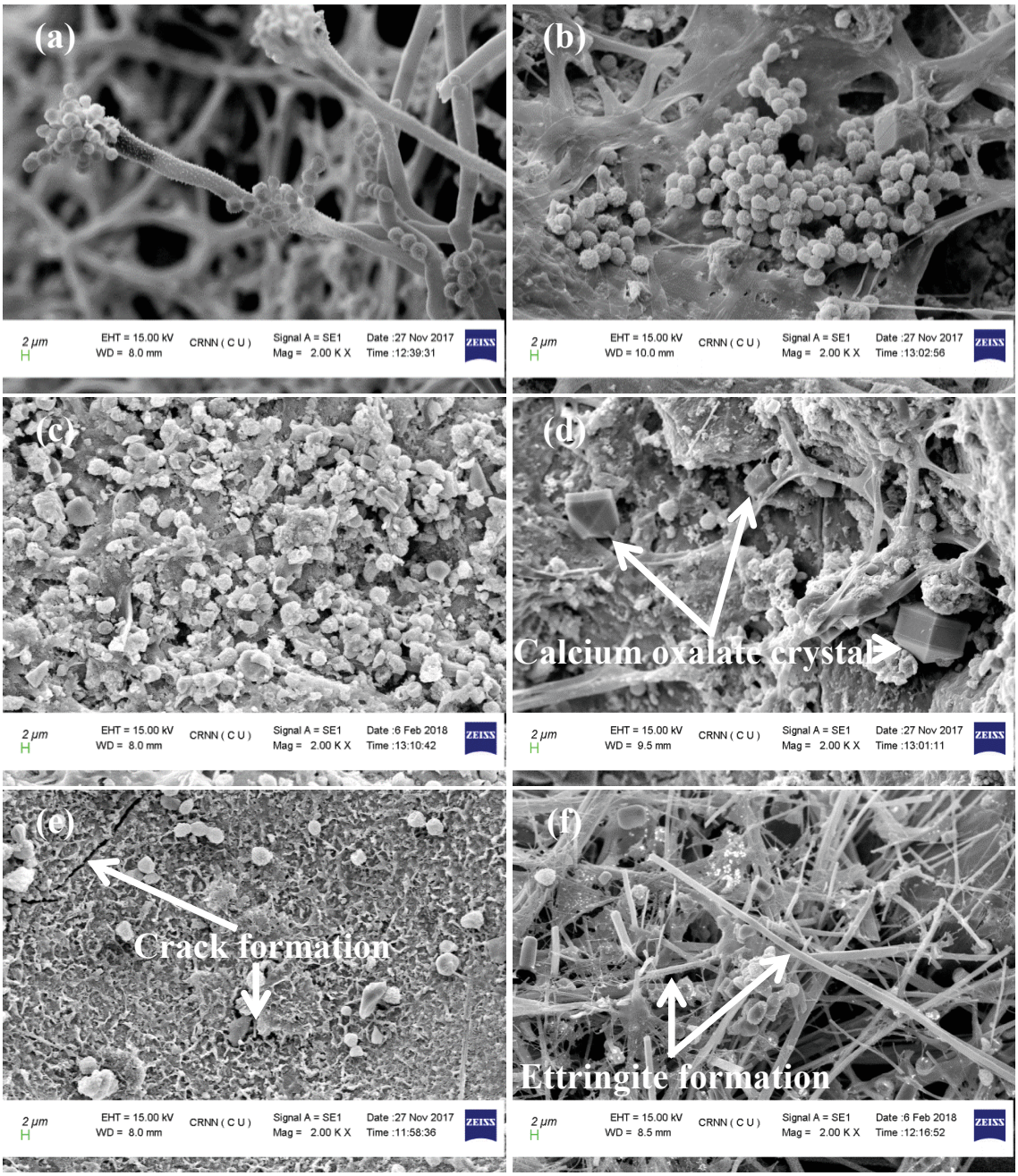

Fig. 5.27 SEM images of *A. tamarii* infected concrete samples: a) 1 month; b) 3 month; c) 6 month; d) calcium oxalate crystal formation e) crack formation f) ettringite formation.

The examination of concrete sample using SEM images was taken after 1, 3 and 6 months interval of the biodeterioration study. After one month of fungal inoculation, the growth of the fungal biofilm was visible. The surface biofilms on the stones frequently contain fungi, to use organic substrates like carbon, hydrogen and energy sources (Nuhoglu et al., 2006). Fungal spore and hyphae had been noticed on the exterior surface of the concrete cube at this point. When the samples had been inoculated for six months, the surface phenomenon undergone changed. The spore in numbers was increased followed by growing fungal hyphae on the surface penetrated into the concrete materials [Fig. 5.27(a) through Fig. 5.27(c)]. The development of calcium oxalate crystals [Fig. 5.27(d)] and thin needles of ettringite [Fig. 5.27(f)] in samples that had been inoculated for six months further corroborate the effects of *A. tamarii*.

In the end, the effect shown structural deterioration (Gadd et al., 2014), expansion cracking as well as peeling of external layers, color changes and produce stains in the building block (Rosado et al., 2013). Micro cracks were also seen on the concrete sample used in the present study (Fig. 5.27(e)), which could represent a pathway for the growth of surface fungus inside building materials. It causes the damage region to become larger and increases the permeability of salt, water, and gas in concrete, leads to weakening of the building materials. This noticeable effect directly related to the concrete cube's compressive strength in the present investigation. The degradation of the exposed concrete surface caused by microorganisms, were also reported by Sanchez-Silva and Rosowsky., (2008). Similar to the present study, it was also seen a reduction in protective cover depth and an increase in porosity, which in turn had an impact on the occurrence of cracking and the reduction of concrete cube compressive strength [Fig. 5.19 and Fig. 5.27(e)].

5.2.6.2 Stereo zoom microscopy

The M20 and M40 grade concrete cube's surface characteristics were examined using the stereo zoom microscope (Bhattacharyya et al., 2022; Suarez et al., 2018). Compared to the control, the colour of the concrete cube was found to change to yellowish grey (5Y 8/1) according to a geological rock-color chart (Munsell 2009). The six-month-old contaminated concrete cubes displayed a phenomenon of disruption and missing concrete granules instead of a color change (Fig. 5.28). The pigmentation of *A. tamarii*, which may be metabolic products like melanin or by-products of other extracellular polymerization, is one of the prime reasons for color change of the concrete cube (Krumbein 1992). In the present

investigation, corrosion was extensively studied in many folds and results indicated that the concrete surface is corroded by organic acids as produced by microorganisms (Cwalina 2014).

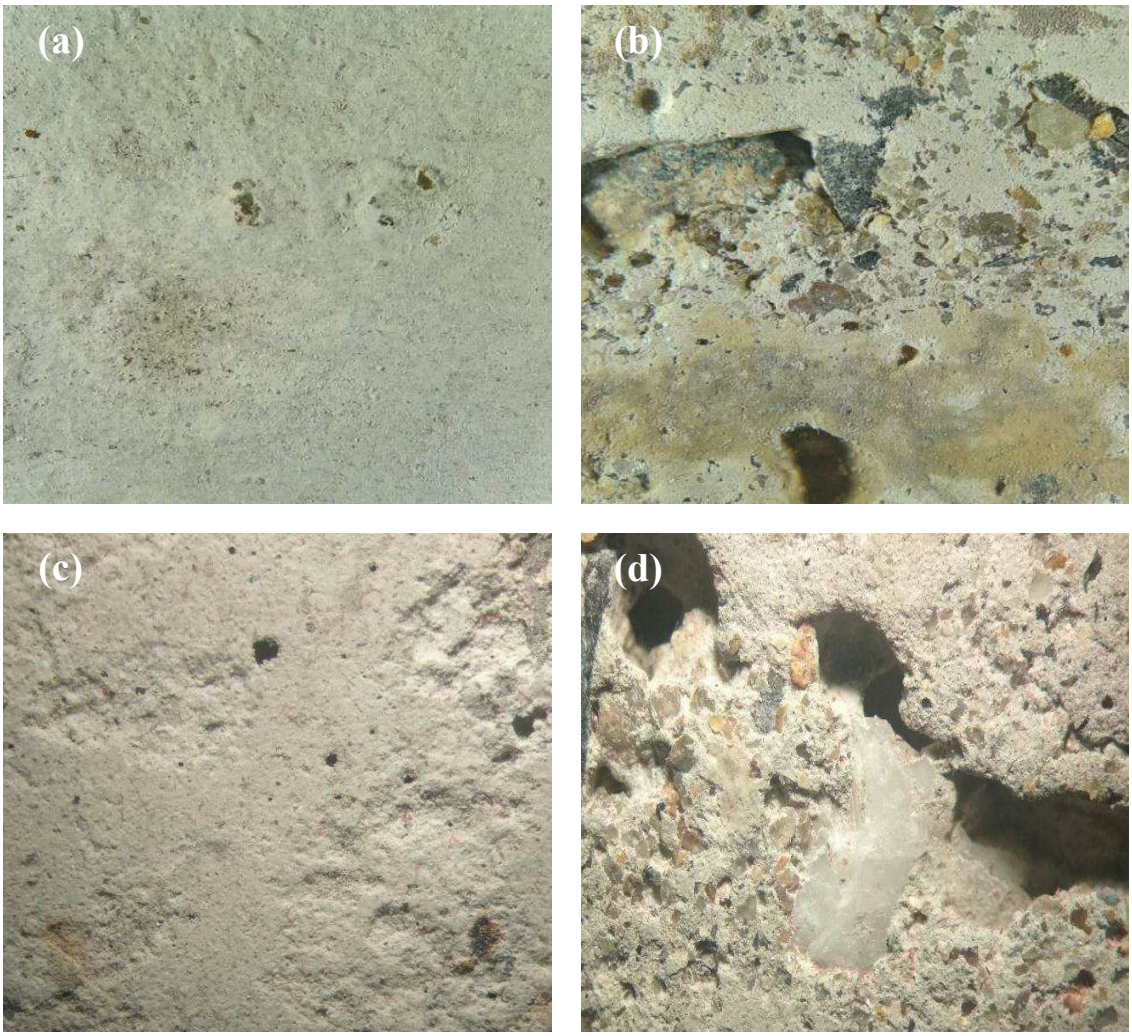

Fig. 5.28 Stereo Microscopic images (1× magnification) of: a) control M20 grade; b) *A. tamarii* infected M20 grade; c) control M40 grade; d) *A. tamarii* infected M40 grade concrete cube surface after 6 months of incubation period.

5.3 Radiation dose selection

5.3.1 Radiosensitivity of *A. tamarii*

The colonies that formed by *A. tamarii* were yellow and white cottony with circular impression and shown in Fig. 5.29. The sensitivity of the isolated fungus to UVC and gamma irradiation was evaluated with the help of Czapek Dox agar plate. Irradiated with different doses of ultraviolet and gamma radiation, the colony diameter (n = 3) were measured and compared to the diameter (n = 3) of the non-irradiated control after 7 days incubation period and exhibited in Fig. 5.29.

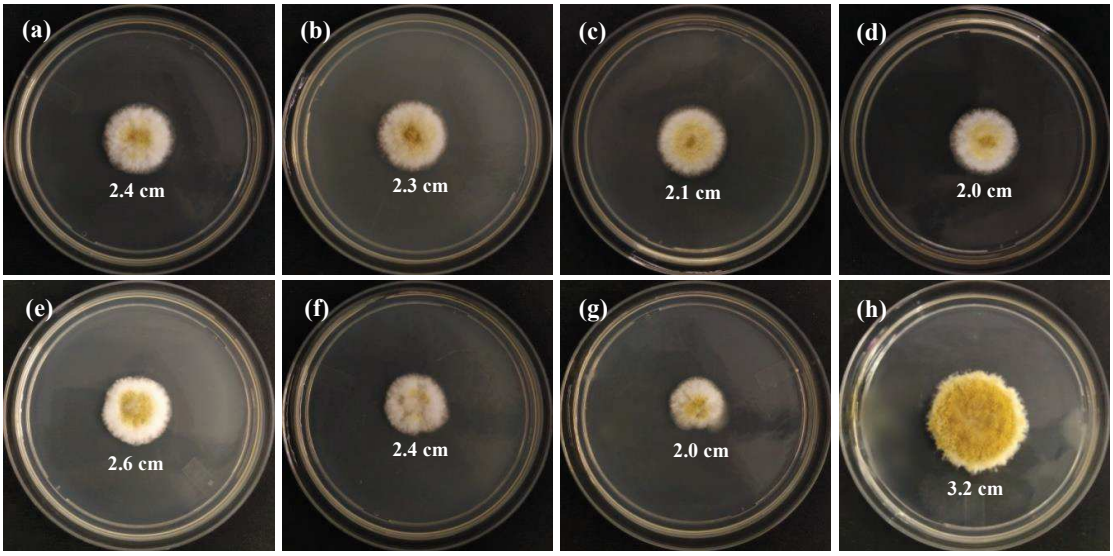

Fig. 5.29 Irradiation effect on *A. tamarii* with doses of: 5 mins a); 10 mins b); 15 mins c); 20 mins d) UVC ray and 0.5 KGy e); 0.75 KGy f); 1 KGy g) gamma ray compared to the control h) after 7-days incubation.

A. tamarii was resistant to ultraviolet exposure after 5, 10, and 15 mins, but was inactivated after 20 mins (Fig. 5.30). The colonies, which had a mean diameter of 2.0 ± 0.05 cm, were initially rendered inactive by the dose of 5 and 10 mins of exposure. Subsequently following a 1 day of incubation, the resistant cells began to grow once more and the colony continued to expand, eventually reaching diameters of 2.4 ± 0.01 and 2.3 ± 0.02 cm after 7 days, while the control colonies had 3.2 ± 0.03 cm diameters after the same incubation period (Fig. 5.30). However for 20 mins UVC, the diameter of the colony remained same after different exposure intervals which were shown in Fig. 5.30. It was noticed that after 45 mins of exposure to UV light (254 nm) the same was sufficient for rendering inactivation of fungus

(Ozcelik 2007). UVC light (250 µW/cm^2) killed most of the *Candida* organisms within 5 min as reported by Ishida et al., (1991).

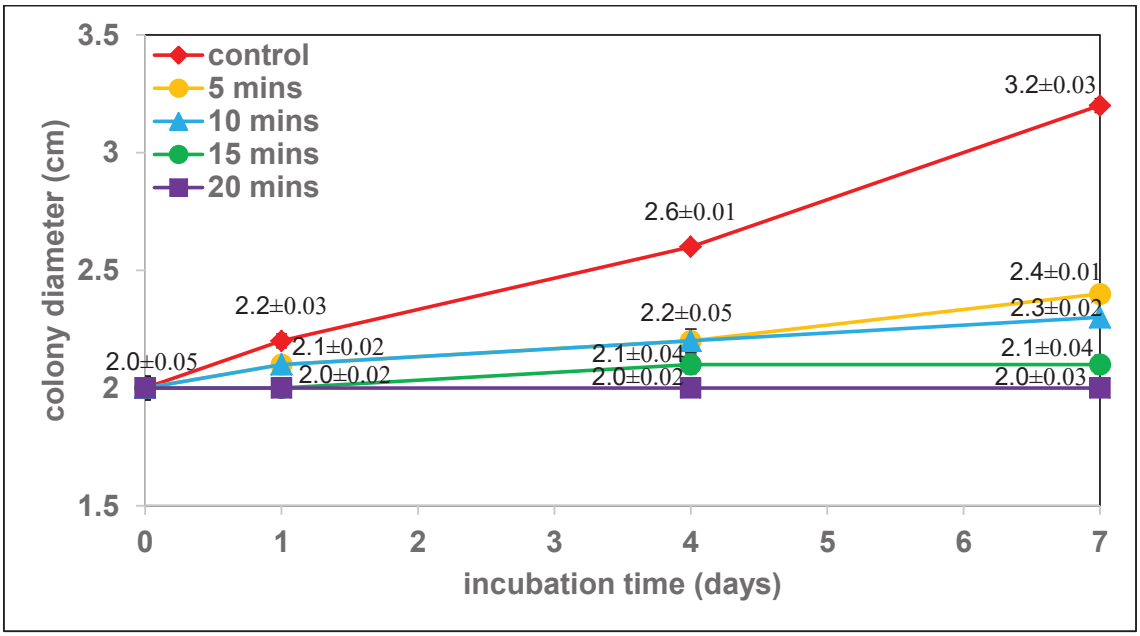

Fig. 5.30 Responses of *A.tamarii* to UVC rays with doses of 5, 10, 15 and 20 mins in accordance to colony diameter (n = 3) during 7-days incubation.

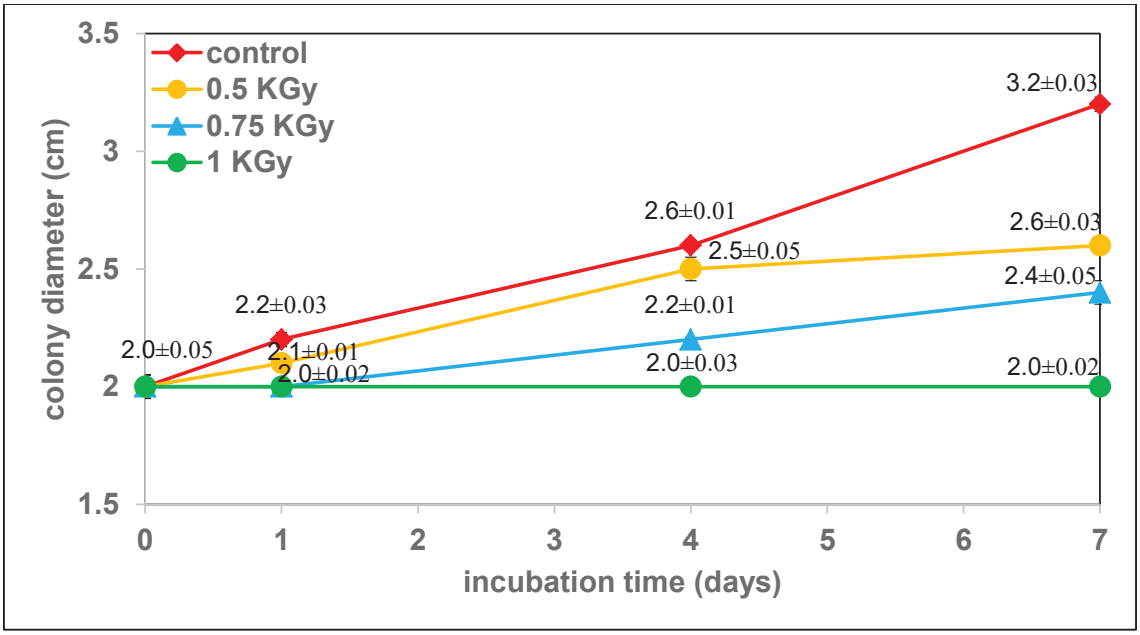

Fig. 5.31 Responses of *A.tamarii* to gamma rays with doses of 0.5, 0.75 and 1 KGy in accordance to colony diameter (n = 3) during 7-days incubation.

The diameter of the gamma irradiated (0.5, 0.75 and 1 KGy) fungal colonies after 7 days of incubation were found to be as 2.6 ± 0.03, 2.4 ± 0.05 and 2.0 ± 0.02 cm respectively (Fig. 5.31). However, it was shown in the plot that in case of gamma radiation with the doses of 0.5 and 0.75 KGy, the growth of *A. tamarii* slowed down compared to the control and finally totally inactive only at a dose equal to or above 1 KGy (Fig. 5.31). The observed phenomenon may have resulted due to complete loss of the fungus capacity to generate spores with the increase of doses of gamma radiation. Subsequently the living fungal cell or spores become inactive due to radiolysis of intercellular water (Maity et al., 2009). Similar kind of figure was obtained after application of gamma radiation where 1 KGy is the optimum dose for complete inactivation of *A. tamarii*. Previously, at doses lower than 2.5 KGy, fungi like *Alternaria alternata*, *Aspergillus flavus*, *Curvularia geniculate,* and *Trichoderma viride* were completely inactive (Maity et al., 2011).

Moreover, some other different studies on the impact of gamma radiation on the viability of fungi on food and plants have been released. When exposed to radiation at a dose of 5 KGy, *A. flavus*, *A. fumigatus*, *A. ochraceus*, and *A. parasiticus* on plants were eradicated (Aziz et al., 1997). Also, it was noted that *Trichoderma* sp. and *Aspergillus* sp. were inhibited at levels of 2 and 3 KGy, respectively, but *Curvularia* sp. and *Alternaria* sp. were only inhibited at 2.5 KGy (Maity et al., 2008). The heterogeneity in the isolated strains may account for the difference in doses needed to inactivate the fungi. Although the 18S rDNA sequencing of the various fungal strains was similar, their various origins accounted for their diverse responses to gamma radiation. Moreover, various experimental conditions could yield various outcomes. Based on the findings of the radiosensitivity of *A. tamarii* in our study, it was decided to use UVC and gamma radiation to treat the concrete cube (Prak et al., 2023; Reches 2019; Borderie et al., 2012; Sommers 1969).

5.3.2 Radiation on concrete cubes

5.3.2.1 Weight variation

The weighting process for control (non-infected and non-irradiated), biodeterioration (infected), control (irradiated), inhibition (infected and irradiated) cube samples was carried out after drying the cube at 110 ^{0}C. These weight reductions were calculated 30 days after exposure, and for control (non-infected and non-irradiated) samples, negligible weight reduction was noticed. After the surface precipitates were cleared away, *A. tamarii* inoculated i.e. biodeteriorated concrete cubes revealed a weight reduction of 0.56 ± 0.01% (Table 5.9).

Table 5.9 Weight loss in percentage for control and biodeteriorated concrete cubes (n = 3) after a month.

	Initial weight (gm)	Final weight (gm)	Difference (gm)	Loss (%)	Average loss (%)	Standard deviation (%)
Control (non-infected and non-irradiated)	345.0 330.5 334.5	345.0 330.5 334.5	0 0 0	0 0 0	0	0
Biodeterioration (infected)	348.0 355.0 347.5	346.0 353.0 345.5	2 2 2	0.57 0.56 0.57	0.56	0.01

Inhibition cube samples showed very marginal reduction of weight after exposed to UV rays for 5 min. After exposed to ultraviolet radiation for 10, 15 and 20 min, the cube samples showed 0.22 ± 0.09%, 0.62 ± 0.01% and 0.99 ± 0.12% weight reduction respectively [Fig. 5.32(a) and Table 5.10], while inhibition cubes lost 0.11 ± 0.09%, 0.34 ± 0.01%, 1.42 ± 0.11% of their weight after being exposed to gamma radiation for 0.5, 0.75 and 1 KGy [Fig. 5.32(b) and Table 5.11].

Table 5.10 Percentage weight losses for UVC irradiated control and inhibition cube samples (n = 3) after a month.

Radiation exposure time (min)	Experimental set-up	Initial weight (gm)	Final weight (gm)	Difference (gm)	Loss (%)	Average loss (%)	Standard deviation (%)
5	Control (irradiated)	331.0 329.5 322.0	331.0 329.5 322.0	0 0 0	0 0 0	0	0
	Inhibition (infected and irradiated)	345.5 351.5 339.5	345.5 351.5 339.5	0 0 0	0 0 0	0	0
10	Control (irradiated)	320.0 337.0 320.0	320.0 337.0 320.0	0 0 0	0 0 0	0	0
	Inhibition (infected and irradiated)	302.0 300.0 307.0	301.5 299.0 306.5	0.5 1 0.5	0.17 0.33 0.16	0.22	0.09
15	Control (irradiated)	323.0 311.0 297.0	322.5 310.5 297.0	0.5 0.5 0	0.15 0.16 0	0.10	0.09

	Inhibition (infected and irradiated)	330.5 317.0 308.0	328.5 315.0 306.0	2 2 2	0.60 0.63 0.65	0.62	0.04
20	Control (irradiated)	350.0 328.0 320.5	349.0 327.5 320.0	1 0.5 0.5	0.28 0.15 0.16	0.20	0.07
	Inhibition (infected and irradiated)	330.0 327.0 353.5	327.0 324.0 349.5	3 3 4	0.91 0.92 1.13	0.99	0.12

Table 5.11 Percentage weight losses for gamma irradiated control and inhibition cube samples (n = 3) after a month.

Radiation dose (KGy)	Experimental set-up	Initial weight (gm)	Final weight (gm)	Difference (gm)	Loss (%)	Average loss (%)	Standard deviation (%)
0.5	Control (irradiated)	349.5 345.0 351.0	349.5 345.0 351.0	0 0 0	0 0 0	0	0
	Inhibition (infected and irradiated)	292.0 305.0 301.5	292.0 304.5 301.0	0 0.5 0.5	0 0.16 0.17	0.11	0.09
0.75	Control (irradiated)	331.0 326.0 307.5	331.0 326.0 307.5	0 0 0	0 0 0	0	0
	Inhibition (infected and irradiated)	280.0 289.0 320.0	279.0 288.0 319.0	1 1 1	0.36 0.35 0.31	0.34	0.03
1	Control (irradiated)	325.5 302.5 307.0	325.0 302.0 306.0	0.5 0.5 1	0.15 0.16 0.33	0.21	0.10
	Inhibition (infected and irradiated)	324.0 280.0 305.0	319.0 276.0 301.0	5 4 4	1.54 1.42 1.31	1.42	0.11

It is interesting to note that variations of concrete weight were also observed for irradiated control cube samples that were run in sterile Czapek Dox medium i.e. negligible after 5 and 10 min UV ray, 0.10 ± 0.09% and 0.20 ± 0.07% after 15 and 20 min UV ray, negligible after 0.5 and 0.75 KGy gamma ray and 0.21 ± 0.10% after 1 KGy gamma exposure (Fig. 5.32). In addition, it was also observed that weight losses of inhibition cubes that had been infected and exposed to radiation were higher ($p < 0.05$, $p < 0.01$ and $p < 0.001$) than those of control samples (irradiated). The loss of weight for the inhibition samples was found less with respect to a gamma dose of 0.5 KGy compared to 0.75 and 1 KGy respectively as shown in Fig. 5.32(b).

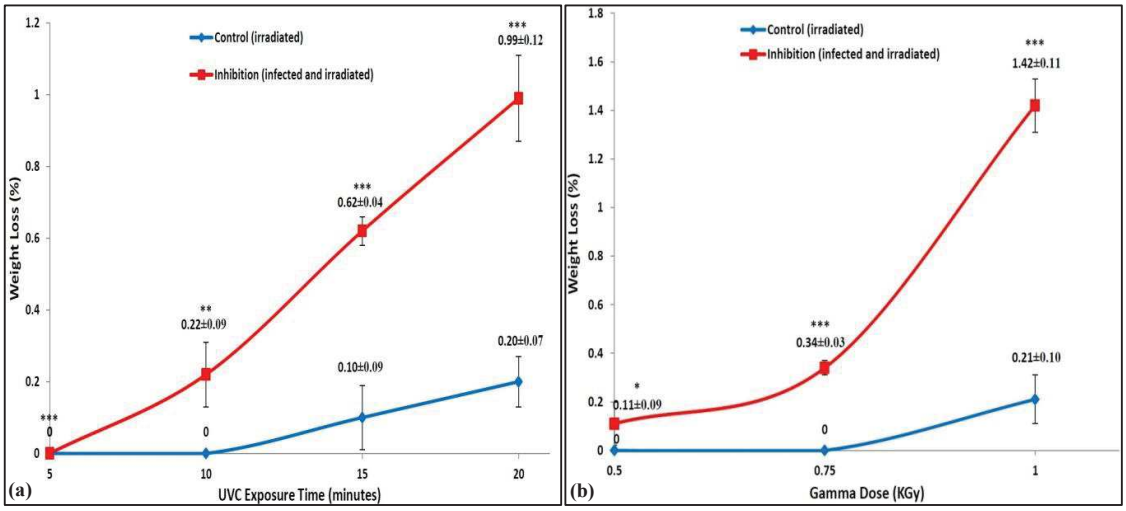

Fig. 5.32 Weight reduction in percentage for: a) ultraviolet; b) gamma radiated cube samples (n = 3) after a month. The asterisks above lines present the *p*-value (*t*-test between the control sample and inhibition sample): *, $p < 0.05$; **, $p < 0.01$; ***, $p < 0.001$.

The loss of weight for inhibited samples was caused by fungus as well as irradiation, whereas for control samples weight loss occurred only due to radiation. Also fungal population depletion was noticed after the infected cube was exposed to gamma radiation at doses of 0.5, 0.75, and 1 KGy, but *A. tamarii* was completely inhibited above or equal to 1 KGy (Fig. 5.31). However, based on weight losses, radiation damage for a concrete was clearly observed after infected cube was exposed to radiation (inhibition) at a dosage of 1 KGy [Fig. 5.32(b)] in contrast to samples that had biodeteriorated (Table 5.9). Cement materials lose weight throughout the irradiation process, which is likely due to the loss of chemically bound or non-evaporable water, physically bound or evaporable water and unbound water. Additionally, present research showed that concrete cubes lost greater weight at higher temperatures or radiation doses (Table 5.9, Table 5.10 and Fig. 5.11). The loss of weight of concrete cube was an indication that it was becoming dehydrated as a result of the increase in radiation doses. Sanchez et al., (2018) and Kontani et al., (2014) claimed that increased weight loss that detected with the escalation of radiation doses due to the concrete samples' dehydration, which is in contrary to the findings of the present investigation. As a result, the pore pressure inside the concrete enhanced, causing the explosive spalling of concrete as reported by Zhang and Ye (2012). Field et al., (2015) explained in their research that large doses of gamma radiation might cause the atomic structure of some aggregates in concrete to

change from crystalline property to deform amorphous, causing a drop in weight and increase in volume.

5.3.2.2 Compressive strength variation

The compressive strength of the concrete cubes was measured in triplicate for every sample, after 30 days of exposure. According to Table 5.12, the average compressive strength for control (non-infected and non-irradiated) and fungal-infected (biodeterioration) 30-day-old cubes were 19.74 ± 0.46 and 18.88 ± 0.43 N/mm^2 respectively and tabulated below in Table 5.12.

Table 5.12 Variation of compressive strength (N/mm^2) for control and biodeteriorated cube samples (n = 3) after a month.

Experimental set-up	Load (KN)	Compressive strength (N/mm^2)	Average strength (N/mm^2)	Standard deviation (N/mm^2)
Control (non-infected and non-irradiated)	49.5 48.1 50.4	19.80 19.24 20.16	19.74	0.46
Biodeterioration (infected)	47.5 46.0 48.1	19.00 18.40 19.24	18.88	0.43

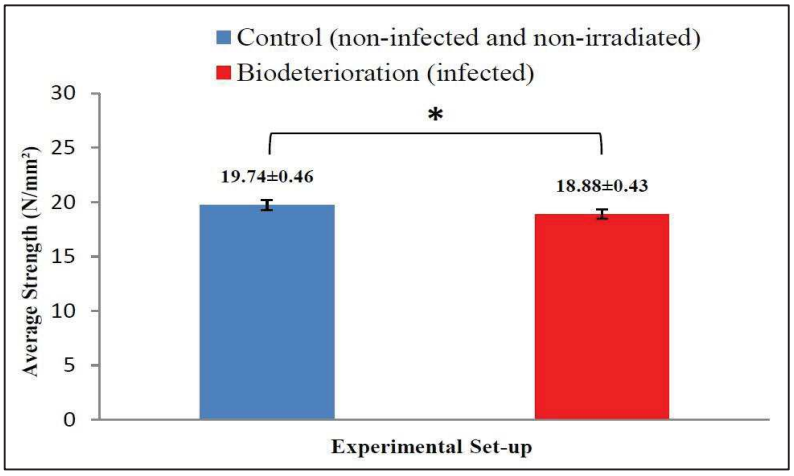

Fig. 5.33 Compressive strength (N/mm^2) variation for control and biodeteriorated cube samples (n = 3) after a month. The asterisks above columns present the *p*-value (*t*-test between the control sample and biodeteriorated sample): *, $p < 0.05$.

These findings demonstrated that compared to the control (non-infected and non-irradiated), *A. tamarii* infection accelerated the process of deterioration, lowering ($p < 0.05$) the compressive strength of the concrete cubes (Fig. 5.33). After microscopic investigation, it was found that fungus was present and grown in the cracks of the damaged concrete structures (Fig. 5.27), but it is still unclear how far the fungi had penetrated the inside of the concrete structures. *Aspergillus* has a cell wall consisting of chitin and complex carbohydrates that is strong and flexible, allowing the apex part of the fungus to infiltrate concrete structures (Tong 2018; Money 2004). So the primary process causing fungal influenced deterioration (FID) of concrete is fungal hyphae extension inside the concrete materials. Organic acid as produced by fungi is one of the main causes of concrete structure corrosion and reduction of the compressive strength of concrete (Davis et al., 1998).

Radiation doses and concrete cube compressive strength are inversely related. Loss of strength would be greater if the dose is increased, and vice versa. According to Craeye et al., (2015), compressive strength reduced as radiation exposure increased.

Table 5.13 Variation of compressive strength (N/mm^2) for UVC irradiated control and inhibition cube samples (n = 3) after a month.

Radiation exposure time (min)	Experimental set-up	Load (KN)	Compressive strength (N/mm^2)	Average strength (N/mm^2)	Standard deviation (N/mm^2)
5	Control (irradiated)	54.3 52.9 54.2	21.72 21.16 21.68	21.52	0.31
	Inhibition (infected and irradiated)	51.5 50.0 50.0	20.60 20.00 20.00	20.20	0.34
10	Control (irradiated)	54.7 53.9 52.6	21.88 21.56 21.04	21.49	0.42
	Inhibition (infected and irradiated)	48.5 47.4 48.6	19.40 18.96 19.44	19.26	0.26
15	Control (irradiated)	51.5 49.9 51.6	20.60 19.96 20.64	20.40	0.38
	Inhibition (infected and irradiated)	50.4 42.2 45.9	18.86 18.18 18.46	18.46	0.34

20	Control (irradiated)	48.5 50.2 49.2	19.40 20.08 19.68	19.72	0.34
	Inhibition (infected and irradiated)	45.4 44.1 44.3	18.16 17.64 17.72	17.84	0.28

Table 5.14 Strength variation (N/mm^2) for gamma irradiated control and inhibition cube samples (n = 3) after a month.

Radiation dose (KGy)	Experimental set-up	Load (KN)	Compressive Strength (N/mm^2)	Average Strength (N/mm^2)	Standard deviation (N/mm^2)
0.5	Control (irradiated)	51.8 52.9 51.1	20.72 21.16 20.44	20.77	0.36
	Inhibition (infected and irradiated)	50.3 49.9 49.3	20.12 19.96 19.72	19.93	0.20
0.75	Control (irradiated)	51.3 49.7 51.5	20.52 19.88 20.60	20.34	0.39
	Inhibition (infected and irradiated)	46.0 47.8 46.8	18.40 19.12 18.72	18.75	0.36
1	Control (irradiated)	49.7 48.7 47.7	19.88 19.48 19.08	19.48	0.28
	Inhibition (infected and irradiated)	41.9 42.5 43.8	16.76 17.00 17.52	17.10	0.38

The lowest ($p < 0.001$) compressive strength 17.84 ± 0.28 N/mm^2 was found in UVC-irradiated infected (inhibition) concrete cubes after 20 min of exposure [Fig. 5.34(a) and Table 5.13]., followed by samples exposed for 5, 10, and 15 min (20.20 ± 0.34, 19.26 ± 0.26 and 18.46 ± 0.34 N/mm^2). The compressive strength of infected cubes after undergoing 5 and 10 min of ultraviolet ray (inhibition) showed higher strength [Fig. 5.34(a) and Table 5.13] in comparison to *A.tamarii* infected (biodeteriorated) cubes (Fig. 5.33 and Table 5.12). The most dangerous waveband, UVC, probably destroys both *A. tamarii* conidia and spores. As a result, the population and spread of fungus on concrete cubes would be reduced.

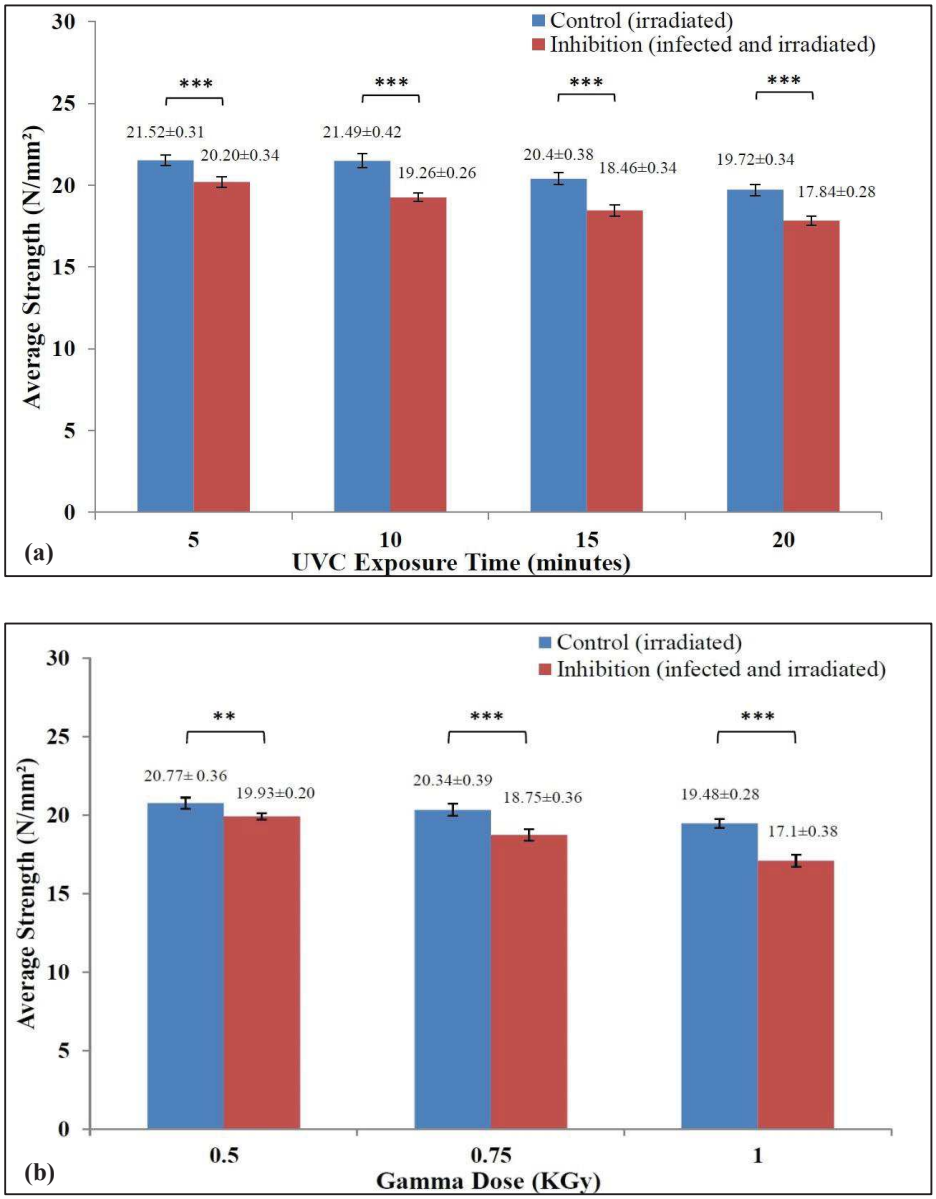

Fig. 5.34 Compressive strength (N/mm^2) variation for: a) ultraviolet; b) gamma irradiated cube samples (n = 3) after a month. The asterisks above columns present the *p*-value (*t*-test between the control sample and inhibition sample): ** $p < 0.01$; ***, $p < 0.001$.

Similarly gamma irradiation with a dose of 0.5 KGy reducing ($p < 0.01$) compressive strength from 20.77 ± 0.36 N/mm^2 (control) to 19.93 ± 0.20 N/mm^2 (inhibition), whereas 19.48 ± 0.28 N/mm^2 (control) to 17.10 ± 0.38 N/mm^2 (inhibition) strength loss ($p < 0.001$) had been also observed after irradiating the cube with 1 KGy dose of gamma radiation [Fig. 5.34(b) and Table 5.14]. Craeye et al., (2015) found that samples aged for a longer period of time prior to irradiation at high dose rates (1.36 KGy/h) showed a larger decrease in

compressive strength. In case of lower dosage rates no impact is traced. According to a study by Sommers (1969), concrete compressive strength descended as gamma radiation exposure has been increased. Depending on the degree of dryness, the strength of the concrete may decrease or rise. Loss of compressive strength is also correlated with water hydration in the cement plus pore water radiolysis or pore water evaporation under radiation heat. The cement's hydration level and strength were decreased during irradiation due to a loss of oxygen and hydrogen radiolytic species (Soo and Milian 2001). Vodak et al., (2005) described this mechanism as a series of chemical reactions on the concrete, starting with water radiolysis and ending with the creation of calcite crystal ($CaCO_3$). As a result, the tobermorite gel is destroyed after the pore size is reduced. By lowering their crystallisation pressure, calcium silicate hydrates (CSH) minerals weaken concrete cubes compressive strength.

5.3.2.3 Variation in elemental composition

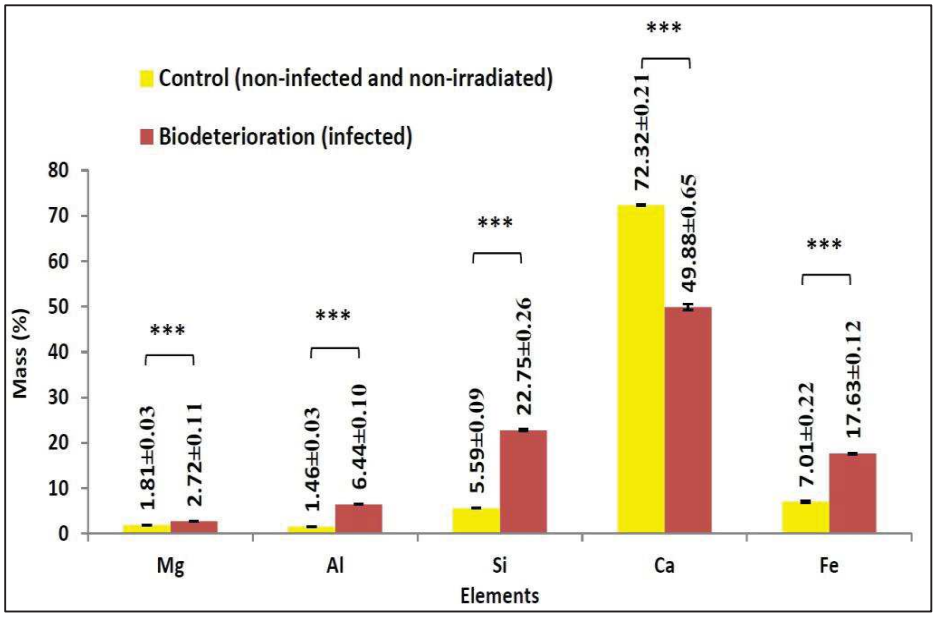

Fig. 5.35 Mass fraction (%) of major elements for control and biodeteriorated samples (n = 3) after a month. The asterisks above columns present the *p*-value (*t*-test between control and biodeteriorated concrete sample): ***, $p < 0.001$.

To determine the percentage of trace elements contained in control (non-infected and non-irradiated), biodeterioration (infected), control (irradiated) and inhibition (infected and irradiated) concrete samples, an EDXRF investigation was carried out. Calcium and silica were the two elements whose composition variability was most apparent (Fig. 5.35 and Fig.

5.36). Before irradiation, the calcium percentage in the infected concrete (49.88 ± 0.65%) was lower ($p < 0.001$) than control sample (72.32 ± 0.21%) because *A. tamarii* assisted in the leaching of calcium ions from the concrete cube (Fig. 5.35). Additionally, this phenomenon has been discussed in some other studies as reported in the literature (Sanchez-Silva and Rosowsky 2008; Gu et al., 1998). Simultaneously, as the amount of calcium leaching was reduced, the percentage of silica was found to be decreased.

Infected concrete as exposed to UV radiation (inhibition) for 5, 10, 15, and 20 minutes had mass percentages of calcium of 75.75 ± 0.16%, 69.12 ± 0.22%, 48.54 ± 0.17%, and 36.54 ± 0.27%, respectively [Fig. 5.36(a)]. Samples exposed to UVC radiation for 15 and 20 mins (inhibition) showed greater calcium losses than samples exposed to 5 and 10 mins UVC radiation. However, compared to the control (irradiated) samples, the mass % of calcium was around the same for the 5 and 10 min irradiated infected (inhibition) samples and statistically significant [Fig. 5.36(a)]. Another finding from the EDXRF analysis was that the calcium concentration of infected cubes following exposure to 5 and 10 minutes of UVC radiation (inhibition) exhibited greater calcium content compared to only infected i.e. biodeteriorated cubes [Fig. 5.35 and Fig. 5.36(a)]. The results of the present investigation thus revealed that the exposure to ultraviolet light for 5 and 10 mins had been beneficial for reducing calcium leaching from concrete and preventing fungal biodeterioration of concrete. Comparing irradiated control samples to non-infected and non-irradiated control samples, a slight percentage of calcium loss was also seen (Fig. 5.35 and Fig. 5.36). Also, as radiation doses increased, the mass (%) of calcium in control (irradiated) samples dropped (Fig. 5.36). All samples included a mass proportion of magnesium, however the mass variances were barely noticeable. Also found in trace amounts at first were chromium, manganese, zinc, and nickel, but they gradually diminished after the 30-day incubation period.

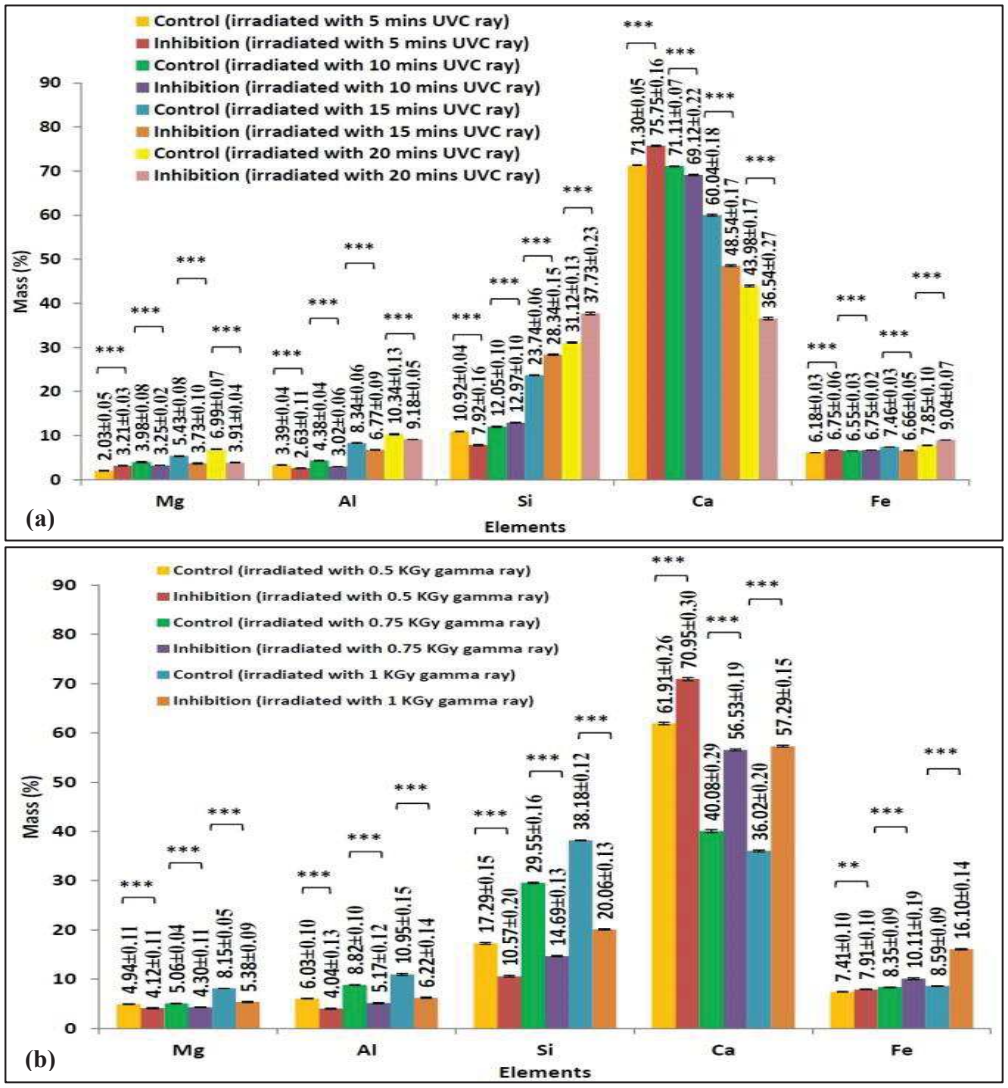

Fig. 5.36 Mass fraction (%) of major elements for: a) UVC; b) gamma irradiated control and inhibition samples (n = 3) after a month. The asterisks above columns present the *p*-value (*t*-test between the control and inhibition concrete sample): **, $p < 0.01$; ***, $p < 0.001$.

For analysis of experimental result, an effort was also endeavoured for using the micro EDXRF technique to analyse the proportion of trace elements in gamma-irradiated (control and inhibition) concrete samples. In a bar graph [Fig. 5.36(b)], the mass (%) and elemental composition of various concrete elements are shown. When compared to calcium percentage (70.95 ± 0.30%) of concrete samples after exposed to 0.5 KGy of radiation (inhibition), the percentages of calcium (56.53 ± 0.19% and 57.29 ± 0.15%) were decreased after the application of 0.75 and 1 KGy gamma doses [Fig. 5.36(b)]. In fact the production of the very insoluble phase $CaO_2.8H_2O$, which results in the eradication of ettringite and portlandite, is

mainly due to the dropping of calcium percentage in concrete exposed to large doses of gamma radiation (Bouniol and Aspart 1998). Additionally, it was observed that the changes in the dissolution rate caused rotations and distortions of carbonate groups with regard to the locations of calcium atoms, which led to a change in calcite density (Pignatelli et al., 2016). With the increase in radiation doses, the mass (%) of additional trace elements like silica, iron, and aluminium also increased (Fig. 5.36). This observation indicates that larger radiation doses (0.75 and 1 KGy) could worsen more the concrete cube than lower ones.

5.3.2.4 Changes in functional groups

Fig. 5.37 and Fig. 5.38 show the results of FTIR analysis performed on control (non-infected and non-irradiated), biodeterioration (infected), control (irradiated) and inhibition (infected and irradiated) concrete samples after 30 days of exposure. All concrete samples' infrared spectra at 3640 cm^{-1} revealed portlandite's hydroxyl vibrations. Portlandite [$Ca(OH)_2$] was transformed during the carbonation and leaching process. Calcium carbonate ($CaCO_3$) was formed during the natural carbonation of concrete (Wiktor et al., 2009). Concrete samples (control and inhibition) which were exposed to ultraviolet ray for 5 mins peaked at 1400, 874 and 705 cm^{-1} respectively and displayed a prominent symmetrical stretching band (C-O) of calcium carbonate. After being exposed to ultraviolet radiation for 10, 15, and 20 mins respectively, the C-O absorption band became medium and weak (Fig. 5.37). In IR spectra obtained from irradiated concrete samples earlier, Nagabhushana et al. (2008) also observed such band behaviour, which showed a shift towards lower wavenumbers and a decrease in the intensity of the calcite (1350, 874, and 712 cm^{-1}) stretching modes. The deformation and fracture of the carbonate groups found in calcite, as well as greater radiation dosages and fungus, have all been linked to this alteration in IR spectra. All of the concrete samples showed an envelope-shaped strong and broad symmetrical band (O-H) of water at 3450 cm^{-1}. The decrease in intensity of the broad band at 3400 cm^{-1} (Fig. 5.37 and Fig. 5.38) in biodeterioration and inhibition (except lower radiation dose) samples as compared to both control (non-infected and non-irradiated as well as only irradiated) demonstrated the clear indication of the decrease in H_2O content.

Very weak stretching band (C=C) remained unaltered in every sample that was tested. After receiving a high dose of radiation, another asymmetrically stretching strong band (980 cm^{-1}) from the C-S-H of the crystalline silica mineral quartz (Si-O) became medium that was both for control (irradiated) and inhibition concrete samples (Fig. 5.37 and Fig. 5.38).

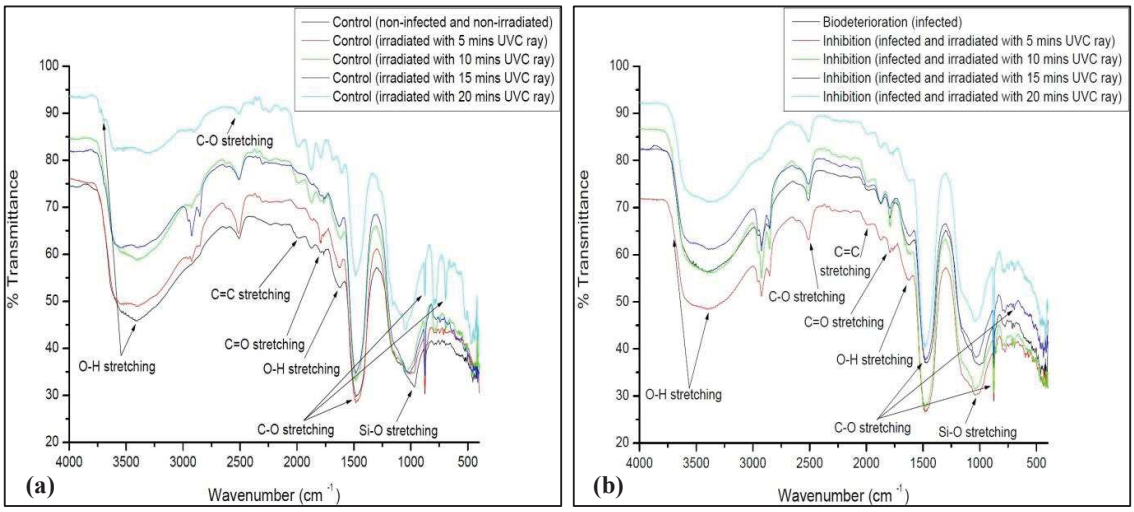

Fig. 5.37 FTIR transmittance spectrum of: a) control concrete (non-irradiated and UVC irradiated); b) biodeterioration concrete and inhibition concrete (UVC irradiated) samples after a month.

Si-O is typically a covalent chemical bond. Consequently, gamma radiation could degrade materials made of silica (Pomaro 2016; Battaglin et al., 1992; Mazzoldi et al., 1991). These findings support the present phenomena that, when calcite ($CaCO_3$) is exposed to greater doses of radiation, quartz also experiences some damage and becomes disordered.

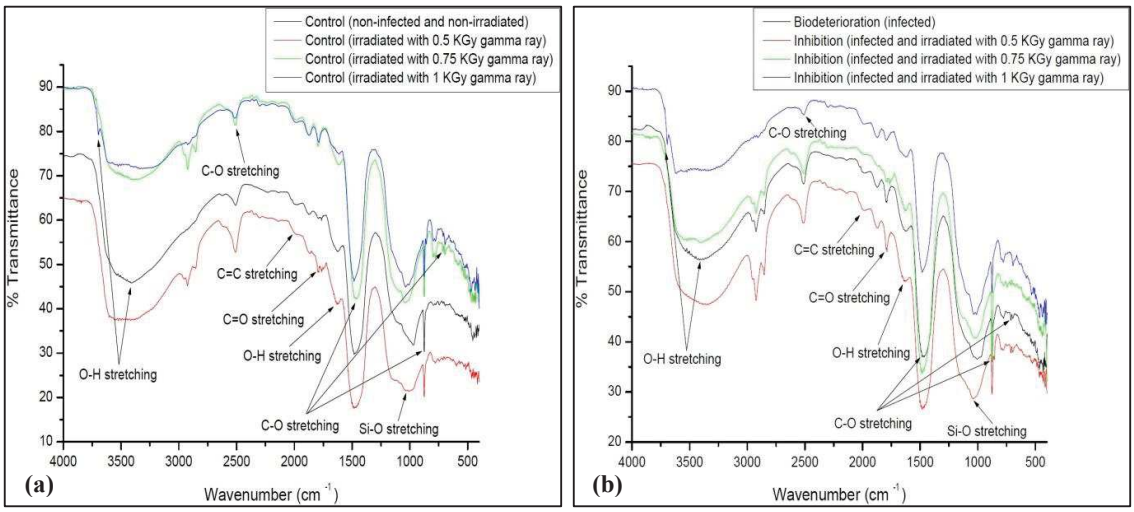

Fig. 5.38 FTIR transmittance spectrum of: a) control concrete (non-infected and gamma irradiated); b) biodeterioration concrete and inhibition concrete (gamma irradiated) samples after a month.

In the mid-IR region of the studied concrete samples, the major bands observed include carbonate, silicate, and water. After 30 days of incubation, these bands in the fungus-affected (biodeteriorated) concrete became medium and thereafter weakened compared to the non-infected and non-irradiated concrete sample (Fig. 5.37 and Fig. 5.38). These bands were found weaker after 180 days of exposure and were eventually be broken by fungus. This is dependent on a number of variables, including mineral content, texture and pH. The bands also weakened as a result of radiation damage when control and inhibition samples were exposed to 0.75 and 1 KGy doses of gamma radiation (Fig. 5.38). As a result, the cement's hydration products changed, weakening the concrete's matrix and lowering compressive strength. However, the band was stronger after 0.5 KGy dose of gamma irradiation in the irradiated (control and inhibition) concrete sample than the infected (biodeteriorated) concrete sample (Fig. 5.38). In contrast to exposure with *A. tamarii* i.e. biodeteriorated sample, concrete degraded more (except lower radiation dose) as a result of exposure to both higher dosage irradiation and *A. tamarii*.

5.4 Inhibition of biodeterioration with selected radiation dose

5.4.1 Characterisation of concrete cubes

5.4.1.1 Weight variation

The variation of weight percentage for non-irradiated (control and infected), UVC (625 $\mu w/cm^2$ x 5 min) and gamma (0.5 KGy) irradiated (control and infected) concrete cubes was measured after 6 months incubation period. The weight loss percentage in UVC irradiated infected concrete cubes (0.28 ± 0.09%) was observed to be the lowest, followed by gamma irradiated infected (0.72 ± 0.08%) and non-irradiated infected (2.22 ± 0.04%) cubes (Table 5.15 and Fig. 5.39). The percentage of weight loss was consistent with other investigations that came to the same conclusion about the weight loss caused by the fungal biodeterioration of concrete (Bhattacharyya et al., 2022; Sanchez-Silva and Rosowsky 2008; Gu et al., 1998). Additionally, when the concrete cube was kept in fungal medium, it shows almost negligible weight loss (0.85 ± 0.02%) over time as shown in tabular form (Table 5.15).

Table 5.15 Weight loss (%) of non-irradiated and irradiated concrete cubes (n =1) after 6 months.

	Experimental set-up	Initial weight (gm)	Final weight (gm)	Difference (gm)	Loss (%)	Average loss (%)	Standard deviation (%)
Non-irradiated	Control	0.352 0.340 0.360	0.349 0.338 0.357	0.003 0.003 0.003	0.85 0.88 0.83	0.85	0.02
	Infected	0.320 0.308 0.316	0.313 0.301 0.309	0.007 0.007 0.007	2.18 2.27 2.21	2.22	0.04
UVC irradiated	Control	325.5 321.5 307.5	325.0 321.0 307.5	0.5 0.5 0	0.15 0.15 0	0.10	0.08
	Infected	302.0 299.5 304.0	301.0 299.0 303.0	1 0.5 1	0.33 0.17 0.33	0.28	0.09
Gamma irradiated	Control	335.0 310.5 309.5	334.5 310.0 309.0	0.5 0.5 0.5	0.15 0.16 0.16	0.15	0.01
	Infected	304.0 295.5 310.0	302.0 293.5 307.5	2 2 2.5	0.66 0.68 0.81	0.72	0.08

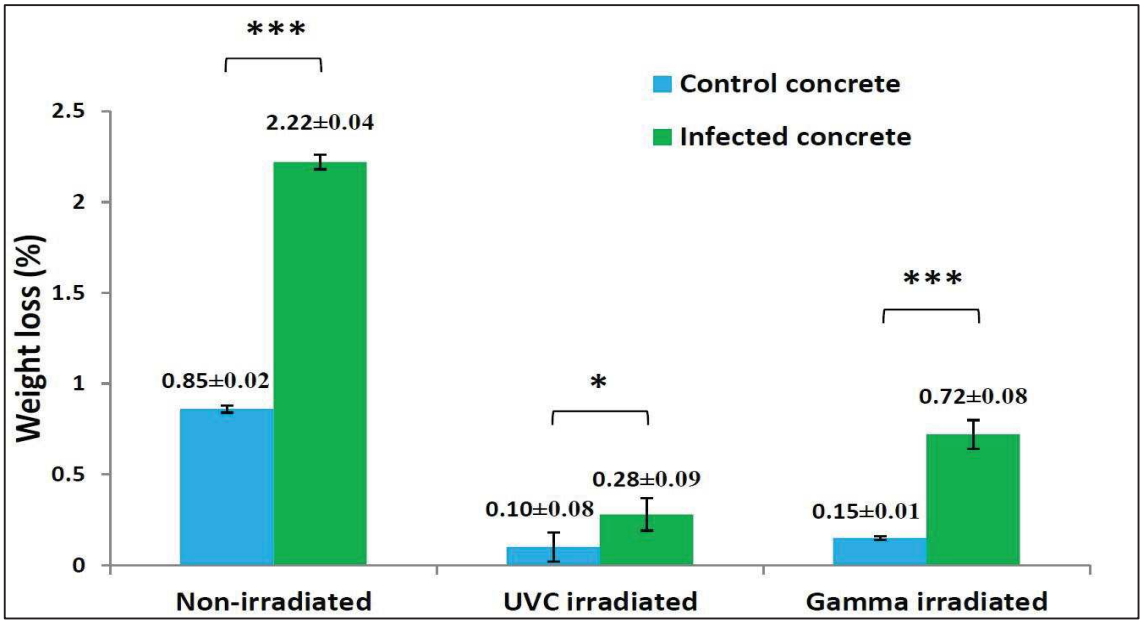

Fig. 5.39 Weight loss of non-irradiated, ultraviolet and gamma irradiated concrete cubes (n = 3) after 6 months. The asterisks above columns present the *p*-value (*t*-test between the control and infected concrete sample): * $p < 0.05$; ***, $p < 0.001$.

Also some weight losses that observed for UVC (0.28 ± 0.09%) and gamma (0.72 ± 0.08%) irradiated cubes (Table 5.15 and Fig. 5.39) because from radiosensitivity study complete depletion of *A. tamarii* was not observed with chosen radiation dose (Fig. 5.30 and Fig. 5.31) without affecting weight properties of concrete due to radiation damage (Fig. 5.32). After irradiation, the colony of *A. tamarii* was still found to persist and being deteriorated the concrete cubes. However, complete inhibition of fungal population and losses weight of concrete cubes were observed even when samples were irradiated with higher doses of radiation. Therefore, it was first priority to inhibit fungal effect without disturbing the concrete properties for conservation of historic building.

5.4.1.2 Compressive strength variation

Table 5.16 Compressive strength (N/mm^2) of non-irradiated and irradiated concrete cubes (n = 3) after 6 months.

	Experimental set-up	Load (KN)	Compressive strength (N/mm^2)	Average strength (N/mm^2)	Standard deviation (N/mm^2)
Non-irradiated	Control	46.3 46.0 46.4	18.52 18.40 18.56	18.50	0.08
	Infected	37.1 36.8 36.8	14.84 14.74 14.72	14.77	0.06
UVC irradiated	Control	69.2 70.1 69.5	27.68 28.04 27.80	27.84	0.18
	Infected	66.2 67.1 66.0	26.48 26.84 26.40	26.58	0.23
Gamma irradiated	Control	64.6 64.1 64.2	25.84 25.64 25.68	25.72	0.11
	Infected	58.8 58.5 58.1	23.52 23.40 23.24	23.38	0.14

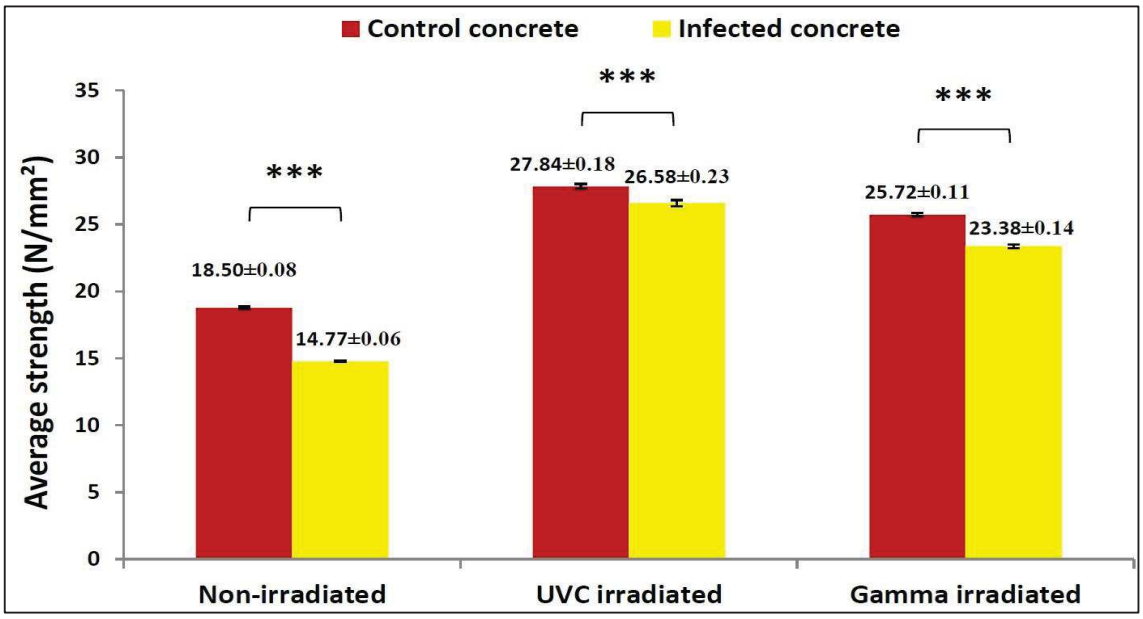

Fig. 5.40 Compressive strength loss (N/mm^2) of non-irradiated, ultraviolet and gamma irradiated concrete cubes (n = 3) after 6 months. The asterisks above columns present the *p*-value (*t*-test between the control and infected concrete sample): ***, $p < 0.001$.

The compressive strength for non-irradiated (control and infected), UVC and gamma irradiated (control and infected) cube samples was measured after 6 months (Table 5.16 and Fig. 5.40). The compressive strength of non-irradiated control and infected cubes were 18.50 ± 0.08 and 14.77 ± 0.06 N/mm^2 respectively. For non-irradiated control samples, Czapek Dox medium will cause deterioration on its own because it contains magnesium sulfate which will accelerate the compressive strength loss of the concrete cube. Moreover, our present investigation agreed with the results of some other researcher's reports on concrete cube as referred below, which revealed that due to fungal infection compressive strength of concrete have been decreased with time (Bhattacharyya et al., 2022; Yakovleva et al., 2018; Marquez-Penaranda et al., 2016). For the irradiated control samples, where Czapek Dox medium was added initially after irradiated and fungal activity was found absent, the increment of compressive strength (27.84 ± 0.18 and 25.72 ± 0.11 N/mm²) were observed compared to the non-irradiated control samples (18.50 ± 0.08 N/mm²). Significant increase in compressive strength was also observed for UVC (26.58 ± 0.23 N/mm²) and gamma (23.38 ± 0.14 N/mm²) radiated infected concrete cubes compared to the non-irradiated infected samples (14.77 ± 0.06 N/mm²) after 180 days of incubation (Fig. 5.40). In contrast to the findings of Rezaei-Ochbelagh et al., (2010) our experimental findings demonstrate that compressive strength of radiated concrete cube has been improved due to gamma effect. Before irradiation, the cubes

were dipped in Czapek Dox medium within the plastic containers and their micro pores filled with water. As a result, water molecules that interact with gamma rays were broken down into H and OH. The hydrogen (H) flows to the concrete's surface and the OH participate on alkali-silica reaction. Micro pores can be eliminated in this manner. As a result, radiating concrete will improve its strength (Rezaei-Ochbelagh et al., 2010; Mobasher et al., 2015).

5.4.1.3 Variation in elemental composition

The primary elements whose composition diversity was clearly visible were silicon, calcium, magnesium, aluminium, and iron (Fig. 5.41 and Fig. 5.42). The calcium content of the non-irradiated infected cubes was found to be decreased ($p < 0.001$) compared to non-irradiated control ones because *A. tamarii* helps to leach calcium from concrete cube as discussed earlier. Czapek medium will degrade non-irradiated control concrete samples on its own because it includes potassium chloride and sodium nitrates, which speed up calcium leaching. But the mass percentage of calcium was found to be increased in UVC and gamma irradiated (infected) concrete whereas the mass percentage of silicon was decreased as compared to the non-irradiated (infected) sample. Hence the chosen ultraviolet and gamma radiation dose were effective to decrease the leaching rate of calcium from the concrete cube. Consequently, the decrease in silicon concentration leads to an increase in calcium concentration. The chemical composition of all elements of concrete cubes must always add up to 100%.

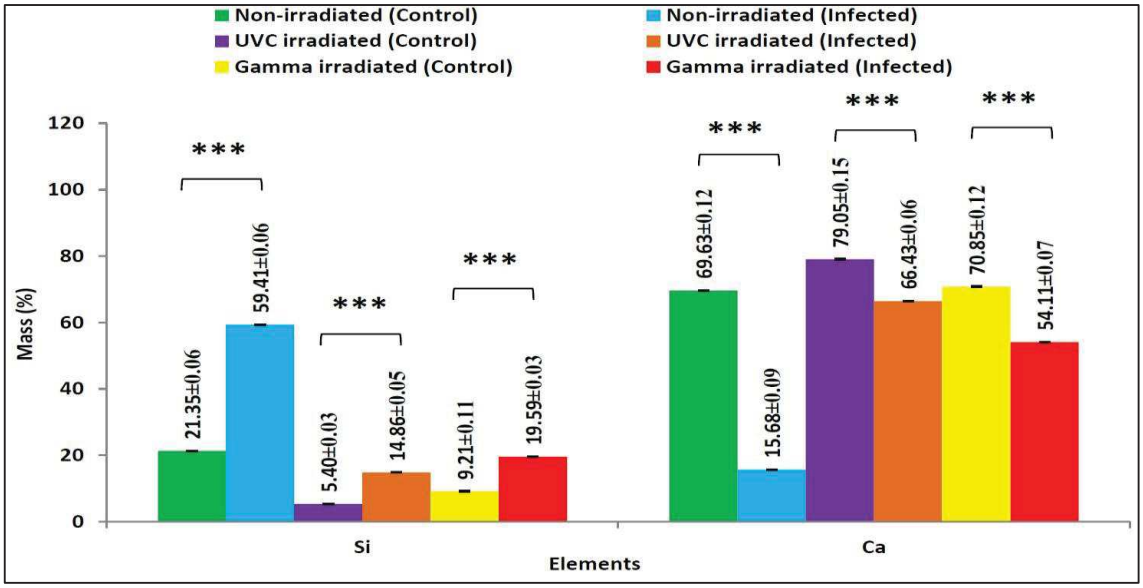

Fig. 5.41 Mass fraction of silicon and calcium of non-irradiated and irradiated concrete samples (n = 3) after 6 months. The asterisks above columns present the *p*-value (*t*-test between the control and infected concrete sample): ***, $p < 0.001$.

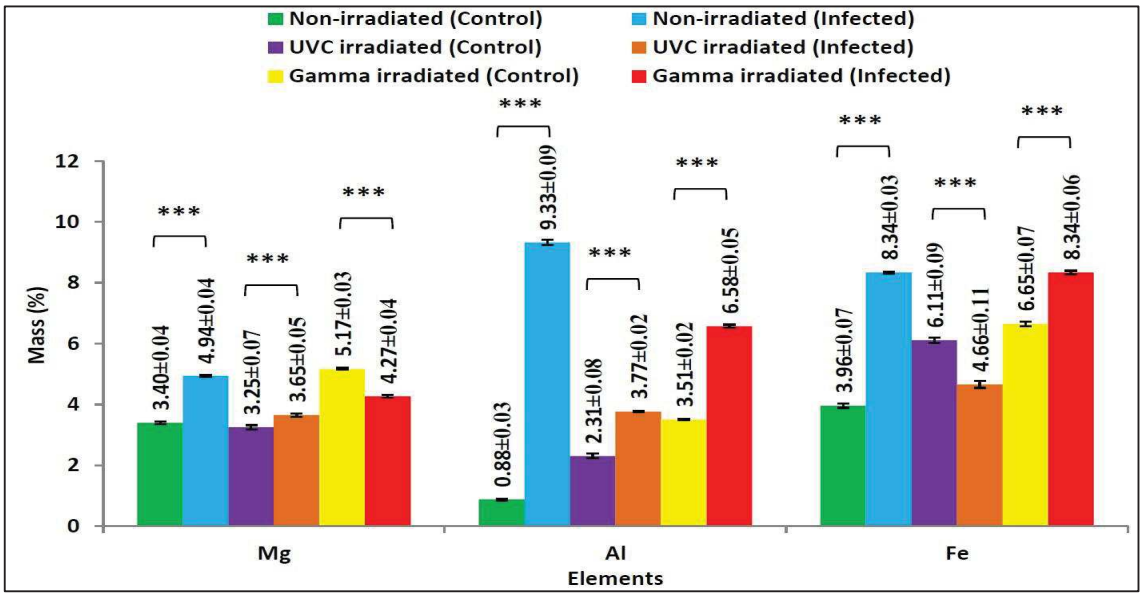

Fig. 5.42 Mass fraction of magnesium, aluminium and iron of non-irradiated and irradiated concrete samples (n = 3) after 6 months. The asterisks above columns present the *p*-value (*t*-test between the control and infected concrete sample): ***, $p < 0.001$.

It has been observed that infected sample also after irradiation, the percentages of magnesium, aluminium and iron were decreased compared to the non-irradiated (infected) ones (Fig. 5.42). Analysis of 30 years old gamma irradiated concrete sample from a recent study by Potts et al., (2021) revealed that the mass fraction of silicon, magnesium, aluminium and iron are also decreasing. Other elements including sulphur, titanium, potassium, chromium, and manganese were found in all of the specimens, but their compositions changed far less than those of the other elements.

5.4.1.4 Variation in functional groups

The mid-IR region (4000–500 cm^{-1}) spectrum of control and infected concrete after 180 days incubation period shown in Fig. 5.43 was perfect for interpreting specimens' basic structures and locating well-defined absorption bands of functional groups. Wide stretched bands centred around 3650 cm^{-1} represents the hydroxyl groups (OH) of the portlandite [$Ca(OH)_2$]. This band was subsequently broken and faded completely after 6 months in *A. tamarii* infected (non-irradiated) samples. After irradiation, this stretching band in the infected sample became strong or remains unchanged (Fig. 5.43).

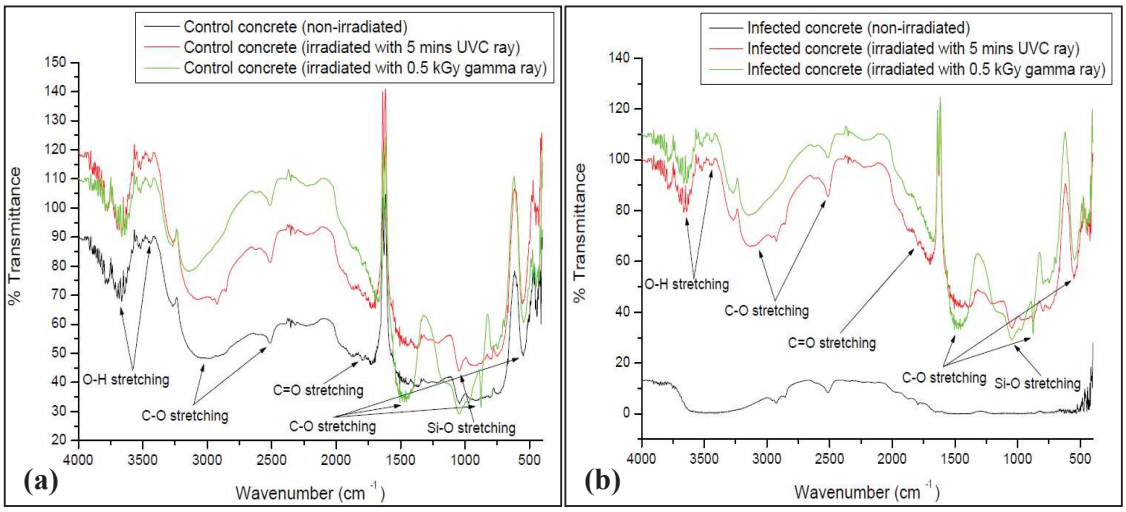

Fig. 5.43 Mid-infrared spectra of: a) control; b) infected concrete samples after 6 months.

The sharp and strong C-O stretches in all the control IR spectrum at 1400, 874 and 611 cm^{-1} indicate the presence of calcite ($CaCO_3$). Similar strong peaks can be observed in the IR spectra of the UVC and gamma irradiated infected cubes after 6 months. Additionally this band can be seen to gradually flatten after six months in *A. tamarii* infected (non-irradiated) sample [Fig. 5.43(b)]. The carbon double bond region 1800 cm^{-1} – 1500 cm^{-1} displayed the existence of C=O stretching in every samples except infected concrete (non-irradiated) set-up. At 980 cm^{-1} to 1000 cm^{-1}, a weak asymmetric stretching band (Si-O) of the crystalline silica material quartz was observed in irradiated (control and infected) specimens, but it completely disappeared after the fungal deterioration (infected and non-irradiated) (Fig. 5.43). It shows that the chosen dose of UVC and gamma radiation helps the depletion of fungal population, thereby improves the chemical properties of concrete.

5.4.1.5 Stereo zoom microscopic observation

The stereomicroscopic images showed that after irradiation *A. tamarii* infected concrete cube surface remains same as compared to the irradiated control samples. Also no cavities were formed in UVC and gamma radiated infected cube surface (Fig. 5.44 and Fig. 5.45) compared to the only *A. tamarii* infected samples (Fig. 5.28). But the color of irradiated as well as infected cube surface becomes yellowish because after irradiation fungus (not completely inhibited) may also have some ability to produce their metabolic products melanin which was the main reason for the pigmentation of the cube surface.

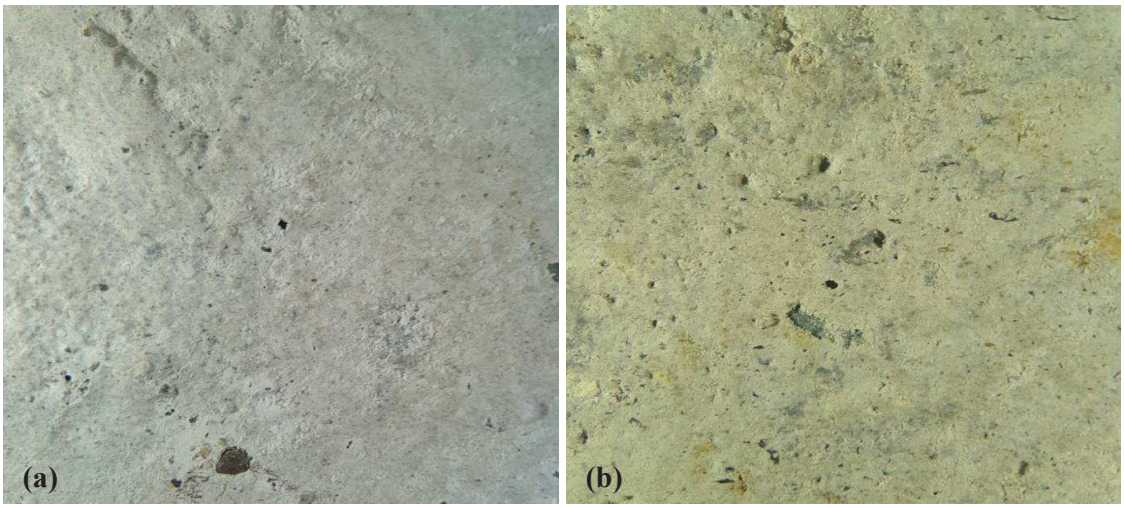

Fig. 5.44 Stereo microscopic images (1× magnification) of UVC irradiated: a) control; b) *A. tamarii* infected concrete cube surface after 6 months.

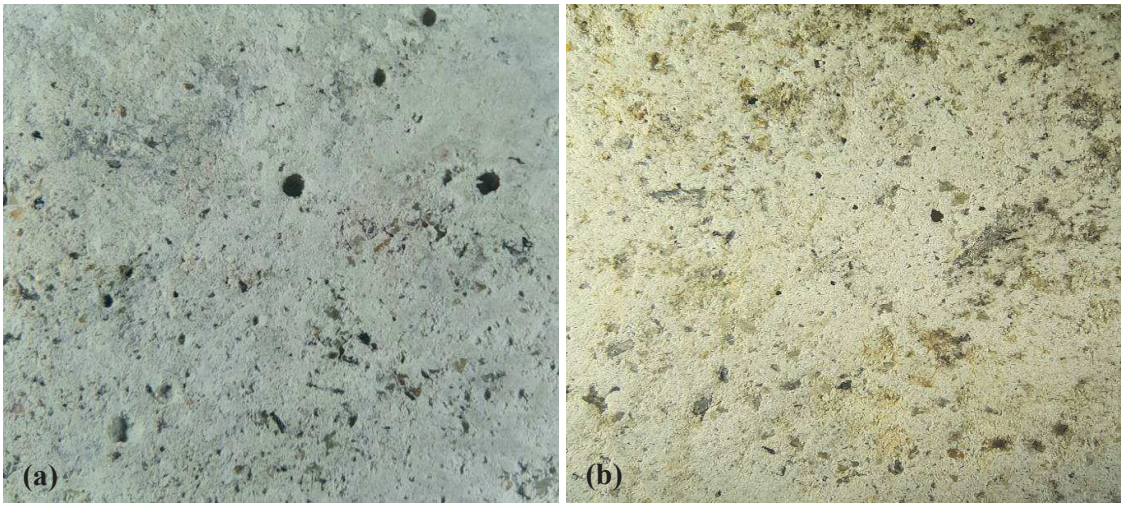

Fig. 5.45 Stereo microscopic images (1× magnification) of gamma irradiated: a) control; b) *A. tamarii* infected concrete cube surface after 6 months.

The effectiveness of selected doses of UVC and gamma radiation against the biodeterioration of concrete by *Aspergillus tamarii* was determined to be positive based on variations in weight, strength, elemental composition, stereo microscopic image, and characteristics of functional bands from FTIR study.

5.4.2 *In situ* model for conservation of heritage building

Based on the findings of this study, an *in situ* model for conservation effect of heritage buildings made of concrete is recommended (Fig. 5.46). According to this model, five UVC

lights will be installed (4 side wall lights and 1 upper wall light) with an intensity of 625 µw/cm^2 and a peak wavelength of 254 nm at a distance of 15 cm from the walls. Another option will to place radioactive material that releases gamma rays in a properly constructed collimator inside the room. The duration of the UV exposure shall be 5 mins, whereas 0.5 KGy dose of gamma radiation needed to prevent the growth of mould on concrete walls at least twice a year. The concrete walls will be better and fungal-free as a consequence, which save time and money and being non-destructive.

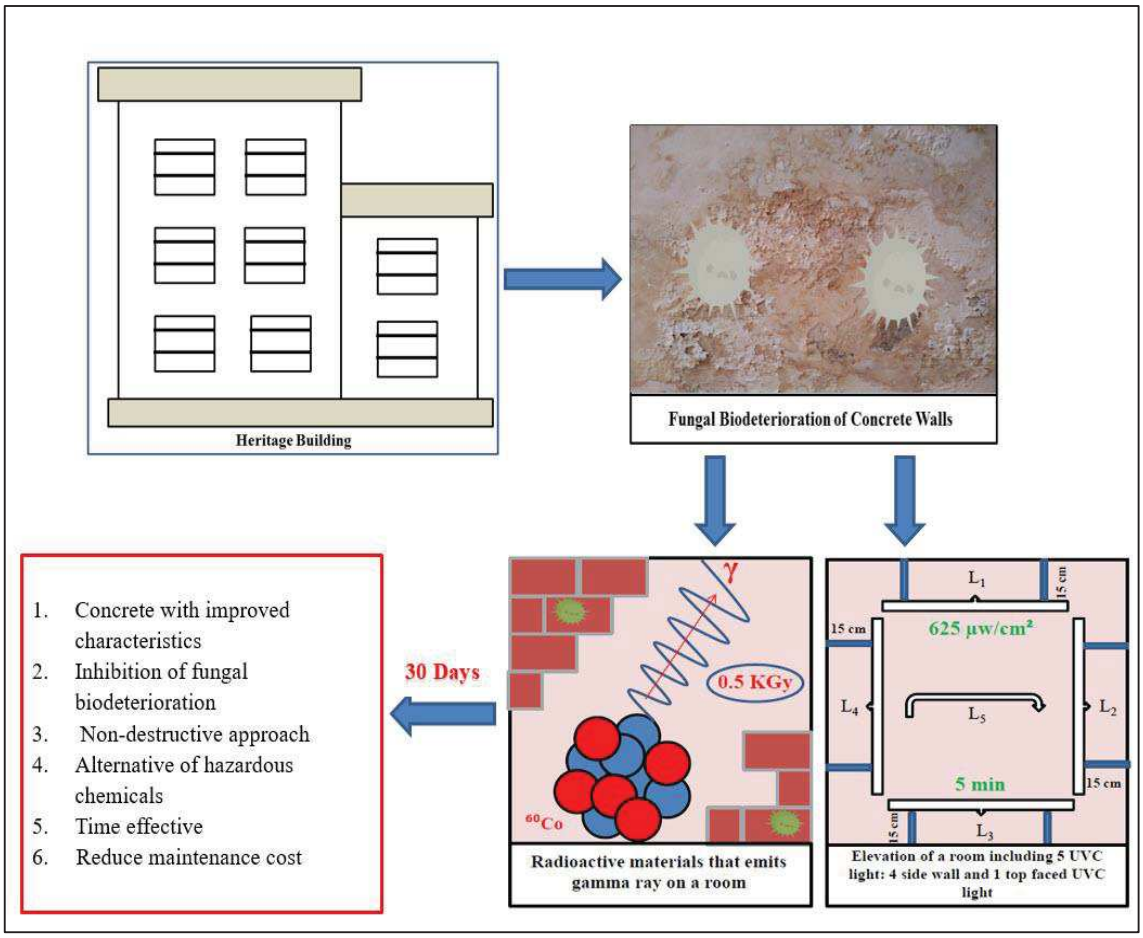

Fig. 5.46 *In situ* model for preventing fungal biodeterioration of historic building.

UVC radiation appears to be a much more effective, safe, and affordable way to get rid of fungi from surfaces and indoor spaces than gamma radiation. These are specialised lights with fungicidal qualities that can be mounted on surfaces or mounted on stands. The luminaires can be used with humans inside when the flow mode is on. The flow mode's strong airflow and reliable UVC light shielding are its defining features.

CHAPTER – 6

CONCLUSIONS AND FUTURE SCOPE OF WORK

6.1 Conclusions

An assessment of the airborne fungi in the indoor environment was experimentally investigated in the present study. This experiment was conducted in five different indoor environment using Two-Stage Andersen air sampler during the monsoon season. The results of air sampling revealed that the highest percentage of culturable airborne fungi was *Aspergillus* sp. followed by *Penicillium* sp., *Rhizopus* sp., *Cladosporium* sp., *Curvularia* sp., *Paecilomyces* sp. and *Alternaria* sp. Fungi were then isolated from three distinct locations of the fungal infected surface (4 cm^2 area) of the wall of Tagore's house by rubbing a sterilized cotton swab. The sampling results revealed that the highest number of colony in this heritage building was found for *Aspergillus* sp. followed by *Penicillium* sp. Similar observations were noticed earlier by several research groups and reported that the highest percentage of spores were found for *Aspergillus* sp. followed by *Penicillium* sp. in different indoor environment (Staszowska 2023; Chegini et al., 2020; Naji et al., 2014; Yassin et al., 2010; Mui et al., 2007). Thereafter concrete pieces were inoculated with these fungi. The weight loss (%) and calcium release of concrete piece, color change, fungal growth and organic acid analysis of the fungal medium after 30 days of observation indicated that *Aspergillus tamarii* imparted maximum loss as compared to *Aspergillus niger*, *Aspergillus flavus* and *Penicillium oxalicum*. The Scanning Electron Microscope (SEM) images displayed fungal colonization, ettringite and crack formation on *A. tamarii* infected concrete surface which also supports the present phenomenon. Hence, all subsequent investigations in the present research were done with *A. tamarii* only.

The second part of this study the *Aspergillus tamari* was applied to infect concrete cubes (M20 and M40) for 60, 120 and 180 days. This study focused on detection of organic acids in infected liquid medium, observation of fungal growth, changes in weight, compressive strength, elemental compositions, functional groups, and surface properties of concrete cubes. The organic acids present in the *A. tamarii* infected medium can damage concrete cubes were due to oxalic acid, malic acid, lactic acid and acetic acid. The results of the experiment showed that the 5cm x 5cm x 5cm (M20) and 10cm x 10cm x 10cm (M40) cube samples infected by the spore suspension of *Aspergillus tamarii* after 180 days of incubation showed the largest effect of biodeterioration with smaller weight loss (2.22 ± 0.04% & 1.20 ± 0.01%) and lower final strength (about 25.17 ± 0.12% & 24.34 ± 0.16% of their initial strength). Successful results achieved in elemental composition analysis, after six months reduction of mass fraction of calcium for M20 and M40 graded concrete were 15.68 ± 0.09% & 25.36 ±

0.05% and also observed the absence of several absorption bands in each region when it can be compared to control specimens. The fungal development and expansion of fungal hyphae into the interior of concrete cubes, which are responsible for crack formation, were clearly visible in the stereo zoom and SEM microscope photos. The evidential examination suggested that isolated fungi *Aspergillus tamarii* was present in Tagore's house could enhance the deterioration phenomena of concrete wall in different ways and also impose changes in their physical, mechanical, and chemical properties that leads to decrease in the lifespan of concrete structure. Additionally, our present study agreed with the results of other researcher's reports (Jiang et al., 2022; Yakovleva et al., 2018; Marquez-Penaranda et al., 2016; Wiktor et al., 2009; Sanchez-Silva et al., 2008; Gaylarde et al., 2003; Gu et al., 1998).

Radiosensitivity test was performed with several doses of UVC (5, 10, 15 and 20 mins) and gamma (0.5, 0.75 and 1 KGy) radiation to select the most of the potent dose for complete inhibition of *A.tamarii*. The results revealed that *A. tamarii* was resistant after 5 min UVC and 0.5 KGy gamma exposure but 20 min UVC and 1 KGy gamma radiation were needed for complete depletion of fungal population. Simultaneously, both kind of radiation such as UVC (5, 10, 15 and 20 mins) and gamma (0.5, 0.75 and 1 KGy) as applied on the *A.tamarii* infected concrete cubes for 30 days. Based on weight losses, strength losses, changes in elemental composition and functional groups, radiation damage in concrete was clearly evidenced after infected cube was exposed to different type of radiation with the increment of doses in contrast to samples that had only infected with *A. tamarii*. Hence the further study revealed that 5 mins UVC and 0.5 KGy gamma radiation dose showed negligible loss of physical, mechanical and chemical properties of concrete after 30 days of incubation. Considering observations from short term inhibition study, it was chosen a 5 min UVC exposure and 0.5 KGy doses of gamma radiation for subsequent study. It was a priority to inhibit some fungal effect without disturbing the concrete properties in the case of conservation of historic building. Additionally, ultraviolet ray has been more effective to prevent fungal biodeterioration of concrete than gamma radiation.

Inhibition study was showed the efficacy of the selected doses (5 mins for UVC and 0.5 KGy for gamma) of radiation. This study also concentrated on weight, compressive strength, elemental compositions, functional groups, and surface properties of concrete cubes. The results revealed that UVC and gamma radiation inhibits the growth of fungus and as a consequence concrete cubes has been found to be very negligible weight losses (0.28 ± 0.09% and 0.72 ± 0.08%) compared to the only infected samples (2.22 ± 0.04%) after 180

days of incubation. Furthermore, a significant increase in compressive strength was observed for infected concrete cubes exposed to UVC (26.58 ± 0.23 N/mm^2) and gamma (23.38 ± 0.14 N/mm^2) radiation as compared to only infected samples (14.77 ± 0.06 N/mm^2). Strong symmetrical stretching bands of inhibition (infected and irradiated) concrete were observed by FTIR and EDXRF analysis as shown found to be greater calcium content in inhibited cubes (66.43 ± 0.06% and 54.11 ± 0.07%) than the only infected ones (15.68 ± 0.09%). In contrast to biodeteriorated (infected) samples, no holes or cavities has been developed on the infected cube surface after exposure to UVC and gamma radiation. The present experimental investigations suggest that chosen dose of radiation which improves physical, mechanical, chemical and aesthetic properties of infected concrete after 180 days.

This thesis presents for the first time the combined studies i.e. (i) isolation and identification of some potent airborne micro-fungi from different indoor environment (ii) evaluation of biodeterioration of M20 and M40 grade concrete using fungus (*A. tamarii*) as biodegrading agent with some exposure interval (iii) standardization of some non-destructive method i.e. application of ultraviolet and gamma radiation for inhibition of fungal biodeterioration. Prior to this work, no integrated comprehensive investigation has been conducted in detail to identify the fungi, loss determination and prevention by some important physical radiological phenomenon to eradicate the problem. The present research is addressed for the reduction of such gap and fulfils the desired objectives of this thesis.

6.2 Future scope of work

The following activities can be performed in near future for further investigations on inhibition of fungal biodeterioration of concrete.

- Other microorganisms like bacteria or algae can also be used to test the deterioration in concrete.
- Inhibition of fungal biodeterioration of concrete can be done in large scale using the methods like chemical treatment i.e. application of liquid biocides and paints, biological treatments with compound of natural origin etc.
- In order to more clearly explain the efficiency of radiation, it is also advised that biodeterioration as well as inhibition with radiation of fungal biodeterioration of concrete can be expanded for extended periods of time.
- The scope of future research work can be widened using the technique *in situ* on actual colonized concrete-based buildings.

CHAPTER – 7

REFERENCES

Adhikary, S. P., & Sahu, J. K. (1998). UV protecting pigment of the terrestrial cyanobacterium Tolypothrix byssoidea. Journal of plant physiology, 153(5-6), 770-773.

Aldosari, M. A., Darwish, S. S., Adam, M. A., Elmarzugi, N. A., & Ahmed, S. M. (2019). Using ZnO nanoparticles in fungal inhibition and self-protection of exposed marble columns in historic sites. Archaeological and Anthropological Sciences, 11, 3407-3422.

Allsopp, D. (2011). Worldwide wastage: the economics of biodeterioration. Microbiol Tod, 38(4), 150-153.

Allsopp, D., Seal, K. J., & Gaylarde, C. C. (2004). Introduction to biodeterioration, 2nd edn. Cambridge University Press.

Amann, R. I., Krumholz, L., & Stahl, D. A. (1990). Fluorescent-oligonucleotide probing of whole cells for determinative, phylogenetic, and environmental studies in microbiology. Journal of bacteriology, 172(2), 762-770.

Andersen, A. A. (1958). New sampler for the collection, sizing, and enumeration of viable airborne particles. Journal of bacteriology, 76(5), 471-484.

Anna, W., Dorota, R., Mansur, R., & Sławomir, W. (2020). Microorganisms colonising historical cardboard objects from the Auschwitz-Birkenau State Museum in Oświęcim, Poland and their disinfection with vaporised hydrogen peroxide (VHP). International Biodeterioration & Biodegradation, 152, 104997.

Aquino, R. S. S., Silveira, S. S., Pessoa, W. F. B., Rodrigues, A., Andrioli, J. L., Delabie, J. H. C., & Fontana, R. (2013). Filamentous fungi vectored by ants (Hymenoptera: Formicidae) in a public hospital in north-eastern Brazil. Journal of Hospital Infection, 83(3), 200-204.

ASTM, Standard Practice for Using the Fricke Reference-Standard Dosimetry System. In: E1026-04e1, Annual book of ASTM Standard, Vol. 12.02, American Society for Testing and Materials, PA, USA, 2007.

Aziz, N. H., El-Fouly, M. Z., Abu-Shady, M. R., & Moussa, L. A. A. (1997). Effect of gamma radiation on the survival of fungal and actinomycetal florae contaminating medicinal plants. Applied Radiation and Isotopes, 48(1), 71-76.

Badarloo, B., Lehner, P., & Bakhtiari Doost, R. (2022). Mechanical properties and gamma radiation transmission rate of heavyweight concrete containing barite aggregates. Materials, 15(6), 2173.

Barkai-Golan, R., Padova, R., Ross, I., Lapidot, M., Davidson, H., & Copel, A. (1993). Combined hot water and radiation treatments to control decay of tomato fruits. Scientia horticulturae, 56(2), 101-105.

Basu, C., Bhattacharyya, S., Chaudhuri, A., Akhtar, S., Chatterjee, A., Thakur, B., Guha, H., & Chaudhuri, P. (2021). Assessment of Potential Damage Factor: A Case Study of St. Paul's Cathedral, Kolkata. Journal of Heritage Management, 6(1), 53-68.

Battaglin, G., Boscolo-Boscoletto, A., Caccavale, F., De Marchi, G., Mazzoldi, P., & Arnold, G. W. (1992). Etching effects in ion Implanted SiO_2. Modifications Induced by Irradiation in Glasses, 91-96.

Becerra, J., Mateo, M. P., Nicolás, G., & Ortiz, P. (2019). Evaluation of the penetration depth of nano-biocide treatments by LIBS. In Science and Digital Technology for Cultural Heritage (pp. 368-372). CRC Press.

Bertrand, L., Schöder, S., Joosten, I., Webb, S. M., Thoury, M., Calligaro, T., Anheim, E., & Simon, A. (2023). Practical advances towards safer analysis of heritage samples and objects. TrAC Trends in Analytical Chemistry, 117078.

Bertron, A. (2014). Understanding interactions between cementitious materials and microorganisms: a key to sustainable and safe concrete structures in various contexts. Materials and Structures, 47, 1787-1806.

Bhattacharyya, S., Akhtar, S., Chaudhuri, A., Mahanty, S., Chaudhuri, P., & Sudarshan, M. (2022). Affirmative nanosilica mediated approach against fungal biodeterioration of concrete materials. Case Studies in Construction Materials, 17, e01258.

Bhattacharyya, S., Mukherjee, D., & Chaudhuri, P. (2016). Biodeterioration risk index of exhibit present in museum galleries of tropical climate. Museum Management and Curatorship, 31(3), 268-282.

Bielefeldt, A., Gutierrez-Padilla, M. G. D., Ovtchinnikov, S., Silverstein, J., & Hernandez, M. (2010). Bacterial kinetics of sulfur oxidizing bacteria and their biodeterioration rates of concrete sewer pipe samples. Journal of Environmental Engineering, 136(7), 731-738.

Bogdan, S., Deya, C., Micheloni, O., Bellotti, N., & Romagnoli, R. (2018). Natural products to control biofilm on painted surfaces. Pigment & Resin Technology, 47(2), 180-187.

Borderie, F., Alaoui-Sossé, B., & Aleya, L. (2015). Heritage materials and biofouling mitigation through UV-C irradiation in show caves: state-of-the-art practices and future challenges. Environmental Science and Pollution Research, 22, 4144-4172.

Borderie, F., Alaoui-Sehmer, L., Bousta, F., Orial, G., Rieffel, D., Richard, H., & Alaoui-Sosse, B. (2012). UV irradiation as an alternative to chemical treatments: a new approach against algal biofilms proliferation contaminating building facades, historical monuments and touristic subterranean environments. Algae: ecology, economic uses and environmental impact. Nova Science Publishers, Inc. Hauppauge, New York, 1-28.

Bouniol, P., & Aspart, A. (1998). Disappearance of oxygen in concrete under irradiation: the role of peroxides in radiolysis. Cement and concrete research, 28(11), 1669-1681.

Burford, E. P., Fomina, M., & Gadd, G. M. (2003). Fungal involvement in bioweathering and biotransformation of rocks and minerals. Mineralogical Magazine, 67(6), 1127-1155.

Cabral, J. P. (2010). Can we use indoor fungi as bioindicators of indoor air quality? Historical perspectives and open questions. Science of the total environment, 408(20), 4285-4295.

Caneva, G., Nugari, M. P., Nugari, M. P., & Salvadori, O. (Eds.). (2008). Plant biology for cultural heritage: biodeterioration and conservation. Getty Publications.

Caneva, G., Nugari, M. P., & Salvadori, O. (2008). Control of biodeterioration and bioremediation techniques. Plant Biology for Cultural Heritage. Biodeterioration and Conservation; Caneva, G., Nugari, MP, Salvadori, O., Eds, 309-345.

Casiglia, S., Bruno, M., Scandolera, E., Senatore, F., & Senatore, F. (2020). Influence of harvesting time on composition of the essential oil of Thymus capitatus (L.) Hoffmanns. & Link. growing wild in northern Sicily and its activity on microorganisms affecting historical art crafts. Arabian Journal of Chemistry, 12(8), 2704-2712.

Chaudhuri, A., & Bhattacharyya, S. (2019). Foldscopic visualization and identification of airborne fungi in museum and library environment. Journal of Emerging Technologies and Innovative Research, 6(6), 838-41.

Chegini, F. M., Baghani, A. N., Hassanvand, M. S., Sorooshian, A., Golbaz, S., Bakhtiari, R., Ashouri, A., Joubani, M. N. & Alimohammadi, M. (2020). Indoor and outdoor airborne bacterial and fungal air quality in kindergartens: Seasonal distribution, genera, levels, and factors influencing their concentration. Building and environment, 175, 106690.

Choi, J. I., & Lim, S. (2016). Inactivation of fungal contaminants on Korean traditional cashbox by gamma irradiation. Radiation Physics and Chemistry, 118, 70-74.

Chuang, C. C., Kuo, Y. L., Chao, C. C., & Chao, W. L. (2007). Solubilization of inorganic phosphates and plant growth promotion by Aspergillus niger. Biology and Fertility of Soils, 43, 575-584.

Cody, R. D., Cody, A. M., Spry, P. G., & Lee, H. (2001). Reduction of concrete deterioration by ettringite using crystal growth inhibition techniques (No. TR-431,). Department of Geological and Atmospheric Sciences, Iowa State University.

Craeye, B., De Schutter, G., Vuye, C., & Gerardy, I. (2015). Cement-waste interactions: Hardening self-compacting mortar exposed to gamma radiation. Progress in Nuclear Energy, 83, 212-219.

Cwalina, B. (2014). Biodeterioration of concrete, brick and other mineral-based building materials. Understanding biocorrosion, 281-312.

Davis, J. L., Nica, D., Shields, K., & Roberts, D. J. (1998). Analysis of concrete from corroded sewer pipe. International Biodeterioration & Biodegradation, 42(1), 75-84.

da Silva, M., Moraes, A. M. L., Nishikawa, M. M., Gatti, M. J. A., de Alencar, M. V., Brandão, L. E., & Nóbrega, A. (2006). Inactivation of fungi from deteriorated paper materials by radiation. International Biodeterioration & Biodegradation, 57(3), 163-167.

De Windt, L., & Devillers, P. (2010). Modeling the degradation of Portland cement pastes by biogenic organic acids. Cement and Concrete Research, 40(8), 1165-1174.

Di Giulio, M., Grande, R., Di Campli, E., Di Bartolomeo, S., & Cellini, L. (2010). Indoor air quality in university environments. Environmental monitoring and assessment, 170, 509-517.

Dresler, C., Saladino, M. L., Demirbag, C., Caponetti, E., Martino, D. F. C., & Alduina, R. (2017). Development of controlled release systems of biocides for the conservation of cultural heritage. International Biodeterioration & Biodegradation, 125, 150-156.

Duggal, S. K. (2017). Building materials. Routledge.

Dutton, M. V., & Evans, C. S. (1996). Oxalate production by fungi: its role in pathogenicity and ecology in the soil environment. Canadian journal of microbiology, 42(9), 881-895.

Favero-Longo, S. E., Benesperi, R., Bertuzzi, S., Bianchi, E., Buffa, G., Giordani, P., & Vannini, A. (2017). Species-and site-specific efficacy of commercial biocides and application solvents against lichens. International Biodeterioration & Biodegradation, 123, 127-137.

Field, K. G., Remec, I., & Le Pape, Y. (2015). Radiation effects in concrete for nuclear power plants–Part I: Quantification of radiation exposure and radiation effects. Nuclear Engineering and Design, 282, 126-143.

Fomina, M., Podgorsky, V. S., Olishevska, S. V., Kadoshnikov, V. M., Pisanska, I. R., Hillier, S., & Gadd, G. M. (2007). Fungal deterioration of barrier concrete used in nuclear waste disposal. Geomicrobiology Journal, 24(7-8), 643-653.

Fuentes, E., Perez-Velon, D., & Prieto, B. (2022). Effects of changes in UV-B radiation levels on biofilm-forming organisms commonly found in cultural heritage surfaces. Environmental Research, 214, 114061.

Gadd, G. M., Bahri-Esfahani, J., Li, Q., Rhee, Y. J., Wei, Z., Fomina, M., & Liang, X. (2014). Oxalate production by fungi: significance in geomycology, biodeterioration and bioremediation. Fungal Biology Reviews, 28(2-3), 36-55.

Gaylarde, C., Ribas Silva, M., & Warscheid, T. (2003). Microbial impact on building materials: an overview. Materials and structures, 36, 342-352.

Geba, M., Lisa, G., Ursescu, C. M., Olaru, A., Spiridon, I., Leon, A. L., & Stanculescu, I. (2014). Gamma irradiation of protein-based textiles for historical collections decontamination. Journal of Thermal Analysis and Calorimetry, 118, 977-985.

Genova, C., Grottoli, A., Zoppis, E., Cencetti, C., Matricardi, P., & Favero, G. (2020). An integrated approach to the recovery of travertine biodegradation by combining phyto-cleaning with genomic characterization. Microchemical Journal, 156, 104918.

George, R. P., Ramya, S., Ramachandran, D., & Mudali, U. K. (2013). Studies on Biodegradation of normal concrete surfaces by fungus Fusarium sp. Cement and Concrete Research, 47, 8-13.

Geweely, N. S., Afifi, H. A., Abdelrahim, S. A., & Alakilli, S. Y. (2014). Novel comparative efficiency of ozone and gamma sterilization on fungal deterioration of archeological painted coffin, Saqqara excavation, Egypt. Geomicrobiology Journal, 31(6), 529-539.

Ghosh, S. N., & Handoo, S. K. (1980). Infrared and Raman spectral studies in cement and concrete. Cement and Concrete Research, 10(6), 771-782.

Giannantonio, D. J., Kurth, J. C., Kurtis, K. E., & Sobecky, P. A. (2009). Effects of concrete properties and nutrients on fungal colonization and fouling. International Biodeterioration & Biodegradation, 63(3), 252-259.

Gu, J. D. (2003). Microbiological deterioration and degradation of synthetic polymeric materials: recent research advances. International biodeterioration & biodegradation, 52(2), 69-91.

Gu, J. D., Ford, T. E., Berke, N. S., & Mitchell, R. (1998). Biodeterioration of concrete by the fungus Fusarium. International biodeterioration & biodegradation, 41(2), 101-109.

Gutarowska, B., Skora, J., Zduniak, K., & Rembisz, D. (2012). Analysis of the sensitivity of microorganisms contaminating museums and archives to silver nanoparticles. International Biodeterioration & Biodegradation, 68, 7-17.

Hanehara, S., & Oyamada, T. (2010). Reproduction of delayed ettringite formation (DEF) in concrete and relationship between DEF and alkali silica reaction. Monitoring and Retrofitting of Concrete Structures-BH Oh, et al.(eds), Korea Concrete Institute, Seoul.

Hanus, M. J., & Harris, A. T. (2013). Nanotechnology innovations for the construction industry. Progress in materials science, 58(7), 1056-1102.

Hassanein, W. A. (1987). Effect of gamma radiation on growth and activity of *Aspergillus flavus* (Doctoral dissertation, M. Sc., Thesis, Zagazig University, Faculty of Science, Egypt).

Heaton, P. E., Callow, M. E., Butler, G. M., & Milne, A. (1991). Control of mould growth by anti-fungal paints. International Biodeterioration, 27(2), 163-173.

https://mausam.imd.gov.in/kolkata/, accessed on September 25 2022.

Hueck, H.J. (1968). The biodeterioration of materials e an appraisal. In: Walters, A.H., Elphick, J.J. (Eds.), Biodeterioration of materials. Elsevier, London, 6-12.

Hueck, H. J. (1965). The biodeterioration of materials as part of hylobiology. Material und Organismen, 1(1), 5-34.

Ilinskaya, O., Bayazitova, A., & Yakovleva, G. (2018). Biocorrosion of materials and sick building syndrome. Microbiology Australia, 39(3), 129-132.

Ishida, H., Nahara, Y., Tamamoto, M., & Hamada, T. (1991). The fungicidal effect of ultraviolet light on impression materials. The Journal of Prosthetic Dentistry, 65(4), 532-535.

Jeong, S. H., Lee, H. J., Kim, D. W., & Chung, Y. J. (2018). New biocide for eco-friendly biofilm removal on outdoor stone monuments. International Biodeterioration & Biodegradation, 131, 19-28.

Jestin, A., Thouvenot, P., Libert, M., & Bournazel, J. P. (2004). A concrete bio-decontamination process in nuclear substructures: effects of organic acids.

Katusin-Razem, B., Mihaljevic, B., & Razem, D. (2003). Microbial decontamination of cosmetic raw materials and personal care products by irradiation. Radiation Physics and Chemistry, 66(4), 309-316.

Kim, K. Y., Kim, Y. S., Kim, D., & Kim, H. T. (2011). Exposure level and distribution characteristics of airborne bacteria and fungi in Seoul metropolitan subway stations. Industrial health, 49(2), 242-248.

Kontani, O., Ichikawa, Y., Ishizawa, A., Takizawa, M., & Sato, O. (2014). Irradiation effects on concrete structures. Infrastructure systems for nuclear energy, 459-473.

Krumbein, W. E. (1992, May). Colour changes of building stones and their direct and indirect biological causes. In Proceedings of the 7th International Congress on Deterioration and Conservation of Stone: held in Lisbon, Portugal, 15-18 June 1992 (pp. 443-452).

Kumar, J., & Kushwaha, R. K. S. (2014). Screening of fungi efficient in feather degradation and keratinase production. Arch. Appl. Sci. Res, 6(1), 73-78.

Kurth, J. C. (2008). Mitigating biofilm growth through the modification of concrete design and practice (Doctoral dissertation, Georgia Institute of Technology).

Liaud, N., Ginies, C., Navarro, D., Fabre, N., Crapart, S., Gimbert, I. H., Levasseur, A., Raouche, S., & Sigoillot, J. C. (2014). Exploring fungal biodiversity: organic acid production by 66 strains of filamentous fungi. Fungal Biology and Biotechnology, 1(1), 1-10.

Li, Z., Bai, T., Dai, L., Wang, F., Tao, J., Meng, S., Hu, Y., Wang. S., & Hu, S. (2016). A study of organic acid production in contrasts between two phosphate solubilizing fungi: Penicillium oxalicum and Aspergillus niger. Scientific reports, 6(1), 25313.

Ljaljevic-Grbic, M. V., & Vukojevic, J. B. (2009). Role of fungi in biodeterioration process of stone in historic buildings. Zbornik matice srpske za prirodne nauke, (116), 245-251.

Magnuson, J. K., & Lasure, L. L. (2004). Organic acid production by filamentous fungi. Advances in fungal biotechnology for industry, agriculture, and medicine, 307-340.

Maity, J. P., Kar, S., Banerjee, S., Sudershan, M., Chakraborty, A., & Santra, S. C. (2011). Effects of gamma radiation on fungi infected rice (in vitro). International Journal of Radiation Biology, 87(11), 1097-1102.

Maity, J. P., Kar, S., Banerjee, S., Chakraborty, A., & Santra, S. C. (2009). Effects of gamma irradiation on long-storage seeds of Oryza sativa (cv. 2233) and their surface infecting fungal diversity. Radiation Physics and Chemistry, 78(11), 1006-1010.

Maity, J. P., Chakraborty, A., Chanda, S., & Santra, S. C. (2008). Effect of gamma radiation on growth and survival of common seed-borne fungi in India. Radiation Physics and Chemistry, 77(7), 907-912.

Maity, J. P., Mishra, D., Chakraborty, A., Saha, A., Santra, S. C., & Chanda, S. (2005). Modulation of some quantitative and qualitative characteristics in rice (Oryza sativa L.) and mung (Phaseolus mungo L.) by ionizing radiation. Radiation Physics and Chemistry, 74(5), 391-394.

Marquez-Peñaranda, J. F., Sanchez-Silva, M., Husserl, J., & Bastidas-Arteaga, E. (2016). Effects of biodeterioration on the mechanical properties of concrete. Materials and structures, 49, 4085-4099.

Martins, J. A., Dallacort, R., Inoue, M. H., Santi, A., & Coletti, A. J. (2010). Probabilidade de precipitação para a microregião de Tangará da Serra, estado do Mato Grosso. Pesquisa Agropecuária Tropical, 291-296.

Martin-Sanchez, P. M., Nováková, A., Bastian, F., Alabouvette, C., & Saiz-Jimenez, C. (2012). Use of biocides for the control of fungal outbreaks in subterranean environments: The case of the Lascaux Cave in France. Environmental science & technology, 46(7), 3762-3770.

Mazzoldi, P., Carnera, A., Caccavale, F., Favaro, M. L., Boscolo-Boscoletto, A., Granozzi, G., Bertoncello, R., & Battaglin, G. (1991). N and Ar ion-implantation effects in SiO2 films on Si single-crystal substrates. Journal of applied physics, 70(7), 3528-3536.

McNamara, N. P., Black, H. I. J., Beresford, N. A., & Parekh, N. R. (2003). Effects of acute gamma irradiation on chemical, physical and biological properties of soils. Applied soil ecology, 24(2), 117-132.

Mehta, P. K. (1999). Concrete technology for sustainable development. Concrete international, 21(11), 47-53.

Mironenko, N. V., Alekhina, I. A., Zhdanova, N. N., & Bulat, S. A. (2000). Intraspecific variation in gamma-radiation resistance and genomic structure in the filamentous fungus Alternaria alternata: a case study of strains inhabiting Chernobyl reactor no. 4. Ecotoxicology and environmental safety, 45(2), 177-187.

Mobasher, N., Bernal, S. A., Kinoshita, H., Sharrad, C. A., & Provis, J. L. (2015). Gamma irradiation resistance of an early age slag-blended cement matrix for nuclear waste encapsulation. Journal of Materials Research, 30(9), 1563-1571.

Money, N. P. (2004). The fungal dining habit: a biomechanical perspective. Mycologist, 18(2), 71-76.

Mui, K. W., Chan, W. Y., Wong, L. T., & Hui, P. S. (2007). Fungi—an indoor air quality assessment parameter for air-conditioned offices. Building Services Engineering Research and Technology, 28(3), 265-274.

Mukherjee, D., Bhattacharyya, S., & Chaudhuri, P. (2016). Fumigation of eucalyptus oil for controlling strong room fungi at Jorasanko Museum (Tagore's residence), India: a study for sustainable conservation. International Journal of Conservation Science, 7(2).

Munsell, A. H. (2009). Geological Rock-Color Chart, Produced by Munsell Color.

Murthy, J. M., Sundaram, C., Prasad, V. S., Purohit, A. K., Rammurti, S., & Laxmi, V. (2000). Aspergillosis of central nervous system: a study of 21 patients seen in a university hospital in south India. The Journal of the Association of Physicians of India, 48(7), 677-681.

Nagabhushana, H., Prashantha, S. C., Nagabhushana, B. M., Lakshminarasappa, B. N., & Singh, F. (2008). Damage creation in swift heavy ion-irradiated calcite single crystals: Raman and Infrared study. Spectrochimica Acta Part A: Molecular and Biomolecular Spectroscopy, 71(3), 1070-1073.

Nair, P. A. K., Vasconcelos, W. L., Paine, K., & Calabria-Holley, J. (2021). A review on applications of sol-gel science in cement. Construction and building materials, 291, 123065.

Naji, K. M., Abdullah, Q. Y. M., Al-Zaqri, A. Q. M., & Alghalibi, S. M. (2014). Evaluating the biodeterioration enzymatic activities of fungal contamination isolated from some ancient Yemeni mummies preserved in the national museum. Biochemistry research international, 2014.

Nevalainen, A., Täubel, M., & Hyvärinen, A. (2015). Indoor fungi: companions and contaminants. Indoor air, 25(2), 125-156.

Nonthijun, P., Mills, N., Mills, N., Yongsawas, R., Sansupa, C., Suwannarach, N., Churdsak, J., Motanated, K., Chayapakdee, P., Jongjitngam, S., Noirungsee, N., & Disayathanoowat, T. (2023). Seasonal Variations in Fungal Communities on the Surfaces of Lan Na Sandstone Sculptures and Their Biodeterioration Capacities. Journal of Fungi, 9(8), 833.

Nugari, M. P., & Salvadori, O. (2017). Biodeterioration control of cultural heritage: Methods and products. In Molecular biology and cultural heritage (pp. 233-242). Routledge.

Nuhoglu, Y., Oguz, E., Uslu, H., Ozbek, A., Ipekoglu, B., Ocak, I., & Hasenekoglu, I. (2006). The accelerating effects of the microorganisms on biodeterioration of stone monuments under air pollution and continental-cold climatic conditions in Erzurum, Turkey. Science of the total environment, 364(1-3), 272-283.

Okten, S., & Asan, A. (2012). Airborne fungi and bacteria in indoor and outdoor environment of the Pediatric Unit of Edirne Government Hospital. Environmental monitoring and assessment, 184, 1739-1751.

Olarinoye, I. O., Kolo, M. T., Shittu, H. O., & Anumah, A. S. (2023). Estimation of indoor gamma radiation dose rate from concrete blocks constructed from tin mine tailings. Journal of Building Engineering, 66, 105934.

Ottow, J. C., & Glathe, H. (1968). Rose bengal-malt extract-agar, a simple medium for the simultaneous isolation and enumeration of fungi and actinomycetes from soil. Applied Microbiology, 16(1), 170.

Ozcelik, B. E. R. R. İ. N. (2007). The Fungi bacteriostatical static Effect of Ultraviolet Light in 254nm 354nm Wavelengths. Research Journal of Microbiology, 2(1).

Palla, F., Bruno, M., Mercurio, F., Tantillo, A., & Rotolo, V. (2020). Essential oils as natural biocides in conservation of cultural heritage. Molecules, 25(3), 730.

Perfettini, J. V., Revertegat, E., & Langomazino, N. (1991). Evaluation of cement degradation induced by the metabolic products of two fungal strains. Experientia, 47(6), 527-533.

Pfendler, S., Borderie, F., Bousta, F., Alaoui-Sosse, L., Alaoui-Sosse, B., & Aleya, L. (2018). Comparison of biocides, allelopathic substances and UV-C as treatments for biofilm proliferation on heritage monuments. Journal of Cultural Heritage, 33, 117-124.

Pignatelli, I., Kumar, A., Field, K. G., Wang, B., Yu, Y., Le Pape, Y., Bauchy, M., & Sant, G. (2016). Direct experimental evidence for differing reactivity alterations of minerals following irradiation: the case of calcite and quartz. Scientific reports, 6(1), 20155.

Pinar, G., Sterflinger, K. (2009). Microbes and building materials, In: Cornejo, D.N., Haro, J.L., (eds) Building materials: properties, performance and applications, Nova Science Publishers, New York, 163–188.

Pomaro, B. (2016). A review on radiation damage in concrete for nuclear facilities: from experiments to modeling. Modelling and Simulation in Engineering, 2016.

Ponta, C. C. (2008). Irradiation conservation of cultural heritage. Nuclear Physics News, 18(1), 22-24.

Portland Cement Association. (2001). Ettringite formation and the performance of concrete (No. 2166). Portland Cement Association.

Potts, A., Butcher, E., Cann, G., & Leay, L. (2021). Long term effects of gamma irradiation on in-service concrete structures. Journal of Nuclear Materials, 548, 152868.

Prak, L., Sumranwanich, T., & Tangtermsirikul, S. (2023). Experimental investigation on the degradation of coating on concrete surfaces exposed to accelerated and natural UV in chloride environment. Journal of Adhesion Science and Technology, 37(2), 240-256.

Ramachandran, V. S., & Beaudoin, J. J. (2000). Handbook of analytical techniques in concrete science and technology: principles, techniques and applications. Elsevier.

Rashid, M., Khalil, S., Ayub, N., Alam, S., & Latif, F. (2004). Organic acids production and phosphate solubilization by phosphate solubilizing microorganisms (PSM) under in vitro conditions. Pak J Biol Sci, 7(2), 187-196.

Reches, Y. (2018). Nanoparticles as concrete additives: Review and perspectives. Construction and Building Materials, 175, 483-495.

Reddy, M. K., & Srinivas, T. (2017). Mold allergens in indoor play school environment. Energy Procedia, 109, 27-33.

Rezaei-Ochbelagh, D., Mosavinejad, H. G., Molaei, M., Azimkhani, S., & Khodadoost, M. (2010). Effect of low-dose gamma-radiation on concrete during solidification. International Journal of the Physical Sciences, 5(10), 1496-1500.

Ribas, S. (1995). Study of biological degradation applied to concrete. In Transactions of the 13. International conference on structural mechanics in reactor technology. v. 4.

Rosado, T., Gil, M., Mirão, J., Candeias, A., & Caldeira, A. T. (2013). Oxalate biofilm formation in mural paintings due to microorganisms–A comprehensive study. International Biodeterioration & Biodegradation, 85, 1-7.

Rose, A. H. (1981). History and Scientific Basis of Microbial Biodeterioration of Materials. In" Microbial Biodeterioration" Economic Microbiology Vol. 6, (Rose, AH, Ed.).

Sanchez, F., Kosson, D., Brown, K., Delapp, R., Teising, R., Gonzalez, R., Lewis, J., Brown, L., Reches, Y., Helbing, M., Thomson, K., Lacy, M., Regala, M., & Srivastava, A. (2018). Development of nano-modified concrete for next generation of storage systems (No. DOE-Vanderbilt-DE-NE0000734). Vanderbilt Univ., Nashville, TN (United States).

Sanchez-Silva, M., & Rosowsky, D. V. (2008). Biodeterioration of construction materials: state of the art and future challenges. Journal of Materials in Civil Engineering, 20(5), 352-365.

Sand, W., & Bock, E. (1991). Biodeterioration of mineral materials by microorganisms—biogenic sulfuric and nitric acid corrosion of concrete and natural stone. Geomicrobiology Journal, 9(2-3), 129-138.

Sand, W. (1987). Importance of hydrogen sulfide, thiosulfate, and methylmercaptan for growth of thiobacilli during simulation of concrete corrosion. Applied and Environmental Microbiology, 53(7), 1645-1648.

Sarah, A. A., & Ee, A. G. R. (2017). Indoor and outdoor concentrations of bioaerosols and meteorological conditions of selected salons in four areas of Ibadan North local government area. Int J Environ Monit Anal, 5, 83.

Sarkhosh, M., Najafpoor, A. A., Alidadi, H., Shamsara, J., Amiri, H., Andrea, T., & Kariminejad, F. (2021). Indoor Air Quality associations with sick building syndrome: An application of decision tree technology. Building and Environment, 188, 107446.

Sierra-Fernández, A., Gomez Villalba, L. S., Rabanal, M. E., & Fort Gonzalez, R. (2017). New nanomaterials for applications in conservation and restoration of stony materials: A review.

Skora, J., Gutarowska, B., Pielech-Przybylska, K., Stępień, Ł., Pietrzak, K., Piotrowska, M., & Pietrowski, P. (2015). Assessment of microbiological contamination in the work environments of museums, archives and libraries. Aerobiologia, 31, 389-401.

Sommers, J. F. (1969). Gamma radiation damage of structural concrete immersed in water. Health physics, 16(4), 503-508.

Soo, P., & Milian, L. M. (2001). The effect of gamma radiation on the strength of Portland cement mortars. Journal of materials science letters, 20(14), 1345-1348.

Staszowska, A. B. (2023). Exposure to Bacterial and Fungal Aerosol in the University Library-A Case Study. Journal of Ecological Engineering, 24(10).

Sterflinger, K. (2010). Fungi: their role in deterioration of cultural heritage. Fungal biology reviews, 24(1-2), 47-55.

Sterflinger, K. (2000). Fungi as geologic agents. Geomicrobiology Journal, 17(2), 97-124.

Suarez, F., Conchillo, J. J., Galvez, J. C., & Casati, M. J. (2018). Macro Photography as an Alternative to the Stereoscopic Microscope in the Standard Test Method for Microscopical Characterisation of the Air-Void System in Hardened Concrete: Equipment and Methodology. Materials, 11(9), 1515.

Surahyo, A., Surahyo, & Luby. (2019). Concrete construction (pp. 61-88). Springer International Publishing.

Sykes, J. M. (1988). Sick building syndrome: a review. Health and Safety Executive, Technology Division.

Szatmari, I., Tudosie, L. M., Cojocaru, A., Lingvay, M., Prioteasa, P., & VIŞAN, T. (2015). Studies on biocorrosion of stainless steel and copper in Czapek Dox medium with Aspergillus niger filamentous fungus. UPB Sci. Bull., Series B, 77(3), 91-102.

Tayel, A. A., Ebeid, M. M., ElSawy, E., & Khalifa, S. A. (2016). Fungicidal effects of plant smoldering fumes on archival paper-based documents. Restaurator. International Journal for the Preservation of Library and Archival Material, 37(1), 15-28.

Thach, T. Q., Mahirah, D., Dunleavy, G., Nazeha, N., Zhang, Y., Tan, C. E. H., Roberts, A.C., Christopoulos, G., Soh, C. K., & Car, J. (2019). Prevalence of sick building syndrome and its association with perceived indoor environmental quality in an Asian multi-ethnic working population. Building and Environment, 166, 106420.

Tong, G. S. (2018). Processes and Mechanisms Responsible for Microbial Degradation of the Chemical and Structural Integrity of Concrete. Imperial College London.

Toreno, G., Isola, D., Meloni, P., Carcangiu, G., Selbmann, L., Onofri, S., & Zucconi, L. (2018). Biological colonization on stone monuments: A new low impact cleaning method. Journal of Cultural Heritage, 30, 100-109.

Urzì, C., De Leo, F., De Hoog, S., & Sterflinger, K. (2000). Recent advances in the molecular biology and ecophysiology of meristematic stone-inhabiting fungi. Of microbes and art: the role of microbial communities in the degradation and protection of cultural heritage, 3-19.

Van Der Molen, J. M., Garty, J., Aardema, B. W., & Krumbein, W. E. (1980). Growth control of algae and cyanobacteria on historical monuments by a mobile UV unit (MUVU). Studies in Conservation, 25(2), 71-77.

Van der Werf, I. D., Ditaranto, N., Picca, R. A., Sportelli, M. C., & Sabbatini, L. (2015). Development of a novel conservation treatment of stone monuments with bioactive nanocomposites. Heritage Science, 3(1), 1-9.

Vannini, A., Contardo, T., Paoli, L., Scattoni, M., Favero-Longo, S. E., & Loppi, S. (2018). Application of commercial biocides to lichens: Does a physiological recovery occur over time?. International Biodeterioration & Biodegradation, 129, 189-194.

Vazquez, P., Holguin, G., Puente, M. E., Lopez-Cortes, A., & Bashan, Y. (2000). Phosphate-solubilizing microorganisms associated with the rhizosphere of mangroves in a semiarid coastal lagoon. Biology and Fertility of Soils, 30, 460-468.

Vodak, F., Trtík, K., Sopko, V., Kapickova, O., & Demo, P. (2005). Effect of γ-irradiation on strength of concrete for nuclear-safety structures. Cement and concrete research, 35(7), 1447-1451.

Westphal, K. R., Heidelbach, S., Zeuner, E. J., Riisgaard-Jensen, M., Nielsen, M. E., Vestergaard, S. Z., Bekker, N. S., Skovmark, J., Olesen, C. K., Thomsen, K. H., Niebling, S. K., Sorensen, J. L., & Sondergaard, T. E. (2021). The effects of different potato dextrose agar media on secondary metabolite production in Fusarium. International Journal of Food Microbiology, 347, 109171.

Wiktor, V., Grosseau, P., Guyonnet, R., Garcia-Diaz, E., & Lors, C. (2011). Accelerated weathering of cementitious matrix for the development of an accelerated laboratory test of biodeterioration. Materials and structures, 44, 623-640.

Wiktor, V., De Leo, F., Urzì, C., Guyonnet, R., Grosseau, P. H., & Garcia-Diaz, E. (2009). Accelerated laboratory test to study fungal biodeterioration of cementitious matrix. International Biodeterioration & Biodegradation, 63(8), 1061-1065.

Wollenzien, U., De Hoog, G. S., Krumbein, W. E., & Urzi, C. (1995). On the isolation of microcolonial fungi occurring on and in marble and other calcareous rocks. Science of the total Environment, 167(1-3), 287-294.

Yakovleva, G., Sagadeev, E., Stroganov, V., Kozlova, O., Okunev, R., & Ilinskaya, O. (2018). Metabolic activity of micromycetes affecting urban concrete constructions. The Scientific world journal, 2018.

Yassin, M. F., & Almouqatea, S. (2010). Assessment of airborne bacteria and fungi in an indoor and outdoor environment. International journal of environmental science & technology, 7, 535-544.

Yu, C., Wang, Y., Cao, H., Zhao, Y., Li, Z., Wang, H., Chen, M., & Tang, Q. (2020). Simultaneous determination of 13 organic acids in liquid culture media of edible fungi using high-performance liquid chromatography. BioMed Research International, 2020.

Zarzuela, R., Carbú, M., Gil, M. A., Cantoral, J. M., & Mosquera, M. J. (2017). CuO/SiO2 nanocomposites: a multifunctional coating for application on building stone. Materials & Design, 114, 364-372.

Zhang, Q., & Ye, G. (2012). Dehydration kinetics of Portland cement paste at high temperature. Journal of thermal analysis and calorimetry, 110(1), 153-158.

PhD thesis

ORIGINALITY REPORT

12%
SIMILARITY INDEX

PRIMARY SOURCES

1	Liying Jiang, Tim R. Pettitt, Nick Buenfeld, Stephen R. Smith. "A critical review of the physiological, ecological, physical and chemical factors influencing the microbial degradation of concrete by fungi", Building and Environment, 2022 Crossref	483 words — 2%
2	www.mdpi.com Internet	377 words — 1%
3	ondoc.logand.com Internet	108 words — < 1%
4	Mian Adnan Kakakhel, Fasi Wu, Ji-Dong Gu, Huyuan Feng, Khadim Shah, Wanfu Wang. "Controlling biodeterioration of cultural heritage objects with biocides: A review", International Biodeterioration & Biodegradation, 2019 Crossref	101 words — < 1%
5	Jong-il Choi, Sangyong Lim. "Inactivation of fungal contaminants on Korean traditional cashbox by gamma irradiation", Radiation Physics and Chemistry, 2016 Crossref	95 words — < 1%
6	da Silva, M.. "Inactivation of fungi from deteriorated paper materials by radiation",	93 words — < 1%

International Biodeterioration & Biodegradation, 200604
Crossref

7	hal.archives-ouvertes.fr Internet	87 words — < 1%
8	www.slideshare.net Internet	76 words — < 1%
9	Subarna Bhattacharyya, Debleena Mukherjee, Punarbasu Chaudhuri. "Biodeterioration risk index of exhibit present in museum galleries of tropical climate", Museum Management and Curatorship, 2016 Crossref	70 words — < 1%
10	link.springer.com Internet	69 words — < 1%
11	Neveen S. Geweely, Hala A. M. Afifi, Shehata A. Abdelrahim, Saleha Y. M. Alakilli. "Novel Comparative Efficiency of Ozone and Gamma Sterilization on Fungal Deterioration of Archeological Painted Coffin, Saqqara Excavation, Egypt", Geomicrobiology Journal, 2014 Crossref	58 words — < 1%
12	www.scipress.com Internet	54 words — < 1%
13	L. Arora. "Role of Magnification in Conservative Dentistry and Endodontics in Today's Practice-A Review of Literature", International Journal of Medical and Dental Sciences, 2016 Crossref	47 words — < 1%
14	journals.plos.org Internet	44 words — < 1%

15	Sahoo, Ashok Kumar, and Bidyadhar Sahoo. "A comparative study on performance of multilayer coated and uncoated carbide inserts when turning AISI D2 steel under dry environment", Measurement, 2013. Crossref	40 words — < 1%
16	De Belie, N.. "Attack of Concrete Floors in Pig Houses by Feed Acids: Influence of Fly Ash Addition and Cement-bound Surface Layers", Journal of Agricultural Engineering Research, 199710 Crossref	39 words — < 1%
17	www.ncbi.nlm.nih.gov Internet	37 words — < 1%
18	shrishikshayatancollege.org Internet	36 words — < 1%
19	Manuela da Silva, A.M.L. Moraes, M.M. Nishikawa, M.J.A. Gatti, M.A. Vallim de Alencar, L.E. Brandão, A. Nóbrega. "Inactivation of fungi from deteriorated paper materials by radiation", International Biodeterioration & Biodegradation, 2006 Crossref	35 words — < 1%
20	www.science.gov Internet	34 words — < 1%
21	dokumen.pub Internet	33 words — < 1%
22	www.researchgate.net Internet	32 words — < 1%
23	acikbilim.yok.gov.tr Internet	31 words — < 1%

24	coek.info Internet	31 words — < 1%
25	"Environmental Concerns and Sustainable Development", Springer Science and Business Media LLC, 2020 Crossref	30 words — < 1%
26	Neveen S. Geweely, Hala A. Afifi, Dalia M. Ibrahim, Mona M. Soliman. "Efficacy of Essential Oils on Fungi Isolated from Archaeological Objects in Saqqara Excavation, Egypt", Geomicrobiology Journal, 2018 Crossref	30 words — < 1%
27	www.arca.fiocruz.br Internet	30 words — < 1%
28	"Infrastructure Systems for Nuclear Energy", Wiley, 2014 Crossref	29 words — < 1%
29	www.neogen.com Internet	26 words — < 1%
30	Aguirar, Livia Vanessa Ferreira de. "Indoor Biological Agents: Evaluation of Primary Schools Environments", Universidade do Minho (Portugal), 2021 ProQuest	25 words — < 1%
31	mzuir.inflibnet.ac.in Internet	25 words — < 1%
32	Potts, Alexander J.. "The Assessment of Gamma Radiation on the Properties of Structural Concrete", The University of Manchester (United Kingdom), 2022 ProQuest	23 words — < 1%

33	www.innspub.net Internet	23 words — < 1%
34	S. Majumdar. "Accumulation of minor and trace elements in lichens in and around Kolkata, India: an application of X-ray fluorescence technique to air pollution monitoring", X-Ray Spectrometry, 2009 Crossref	22 words — < 1%
35	Neveen S. Geweely, Mona M. Soliman, Rania A. Ali, Hamdi M. Hassaneen, Ismail A. Abdelhamid. "Novel eco-friendly [1,2,4]triazolo[3,4-a]isoquinoline chalcone derivatives efficiency against fungal deterioration of ancient Egyptian mummy cartonnage, Egypt", Archives of Microbiology, 2023 Crossref	21 words — < 1%
36	Gilbert, Christi. "The durability of concrete containing a high-level of fly ash or a ternary blend of supplementary cementing materials", Proquest, 2013. ProQuest	20 words — < 1%
37	www.hindawi.com Internet	20 words — < 1%
38	Francesca Cappitelli, Cristina Cattò, Federica Villa. "The Control of Cultural Heritage Microbial Deterioration", Microorganisms, 2020 Crossref	19 words — < 1%
39	dspace.dtu.ac.in:8080 Internet	19 words — < 1%
40	ebin.pub Internet	19 words — < 1%
41	hal-emse.ccsd.cnrs.fr Internet	

		19 words — < 1%
42	"Recent Advances in Pharmaceutical Innovation and Research", Springer Science and Business Media LLC, 2023 Crossref	18 words — < 1%
43	lands.nv.gov Internet	18 words — < 1%
44	www.statkart.no Internet	18 words — < 1%
45	Rivka Barkai-Golan, Peter A. Follett. "Irradiation for Quality Improvement of Individual Fruits", Elsevier BV, 2017 Crossref	17 words — < 1%
46	agronomyjournal.usamv.ro Internet	17 words — < 1%
47	Sterflinger, Katja, and Guadalupe Piñar. "Microbial deterioration of cultural heritage and works of art — tilting at windmills?", Applied Microbiology and Biotechnology, 2013. Crossref	16 words — < 1%
48	ir.kluniversity.in Internet	16 words — < 1%
49	theconstructor.org Internet	16 words — < 1%
50	Togoro Harada, Hiroshi Takaki, Yoshio Yamada. "Effect of nitrogen sources on the chemical	15 words — < 1%

components in young plants", Soil Science and Plant Nutrition, 1968
Crossref

51	jeq.scijournals.org Internet	15 words — < 1%
52	www.freepatentsonline.com Internet	15 words — < 1%
53	"Methods in Actinobacteriology", Springer Science and Business Media LLC, 2022 Crossref	14 words — < 1%
54	Bhattacharyya, Subarna, Debleena Mukherjee, Paushali Sarkar, Sreya Ghosh, Barnali Samaddar, and Punarbasu Chaudhuri. "Assessment of Viable Fungi in Indoor Air: A Case Study from Tagore's Residence at Jorasanko, India", International Letters of Natural Sciences, 2015. Crossref	14 words — < 1%
55	Santika Widowati, Kartinah W., Guruh Sri Pamungkas. "Identifikasi Jamur Kontaminan yang Bersifat Xerofilik pada Lada Bubuk", Biomedika, 2018 Crossref	14 words — < 1%
56	mafiadoc.com Internet	14 words — < 1%
57	web.fe.up.pt Internet	14 words — < 1%
58	Kristina Matković. "Airborne Fungi in Dwellings for Dairy Cows and Laying Hens", Archives of Industrial Hygiene and Toxicology, 12/01/2009 Crossref	13 words — < 1%
59	answeregy.com	

Internet

13 words — < 1%

60 bmcgenomics.biomedcentral.com
Internet

13 words — < 1%

61 docshare.tips
Internet

13 words — < 1%

62 webpages.uidaho.edu
Internet

13 words — < 1%

63 Feng, Dan. "Towards Socially Interactive Agents: Learning Generative Models of Social Interactions Via Crowdsourcing.", Northeastern University, 2020
ProQuest

12 words — < 1%

64 dolphin.bwc.state.oh.us
Internet

12 words — < 1%

65 dx.doi.org
Internet

12 words — < 1%

66 eprints.uanl.mx
Internet

12 words — < 1%

67 tpesecurity.com
Internet

12 words — < 1%

68 www.biorxiv.org
Internet

12 words — < 1%

69 Ki-Chang Lee, Jong-Heum Park, Jae-Kyung Kim, Ha-Young Park, Yeong-Seok Yoon, Jong-Bang Eun, Beom-Seok Song. "Rapid identification method for gamma-irradiated soybeans using gas chromatography–mass spectrometry coupled with a headspace solid-phase

11 words — < 1%

microextraction technique", Journal of Agricultural and Food Chemistry, 2020
Crossref

70	detail.chiebukuro.yahoo.co.jp Internet	11 words — < 1%
71	koreascience.kr Internet	11 words — < 1%
72	openaccess.iyte.edu.tr Internet	11 words — < 1%
73	repozitorium.omikk.bme.hu Internet	11 words — < 1%
74	www.coursehero.com Internet	11 words — < 1%
75	Agarwal, M.K.. "Studies on the allergenic fungal spores of the Delhi, India, metropolitan area", Journal of Allergy, 196910 Crossref	10 words — < 1%
76	Peerzada R. Hussain, A Omeera, Prashant P. Suradkar, Mohd A. Dar. "Effect of combination treatment of gamma irradiation and ascorbic acid on physicochemical and microbial quality of minimally processed eggplant (Solanum melongena L.)", Radiation Physics and Chemistry, 2014 Crossref	10 words — < 1%
77	Sammy Yin Nin Chan, Xihuang Ji. "Water sorptivity and chloride diffusivity of oil shale ash concrete", Construction and Building Materials, 1998 Crossref	10 words — < 1%

VNUA

78	Publications	10 words — < 1%
79	dzumenvis.nic.in Internet	10 words — < 1%
80	iosrjournals.org Internet	10 words — < 1%
81	patents.google.com Internet	10 words — < 1%
82	pdfs.semanticscholar.org Internet	10 words — < 1%
83	qspace.library.queensu.ca Internet	10 words — < 1%
84	studfile.net Internet	10 words — < 1%
85	timesofindia.indiatimes.com Internet	10 words — < 1%
86	tudr.thapar.edu:8080 Internet	10 words — < 1%
87	www.researchsquare.com Internet	10 words — < 1%
88	www.tandfonline.com Internet	10 words — < 1%
89	A Potts, E Butcher, G Cann, L Leay. "Long Term Effects of Gamma Irradiation on In-Service Concrete Structures", Journal of Nuclear Materials, 2021 Crossref	9 words — < 1%

90	Beata Gutarowska, Andrzej Michalski. "Chapter 2 Microbial Degradation of Woven Fabrics and Protection Against Biodegradation", IntechOpen, 2012 Crossref	9 words — < 1%
91	basicmedicalkey.com Internet	9 words — < 1%
92	code-research.eu Internet	9 words — < 1%
93	cyberleninka.org Internet	9 words — < 1%
94	dash.harvard.edu Internet	9 words — < 1%
95	fdocuments.net Internet	9 words — < 1%
96	ijirset.com Internet	9 words — < 1%
97	rke.abertay.ac.uk Internet	9 words — < 1%
98	www.jiskha.com Internet	9 words — < 1%
99	www.jmbfs.org Internet	9 words — < 1%
100	www.opensciencepublications.com Internet	9 words — < 1%
101	www.rsc.org Internet	9 words — < 1%

102	www.sandhillsci.com Internet	9 words — < 1%
103	"Food Flavour Technology", Wiley, 2010 Crossref	8 words — < 1%
104	Anurak Khieokhajonkhet, Marisa Phoprakot, Niran Aeksiri, Gen Kaneko, Wutiporn Phromkunthong. "Effects of thermal stress responses in goldfish (Carassius auratus): Growth performance, total carotenoids and coloration, hematology, liver histology, and critical thermal maximum", Research Square Platform LLC, 2023 Crossref Posted Content	8 words — < 1%
105	Cabral, J.P.S.. "Can we use indoor fungi as bioindicators of indoor air quality? Historical perspectives and open questions", Science of the Total Environment, 20100915 Crossref	8 words — < 1%
106	Fukuwatari, T.. "Effects of dietary di(2-ethylhexyl)phthalate, a putative endocrine disrupter, on enzyme activities involved in the metabolism of tryptophan to niacin in rats", BBA - General Subjects, 20040503 Crossref	8 words — < 1%
107	Osamu Kontani, Yoshikazu Ichikawa, Akihiro Ishizawa, Masayuki Takizawa, Osamu Sato. "Irradiation Effects on Concrete Structures", Wiley, 2013 Crossref	8 words — < 1%
108	academic.oup.com Internet	8 words — < 1%
109	acikerisim.mersin.edu.tr Internet	8 words — < 1%

110	analesranf.com Internet	8 words — < 1%
111	assets.researchsquare.com Internet	8 words — < 1%
112	digitalscholarship.unlv.edu Internet	8 words — < 1%
113	ethesis.nitrkl.ac.in Internet	8 words — < 1%
114	pubs.rsc.org Internet	8 words — < 1%
115	scholarworks.gsu.edu Internet	8 words — < 1%
116	www.eprint.iitd.ac.in Internet	8 words — < 1%
117	www.prppg.ufpr.br Internet	8 words — < 1%
118	www.pt.bme.hu Internet	8 words — < 1%
119	"Advances and Applications Through Fungal Nanobiotechnology", Springer Science and Business Media LLC, 2016 Crossref	7 words — < 1%
120	Mohamed A. Rizk ., Tarek A. A. Moussa .. "Impact of Gamma Irradiation Stresses I. Response of Gamma-irradiated Sugarbeet Seeds to Infection by Soil-borne Fungal Pathogens", Plant Pathology Journal, 2003 Crossref	6 words — < 1%

121 Rinu K., Anita Pandey. "Slow and steady phosphate solubilization by a psychrotolerant strain of Paecilomyces hepiali (MTCC 9621)", World Journal of Microbiology and Biotechnology, 2010
Crossref

6 words — < 1%

EXCLUDE QUOTES	OFF	EXCLUDE SOURCES	OFF
EXCLUDE BIBLIOGRAPHY	OFF	EXCLUDE MATCHES	OFF